COMBINATION IMMUNOTHERAPY WITH INHIBITOR OF APOPTOSIS (IAP) ANTAGONISTS TO TREAT NEUROBLASTOMA

Matthew Michalicka

A thesis submitted to the
Faculty of Graduate and Postdoctoral Studies
in partial fulfillment of the requirements for the
Master's in Science degree in Microbiology and Immunology

Department of Biochemistry, Microbiology and Immunology
Faculty of Medicine
University of Ottawa

ABSTRACT

Neuroblastoma is the third most common pediatric cancer. Dinutuximab is a recently approved monoclonal antibody targeting GD2, a ganglioside ubiquitously present on neuroblastoma. Recent studies have shown that αGD2 therapy activates PD1-PDL1 signalling, resulting in the inhibition of its full therapeutic potential. The PD1-PDL1 signalling axis is a cellular checkpoint that inhibits immune responses. The blocking of this interaction has been successful in the treatment of numerous cancers, including in combination with anti-GD2 therapy. The Inhibitor of apoptosis (IAP) proteins are commonly upregulated in cancers and prevent cell death through the inhibition of caspases and through the control of NF-κB activity. Smac mimetic compounds (SMCs) have been designed to target IAP activity, thereby promoting cancer cell death. Here, I used the SMC, LCL161, to improve αGD2 antibody treatment against a $GD2^+$ syngeneic neuroblastoma mouse model. I found that murine cell lines NXS2 and N2a were resistant *in vitro* to LCL161-mediated apoptosis, despite expressing apoptotic components often silenced in neuroblastoma. *In vivo*, I observed a slight delay in tumour growth induced by LCL161 and I confirmed an *in vivo* anti-angiogenic effect of LCL161 through ultrasound imaging and necropsy evaluation. I then combined LCL161 and αGD2 antibody (clone ME361-S2a) treatment and reported a delay in NXS2 subcutaneous tumour growth, which was further potentiated with the addition of an αPD-L1 antibody. With optimization, there is potential for SMCs to be used in combination with αGD2 therapy in $GD2^+$ cancers like neuroblastoma.

ACKNOWLEDGEMENTS

My biggest thanks go to Dr. Robert Korneluk for allowing me the opportunity to work in his lab and guiding me throughout my degree. His support and experience were instrumental in my success. Furthermore, his passion for science (probably the only thing keeping him from being an English professor) allowed me to explore as a researcher and truly enjoy my work here. As well, thanks to my thesis advisory committee, Dr. Subash Sad and Dr. Seung-Hwan Lee, for guiding myself and my project through to the end.

I must also acknowledge my other mentors, Drs. Eric LaCasse, Shawn Beug, and Neena Lala, whose discussions improved not only my understanding of the science, but of the field as well. Their additional supervision helped tremendously in progressing my project and thesis.

I also extend my gratitude to the rest of the Korneluk lab. Janelle Holbrook, M(ouse). D(octor). requires a specific mention for her essential contributions with the *in vivo* work. As well, thanks to Martine St. Jean, Nathalie Earl and Danielle Walker for generously answering my questions (often the same ones) and teaching me over my degree. I acknowledge Dr. Stephen Baird for running my immunofluorescence samples. My fellow students were also vital for my sanity over this journey, with Tarun Sanda and Travis Richard providing great support and after hour science discussion when needed. My other student colleagues, Matthew Hunt and Cristin Healy, and the rest of the CHEO Research Institute deserve a specific mention for the great experiences we shared as well. A specific mention to ATCC and medicine (in Germany and in Canada) for teaching me to never give up.

Special thanks go to my friends and family, who always supported me and were always there for me to enjoy my time. I am excited for the next step and am glad you will all be there.

Don’t forget, life is about *BIRC7* not just *BIRC5*.

TABLE OF CONTENTS

LIST OF TABLES

LIST OF FIGURES

LIST OF ABBREVIATIONS

ACVS	Animal Care and Veterinary Service
ADCC	antibody dependent cellular cytotoxicity
ADCP	antibody dependent cellular phagocytosis
ALCAM	activated leukocyte cell adhesion molecule
APC	antigen presenting cells
BIR	baculovirus IAP repeat
CAR	chimeric antigen receptor
CARD	caspase recruitment domain
CDC	complement dependent cytotoxicity
cFlip	cellular FADD-like IL-1β-converting enzyme inhibitor protein
CHEO	Children's Hospital of Eastern Ontario
cIAP	cellular inhibitor of apoptosis
CTLA-4	cytotoxic T-lymphocyte-associated protien-4
DCs	dendritic cells
DISC	death-inducing signalling complex
DMEM	Dulbecco's Modified Eagle Medium
FAK	focal adhesion kinase
FDA	U.S. Food and Drug Administration
Fluc	firefly luciferase
FOXC2	forkhead box protein C2
GM-CSF	granulocyte-macrophage colony-stimulating factor
HAMA	Human anti-mouse antibodies
i.v.	intravenous
IAP	inhibitor of apoptosis
ICI	immune checkpoint inhibitor
IFNy	interferon γ

IgM	immunoglobulin M
Iκβ	inhibitor of κβ
IKKβ	inhibitor of κβ kinase β
IL-2	interleukin-2
IL-4	interleukin-4
ILP2	inhibitor of apoptosis-like protein 2
IVIS	In vivo imaging system
KIR	killer immunoglobulin-like receptor
LAK	lymphokine activated killer cells
LDH	lactate dehydrogenase
LPS	lipopolysaccharide
MFI	mean fluorescence intensity
MHC	major histocompatibility complex
ML-IAP	melanoma inhibitor of apoptosis
N2a	Neuro2a
NAIP	neuronal inhibitor of apoptosis
NB	neuroblastoma
NCAM	neural cell adhesion molecule
NF-κβ	nuclear factor kappa-light-chain-enhancer of activated B cells
NIK	NF-κβ inducing kinase
NK cells	natural killer cells
p.o.	per os
PARP	poly (ADP ribose) polymerase
PBMCs	peripheral blood mononuclear cells
PD-1	programmed death protein-1
PDGF	platelet-derived growth factor
pdl1	programmed death ligand 1
ring	really interesting new gene

RPMI	Roswell Park Memorial Institute
s.c.	subcutaneous
SCLC	small cell lung cancer
SDS-PAGE	sodium dodecyl sulfate-polyacrylamide gel electrophoresis
Smac	second mitochondrial activator of caspases
SMC	Smac mimetic compounds
TAK1	transforming growth factor b activated kinase 1
TNFα	tumor necrosis factor α
tnfr1	TNF receptor 1
TRADD	TNFR type 1-associated death domain
TRAF2	TNF receptor associated factor 2
TRAIL	TNF-related apoptosis inducing ligand
Tregs	Regulatory T cells
VEGF	vascular endothelial growth factor
XIAP	x-linked inhibitor of apoptosis

1.0 INTRODUCTION

My project aims to antagonize the inhibitor of apoptosis (IAP) proteins in neuroblastoma to improve the efficacy of an approved immunotherapy which targets GD2. An explanation of IAP biology, IAP antagonism, immunotherapy, αGD2 therapy, and neuroblastoma follows.

1.1 The Inhibitors of Apoptosis

The IAP proteins represent a group of proteins that control cell death (1,2) and act as regulators of the nuclear factor kappa-light-chain-enhancer of activated B cells (NF-κB) pathway (3,4). The capabilities of the IAP family have led to their overexpression in certain diseases, such as cancers like neuroblastoma (NB) (5,6).

1.1.1 Characteristics of the IAPs

The baculovirus IAP gene family was discovered in the Cydia pomonella granulosis virus by the Miller group (7). Following studies reported the discovery of a mammalian IAP protein, neuronal IAP (NAIP), by the Korneluk group (2). Currently, there are eight proteins classified in the IAP family (8).

The mammalian IAP members can be divided into three classes depending on their domain composition (8). All IAP proteins contain Baculovirus IAP repeat (BIR) domains which are zinc-finger folds that are composed of conserved histidine and cysteine residues (7,9). A first sub-class of IAP proteins are distinguished by their C-terminal Really Interesting New Gene (RING) domain, which has E3-ligase activity (10,11). This class includes the following members: X-linked IAP (XIAP), cellular IAP 1 (cIAP1) and cIAP2, IAP-like protein 2 (ILP2), and melanoma-IAP (ML-IAP, also known as Livin). cIAP1 and cIAP2 also have a Caspase Recruitment Domain (CARD) which interacts with other CARDs to create larger protein complexes. The specific

purpose of the CARD domains on the IAP proteins are currently unknown (12,13). However, outside of IAPs, these CARD domains can be found on mitochondrial and cytoplasmic proteins such as caspases (14,15).

NAIP is the sole member of a second IAP sub-class, which contains three BIR domains but no ligase domain. The third IAP sub-class has two members which have a single BIR domain, Apollon and Survivin (8).

1.1.2 Inhibition of apoptosis

Caspases are protease enzymes which cleave proteins to induce cell death (16). Once activated by cell death stimuli, initiator caspases (caspase-2, -8,, -9, -10) will form complexes to initiate the caspase cascade, activating executioner caspases (caspase-3, -6, -7) (17). These executioner caspases can then cleave other proteins related to cell structure and signalling which leads to DNA fragmentation and nuclear collapse and eventually cell death (18). IAP proteins can inhibit apoptosis and promote cell survival by targeting caspase proteins (Figure 1) (19). The BIR domains permit IAP proteins to bind directly to caspases. The XIAP BIR domains are capable of directly inhibiting both effector and initiator caspases such as caspase-3, -7, and -9 (20). The BIR3 domain of XIAP is capable of binding to and inhibiting inactive caspase-9 monomers, preventing active caspase-9 homodimer formation (21). Comparatively, the XIAP BIR2 domain binds the active sites of caspase-3 and -7 to mediate their inhibition (20). The cIAP1/2 proteins can bind caspases, such as caspase-3 and -7, but do not inhibit their function directly due to key amino acid substitutions found in their BIR domains relative to the XIAP BIR domains (22). Instead, these IAP proteins target effector caspases for ubiquitination, which leads to their degradation (23).

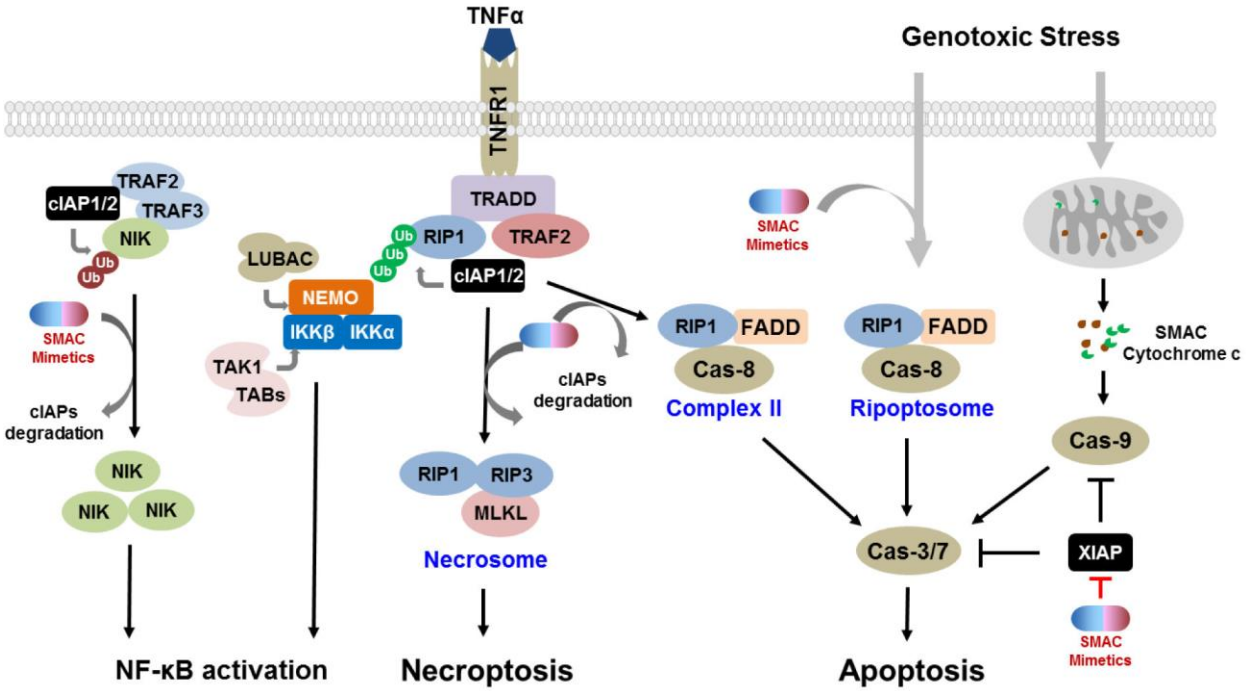
TNFα
TNFR1
Genotoxic Stress
TRADD
RIP1
TRAF2
cIAP1/2
Ub
SMAC Mimetics
LUBAC
NEMO
IKKβ
IKKα
TAK1
TABs
TRAF2
cIAP1/2
TRAF3
NIK
cIAPs degradation
NIK
NIK
NIK
NF-κB activation
cIAPs degradation
RIP1
RIP3
MLKL
Necrosome
Necroptosis
RIP1
FADD
Cas-8
Complex II
RIP1
FADD
Cas-8
Ripoptosome
SMAC Cytochrome c
Cas-9
Cas-3/7
XIAP
SMAC Mimetics
Apoptosis

Figure 1. Role of IAP proteins and SMCs in apoptosis and NF-kB signalling. General overview of how the IAP proteins and SMCs interact with signalling pathways for apoptosis, necroptosis, and NF-κB signalling. cIAP1 and cIAP2 will ubiquitinate NIK, preventing NIK accumulation and inhibiting signalling from alternative NF-κB pathway. cIAP1 and cIAP2 will also ubiquitinate RIP1, preventing formation of the necrosome or complex 2, inhibiting both necroptosis and apoptosis. As well, ubiquitinated RIP1 serves as a scaffold for the TAK1 complex to form, promoting signalling from canonical NF-κB pathway. XIAP is also seen inhibiting caspase-3, -7, and -9 activations. Not shown is XIAP dimerizing with TAK1 to activate canonical NF-κB signalling. Impact of SMCs are also indicated in each pathway and can be seen promoting alternative NF-κB signalling, necroptosis, and apoptosis pathways. Adapted from Bai et al. 2014 (19)

1.1.3 Modulation of NF-κB signalling

In addition to their roles in inhibiting apoptosis, IAP proteins are also regulators of cell signalling (Figure 1). The NF-κB pathway is a family of transcription factors which have roles in regulating important cell processes, such as cytokine production, inflammation, immune responses, and cell survival (24–26). Some of the target genes of the NF-κB pathway that are involved in cell death and immune signalling are tumor necrosis factor α (TNFα) (27), major histocompatibility complex 1 and 2 (MHC 1 and 2) (28–30) , and programmed death receptor ligand 1 (PD-L1) (31). MHC 1 and 2 are important for immune cell recognition of host cells and presented antigens. PD-L1 is the ligand for PD-1 and acts as a stop signal to certain immune cells. The NF-κB pathway can be activated in two ways, canonical/classical and non-canonical/alternative signalling (24,26,32). These two pathways can be distinguished by their signalling components. Canonical signalling requires the activation of the inhibitor of κB (IκB) kinase β (IKKβ) and signals through RelA- or c-Rel-p50 heterodimer to mediate target gene transcription. Non-canonical signalling requires NF-κB-inducing kinase (NIK) accumulation to activate IKKα, leading to RelB-p52 transcription factor heterodimer formation (24,26,32).

Both XIAP and the cIAP1/2 proteins are capable of regulating NF-κB pathway signalling (3,4). The first BIR domain of XIAP binds and activates transforming growth factor β-activated kinase 1 (TAK1), which then phosphorylates IKK. Phosphorylated IKK degrades IκB by phosphorylation, releasing transcription factor dimers into the nucleus for signalling. Thus, XIAP can promote NF-kB signalling through activation of TAK1 (3). As well, TNFα-mediated NF-κB signalling was found to be attenuated by loss of both cIAP1/2 proteins. Due to the functional redundancy of cIAP1 and cIAP2, either of these proteins are able to polyubiquinate Rip1 to permit recruitment of TAK1 and IKK complexes to the TNF receptor 1 (TNF-R1) signalosome (4).

Additionally, the cIAP1/2 proteins also play an important role in inhibiting alternative NF-κB signalling by degrading NIK. Degradation of NIK prevents signalling from the alternative NF-κB pathway by attenuating downstream activation of IKKα (4,33).

1.2 Smac mimetic compounds

1.2.1 Characteristics of Smac mimetic compounds

The ability of the IAPs to play a role in cell survival and NF-κB signalling makes them important targets for cellular regulation (Figure 1)(19). Discovered in 2000 by the Wang lab, second mitochondrial activator of caspases (Smac) is an endogenous protein, which binds and inhibits IAP proteins, preventing caspase inhibition, and promoting programmed cell death (34). Smac is sequestered in the mitochondria and, upon apoptotic stimuli, is released into the cytosol to antagonize IAP proteins. Its ability to target the IAPs, and how its overexpression sensitizes cells to other apoptotic agents, makes Smac a good candidate for drug development (19,34,35).

Smac mimetic compounds (SMCs) have been developed to model the IAP binding motif of Smac. Specifically, SMCs are modelled after a four-amino acid sequence in Smac, Alanine-Valine-Proline-Isoleucine (AVPI) (19,36). The most studied SMC is LCL161, a monomer SMC developed by Novartis (Figure 2). Preclinical studies have been successful in using SMCs, like LCL161, to treat numerous cancer models (37–43). However, limited anti-tumour responses by SMCs have been seen against NB cell lines (5,6,44,45).

1.2.2 Promotion of apoptosis

Smac and SMCs can promote apoptosis by antagonizing IAP proteins, often using an AVPI motif that is capable of binding distinct BIR domains (19,34,36,46). The AVPI motif can bind to BIR2 and BIR3 of XIAP, interfering with XIAP-caspase interactions and thus permitting activation of

caspases (34,47). As well, the AVPI motif can bind the BIR3 domain of cIAP1/2 and cause autoubiquitination, decreasing cellular levels of those IAPs (46). SMC-mediated IAP antagonism increases the sensitivity of cells to TNFα-related cell death by two methods. Firstly, SMC-mediated antagonism will prevent cIAP1/2-mediated inhibition of apoptosome or necrosome formation (48–50). Secondly, SMC will directly bind XIAP and prevent XIAP-caspase interaction, thus permitting caspases to activate and induce cell death (Figure 1) (34,36,47). Additionally, by inducing degradation of cIAP1/2, NIK accumulates and activates the alternative NF-κB pathway (32,51). Activated NF-κB signalling can lead to TNFα production (27). Secretion of TNFα can then induce cell death in the neighbouring cells as well (52,53). This has led to a potential for a bystander killing effect of cancer cells by SMCs, which was observed when LCL161 was used in combination with an oncolytic virus (41). Furthermore, SMCs have even been shown to affect tumour angiogenesis through the promotion of TNFα signalling. Tumour endothelial cells were found to be sensitive to SMC-induced TNFα production in a B16 melanoma tumour model (54). This ability of SMCs to induce vascular shutdown in tumours was confirmed in our lab using an EMT6 model (55). Thus, not only can SMCs be directly tumoricidal, but they can also inhibit tumour growth by inducing vascular collapse through sensitizing endothelial cells to TNFα-induced death. This anti-angiogenic ability of SMCs could warrant their use against highly vascularized tumours, such as neuroblastoma (NB). However, since SMCs regulate the NF-κB pathway, which is important in immune signalling, they can also affect the tumour microenvironment in ways other than promoting vascular shutdown.

1.2.3 Effect on the innate immune system

Since the IAPs are also capable of modulating NF-κB signalling, they have been studied for their role in regulating the innate and adaptive immune system (38,41,56,57). In certain diseases

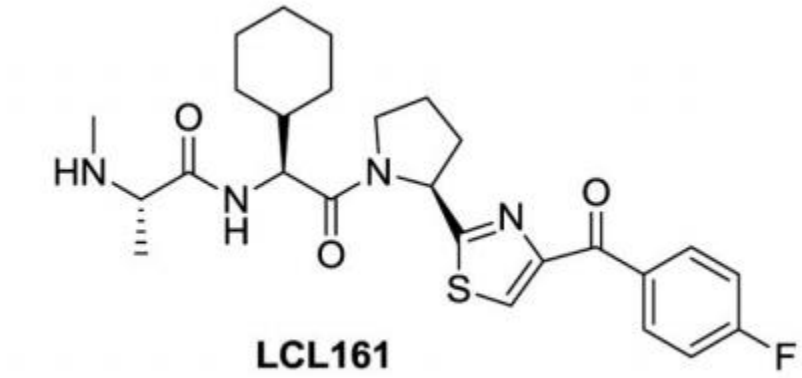

Figure 2. Structure of LCL161, a monovalent SMC from Novartis. Adapted from Bai et al. 2014 (19).

such as cancer, the innate and adaptive immune system is dysregulated and the IAP expression has been shown to be upregulated (58–60). This has made the IAP family a promising therapeutic target since they can be directly antagonized with SMCs.

SMCs and IAPs can both affect the innate immune components. Studies showed that IAP antagonism by SMCs in human NK cells increased TNFα and interferon γ (IFNγ) production and cellular cytotoxicity against various cancer cell lines (61,62). Additionally, granulocyte macrophage colony-stimulating factor (GM-CSF) production was found to increase in mouse natural killer (NK) cells treated with SMCs in the presence of the NK target cell line, Yac-1 (63). As well, it was found that XIAP protected cancer cells from αHer2-antibody dependent cellular cytotoxicity (ADCC) (64) The gene *BIRC3*, encoding cIAP2, was found to be upregulated in activated NK cells in HIV-1-infected patient samples (65). However, after TNFα signalling, NK cells in the tumour microenvironment had increased expression of *BIRC3* and reduced expression of the activating receptor NKp46. This correlated with poor prognosis in patients with gastrointestinal stromal tumour (66). Thus, the complete role of IAP proteins in NK cells still requires further examination.

Several studies have shown the IAP proteins are used to modulate the lifespan of neutrophils. A study reported that the loss of XIAP expression protected neutrophils from lipopolysaccharide (LPS)-induced death, and that neutrophils could be sensitized to LPS by the additional loss of cIAP1/2 proteins (67). Studies also found that neutrophil lifespan was extended through XIAP and cIAP protein overexpression induced by granulocyte colony-stimulating factor (68,69). However, in a cancer model, a SMC was shown to enable a tumoricidal function of BCG-stimulated neutrophils (70).

Studies have also shown the IAP family to regulate monocytes. There have been contested implications of IAP proteins and SMCs on macrophage polarization. In an infection model, the SMC, birinapant, was found to promote an M2 phenotype of macrophages (71). Meanwhile, LCL161 promoted a M1 phenotype in a cancer model (38,39). IAP proteins could mediate the resistance of macrophages to apoptotic stimuli (72–74) but SMCs could also lead to macrophage activation (38,39,75). Oddly, it was observed that cIAP1-mediated degradation of TNF receptor associated factor 2 (TRAF2) to be necessary for monocyte maturation to functional macrophages (76). Studies have also reported that SMCs could activate dendritic cells (DCs), increasing activation markers and MHC expression (39,63,75,77). Interestingly, a group observed that IAP antagonism induced maturation of myeloid DCs and reduced their capacity to cross-present antigen. They also observed that IAP antagonism of peripheral blood mononuclear cells (PBMCs) had increased capacity to prime naïve T-cells (78).

The ability of SMCs to activate and affect polarization of antigen presenting cells (APCs), such as DCs and macrophages, suggests that SMCs could also contribute to generating an adaptive immune response.

1.2.4 Effect on the adaptive immune system

Studies have also found IAP proteins to regulate adaptive immune responses. One lab, using a lentiviral delivery system, was able to treat tumours with cytosolic Smac protein and induce tumour cell death, activate DCs, reduce regulatory T-cells (Tregs) frequencies and stimulate cytotoxic T-lymphocytes (79,80). Another study was able to repolarize immunosuppressive macrophage subsets in a tumour microenvironment with SMCs. This enhanced the activity of exhausted $CD8^+$ T-cells in the tumour (38). Additionally, IAP antagonism was found to have direct co-stimulatory effects on $CD4^+$ and $CD8^+$ effector T-cells. These co-stimulatory effects increased

interleukin-2 (IL-2), IL-4 and IFNγ cytokine production by CD4 and CD8 T-cells, proliferation of CD4 T-cells, and an increase in CD25 activation marker expression (63). Importantly, one study also concluded that i*n vitro* treatment of T-cells had no sensitivity to SMC-mediated cell death, regardless of stimulation status (77). However, in contrast, a report showed that a viral infection model treated with LBW242 impaired control of the viral infection due to TNFα-mediated death of activated T-cells (81). Treg suppressive functionality was also found dependent on XIAP-mediated stabilization of suppressor of cytokine signalling 1 (SOCS1) (82). It was also shown that SMC treatment decreased tumour infiltrating Treg populations while increasing $CD4^+$ and $CD8^+$ T-cell populations (80).

Targeting the IAP family with SMCs can synergize with immunotherapies, such as checkpoint inhibitors (43), cancer cell vaccines (63), and oncolytic viruses (38,40,55). A partial explanation of the basis for this synergy is because of the ability of SMCs to increase cell cytotoxicity and modulate immune cell activation, antigen presentation, and T-cell stimulation. Thus, SMCs are being studied to further potentiate the efficacy of immunotherapies, a class of drugs that have had limited success in treating NB so far.

1.3 Cancer immunotherapy

The immune system is a powerful tool to treat cancer. Two benefits of immunotherapies are the antigenic specificity to target one marker effectively and the possibility to generate a memory response to protect against future repeat events. Immunotherapy is a broad label for biologics such as tumour vaccines, cytokines, adoptive cell transfers, and monoclonal antibodies (83). Each of these can be divided into two dichotomies: passive or active and specific or nonspecific (84,85). Passive immunotherapies are treatments which have intrinsic anti-tumour cytotoxicity. Active immunotherapies are compounds that rely on engaging the host immune system to elicit

their anti-tumour response. Specific immunotherapies will generate an immune response to a particular antigen while non-specific immunotherapies will generate an immune response to antigens not specifically designated. Antibody immunotherapies fall under the passive and specific or active and non--specific immunotherapy category, such as tumour targeting monoclonal antibodies or immune checkpoint blockers, respectively (84,85).

1.3.1 Passive and specific antibody-mediated immunotherapy

Passive and specific antibody-mediated immunotherapy involves the antibody binding the target cell directly and then directing immune effector components, such as complement, NK cells, or granulocytes, to kill the target cell (86,87). There are three main cytotoxic mechanisms an antibody can mediate, namely complement dependent cytotoxicity (CDC) (88–90), antibody dependent cellular cytotoxicity (ADCC) (91–94), and antibody dependent cellular phagocytosis (ADCP) (93,95,96).

CDC occurs when the complement protein C1q binds the Fc region of antibody, which undergoes a conformational change and then recruits and activates a cascade of complement proteins. This process leads to inflammation, opsonization, and eventually cytotoxicity through the formation of the membrane attack complex which disrupts the cell membrane (88–90). ADCC occurs when a target cell is brought into proximity of a cytotoxic cell through an antibody binding the antigen and an Fc receptor. Engaging the Fc receptor on the effector cell releases cytotoxic factors, such as granzyme B and perforin, which lyse the target cell. Typical effector cells for ADCC are NK cells, neutrophils, monocytes, dendritic cells, and eosinophils (91–94). ADCP occurs similarly to ADCC, however the target cell is instead phagocytosed by the effector cell. Phagocytosed cells are lysed, and then possible antigen generation and presentation can occur. Typical effector cells for ADCP are monocytes, macrophages, neutrophils, and dendritic cells (93,95,96).

Table 1. Approved antibody therapeutics that are specific immunotherapies. Adapted and edited from Suzuki et al. 2015 (87)

Scientific name (Commercial name)	**Target**	**Isotype class**	**Cancer approved for**	**Date of FDA approval**
Rituximab (Rituxan)	CD20	Chimeric IgG1	B-cell Non-Hodgkin's lymphoma	1997
Trastuzimab (Herceptin)	Her2	Humanized IgG1	Breast cancer	1998
Alemtuzumab (Campath)	CD52	Humanized IgG1	B-cell chronic lymphocytic leukemia	2001
Cetuximab (Erbitux)	EGFR	Chimeric IgG1	Colorectal, head and neck cancer	2004
Catumaxomab (Removab)	CD3, EpCAM	Chimeric IgG2a/b	Malignant ascites	2009
Mogamulizumab (Poteligeo)	CCR4	Humanized IgG1	T-cell leukemia-lymphoma	2012
Dinutuximab (Unituxin)	GD2	Chimeric IgG1	Neuroblastoma	2015
Avelumab (Bavencio)	PD-L1	Humanized IgG1	Merkel cell carcinoma	2016

Only antibodies with specific Fc isotype classes can bind Fc receptors on the effector components and mediate these immune mechanisms. Human antibody classes capable of mediating CDC are immunoglobulin M (IgM) and IgG, while ADCC and ADCP are only mediated by IgG antibodies (86).

Currently, there are six clinically approved antibodies which function as passive and specific antibody-mediated immunotherapies (Table 1) (87).

1.3.2 Active and non-specific antibody-mediated immunotherapy

Active and non-specific antibody-mediated immunotherapy functions through pathway signalling modulation and typically targets immune checkpoints (84). Known as immune checkpoint inhibitors (ICIs), these antibodies bind either the ligand or receptor and modulate the activity of a signalling pathway. There are three main targets for currently approved ICIs: programmed death protein-1 (PD-1), programmed death-ligand 1 (PD-L1), and cytotoxic T-lymphocyte-associated protein 4 (CTLA-4) (97,98).

The PD-1 molecule, also known as CD279, functions by promoting apoptosis in antigen-specific T-cells while also promoting the survival of Tregs (99–102). The objective of the PD-1 signalling axis is to suppress immune responses and prevent autoimmunity (103,104). The PD-1 molecule is expressed on all T-cells during activation, but also found other immune cells such as B-cells (105), NK cells (106) and DCs (107). Tumour microenvironments can promote the PD-1 signalling axis and inappropriately suppress an effective immune response against tumour cells, causing T-cell exhaustion (104). Blocking the PD-1 signalling axis has been successful in increasing T-cell activation leading to durable cures (43,108,109). The exact function of the PD-1 signalling on other cell types is unknown. However, some reports suggest that PD-1 may have a suppressive effect on these cells which can be abrogated by antibody blocking (106). Nivolumab and

Pembrolizumab are αPD-1 antibodies that were approved in 2014 to treat urothelial carcinoma and metastatic melanoma or non-small cell lung cancer and metastatic melanoma, respectively.

The PD-1 molecule binds to two ligands, PD-L1 (CD274) and PD-L2 (CD273). PD-L1 can be found in tissue cells, immune cells, and cancer cells, while the expression of PD-L2 is less understood (110–112) . Similar to αPD-1 therapy, PD-L1 blockade is used to stimulate the immune system and promote an anti-tumour response by reversing immune exhaustion. Expression of PD-L1 can be stimulated by interferons, as the promoter region contains an interferon response element, and by the NF-κB pathway (31,113). Currently, three antibody therapeutics are approved that target PD-L1: atezolizumab, avelumab, and durvalumab, which were approved in 2016, 2017 and 2017 respectively. Interestingly, avelumab, a human IgG1 antibody, was found capable of also mediating ADCC against numerous human tumour cell lines using PBMCs and NK cells as effector cells (91).

The CTLA-4 molecule (CD152) is another important immune checkpoint that is used as a target in immunotherapy. It is highly expressed on Tregs and is upregulated in T-cells after activation (114–116). If bound to CD80 or CD86 ligands, commonly found on antigen presenting cells, then CTLA-4 will prevent naïve T-cell priming (117,118). The exact mechanism of action for CTLA-4 is unknown but proposed to be sequestering of T-cell co-stimulatory ligands. Studies have suggested that blocking CTLA-4 signalling with an antibody decreases Treg populations, prevents the endocytosis of activating CD80 or CD86 ligands, and promotes naïve T-cell priming. As well, durable responses have been measured in both preclinical (118–121) and clinical studies using αCTLA-4 therapy, with ipilimumab, a human antibody targeting CTLA-4, getting approval by the U.S. Food and Drug Administration (FDA) as a therapy for melanoma patients in 2011.

1.4 Neuroblastoma

1.4.1 Characteristics of disease

Neuroblastoma (NB) is a cancer of the peripheral nervous system. It is the third most common pediatric cancer and the most common extracranial solid tumour in children (122,123). NB tumours originate from immature cells of neuroectodermal origin. Primary tumours can be found anywhere along the sympathetic nervous system from the neck to pelvis area, with the most common location in the adrenal gland (40% of all cases and 60% of metastatic cases) (122,123). Unfortunately, about 66% of NB cases are only found after the cancer has metastasized. Common sites of metastasis for NB are: bone and bone marrow, lymph nodes, liver, orbital, skin and brain (122,124).

NB has some characteristic mutations involving genes *MYCN*, *CASP8*, and *BCL2*. The gene *MYCN* (encoding N-Myc) is amplified in 25% of neuroblastoma cases and correlates with high-risk disease and poor survival. Expression of the gene *CASP8* (caspase-8) is commonly silenced by DNA methylation or gene deletion in NB patients. As well, overexpression of *BCL-2 (*Bcl-2) was present in NB patients with unfavorable histology. There was a strong correlation of NB cases with *MYCN* amplification to also have events of *CASP8* silencing (63% of examined *MYCN*-amplified samples) (125) and *BCL*-2 overexpression (77%) (126).

Cases of NB account for up to 6% of pediatric cancer patients and 15% of pediatric cancer patient deaths in the USA. Patients can be organized into three risk groups based on factors such as degree of cancer stage, amplification of *MYCN*, or age (124,127,128). Patients diagnosed with NB under the age of 18 months tend to undergo spontaneous remission, rendering screening of infants futile. Low and medium risk groups have favourable outcomes, while high risk groups have poor outlooks (129). Even after intense treatment plans, patients in high risk groups have a 40-66% five

year event free survival (122). The incidence rate of NB cases was highest in Caucasians, however African American and Native Americans suffered higher prevalence of high-risk disease and lower event-free survival.

High-risk NB patients undergo aggressive therapy. Depending on the available healthcare resources, treatment plans can include surgery, chemotherapy, radiation, stem cell transplant, retinoic acid, and αGD2 and cytokine immunotherapy (124,130). Therapy is often broken down into three phases: induction, consolidation, and maintenance. The goal of the maintenance phase is to prevent recurrence of the disease. This stage incorporates retinoic acid therapy in combination with αGD2 therapy and immune-activating cytokines IL-2 and GM-CSF (123,124,130).

Preclinical studies have investigated new therapeutics against NB cell lines, such as SMCs and immunotherapies.

1.4.2 IAPs and Smac mimetics in neuroblastoma

The IAP proteins, XIAP and survivin, were found to be overexpressed on NB biopsy samples (5). The study found higher *BIRC4* mRNA (encoding XIAP) expression in relapsed or *MYCN*-amplified tumours. There was increased XIAP protein levels, but not mRNA expression, in a comparison of NB cell lines (Kelly, SK-N-AS, NXS2 and C1300) and patient biopsies to mouse adrenal tissue (5). Another study also confirmed expression of cIAP1/2 and XIAP proteins in six human NB cell lines (Kelly, NB169lluc, SH-EP TET21N, SK-N-AS, SK-N-BE2-M17 and SK-N-SH) (6).

The chromosomal locations of notable IAPs are Xq25 for *BIRC4* and 11q22 for *BIRC2* (encoding cIAP1) and *BIRC3* (cIAP2). It was shown that 11q deletions are prevalent in cases of high-risk NB, with an occurrence of 20-45% (131). Although events of *MYCN* amplification and 11q

deletions are both prevalent in high-risk NB patients, these events very rarely occur simultaneously (one case reported in 165 cases evaluated) (131). However, one should not interpret the lack of *MYCN* amplification in NB cells as deletion of *BIRC2* and *BIRC3* genes. A study reported cIAP1/2 protein expression in *MYCN* non-amplified SK-N-AS and SK-N-SH cell lines (6).

Studies have investigated the efficacy of SMCs *in vitro* or *in vivo* against various NB cell lines. A preclinical screen of pediatric cancer cell lines showed minimal sensitivity *in vitro* of human NB cell lines (NB-1643, NB-EBc1, CHLA-90, CHLA-136) to the SMC, LCL161 (132). The study also tested the *in vivo* response of the cell lines to LCL161. They observed only two of the six tested xenograft tumour models (NB-1771 and NB-EBc1) respond to LCL161 with significant delays in tumour growth (132). Other investigations that examined treating NB cell lines using SMCs typically include a combination with an additional therapeutic. Studies report that SMCs synergize with chemotherapies in a drug class-dependent manner. They concluded that the class of vinca alkaloids was the most successful chemotherapy in combination with SMCs against human NB cell lines *in vitro* (5,6,133,134). Even resistance to the vinca alkaloid, vincristine, in relapsed neuroblastoma samples could be abrogated by LCL161 treatment (45). Typically, vinca alkaloids are used to prevent microtubule polymerization and impair cell division. However, a proposed mechanism of synergy with SMCs was the ability of vinca alkaloids to induce NF-κB activation (3,6). Additionally, studies found that the chemotherapy drug class of topoisomerase inhibitors synergized with SMC treatment to kill lung and colon adenocarcinoma models (135,136). They reported that engaging the RIP1 kinase through TNFα signalling led to formation of the necrosome complex which could enhance topoisomerase inhibitor-induced death of colon adenocarcinoma. Engagement of the RIP1 pathway via TNF-related apoptosis engaging ligand

(TRAIL) receptor-targeting antibodies was also found to synergize with SMC against NB cell lines (SH-EP, CHP-212, Lan-5, and SK-N-AS) and primary cultured cells (137).

1.4.3 Neuroblastoma and immunotherapy

Tumour microenvironments support the expression of immune checkpoints to suppress immune function. Studies have shown that NB tumour samples or cell lines express numerous immune checkpoints (PD-1 and CTLA-4) and their ligand molecules (PD-L1, CD80 and CD86) (138–142). PD-L1 expression in NB tumour samples has been contested in literature, with reports of 0% (143), 14% (144), and 72% (145) samples expressing the molecule. However, αPD-L1 or αCTLA-4 therapies were effective against NXS2 and N2a mouse models when used either in combination (141,146), with a tumour vaccine (140) , or with an αCD4 antibody (147). A recent study showed that αGD2 and IL2 therapy upregulates the expression of PD-L1 in the NB cell lines NXS2 and Lan-1 (109). They then showed that the combination of an αGD2 antibody with an αPD-1 antibody was successful in treating NXS2 tumours and increased mouse survival and cytotoxicity against NXS2 cells. A clinical trial is now being organized to translate using an αPD-1 and αGD2 therapeutic combination (148).

1.4.4 GD2 and αGD2 immunotherapy

The most recently approved therapy for NB is dinutuximab, a monoclonal antibody that targets a disialoganglioside molecule called GD2 (149,150). A GD2 molecule is composed of a glycosphingolipid with two sialic acid moieties (Figure 3). GD2 molecules are synthesized following the ‘b’ pathway of ganglioside biosynthesis (151). First, a ceramide molecule is converted to GM3 through the additions of glucose, galactose, and N-acetylneuraminic acid molecules. GM3 is then converted to GD3 with the addition of another N-acetylneuraminic acid by GD3 synthase.

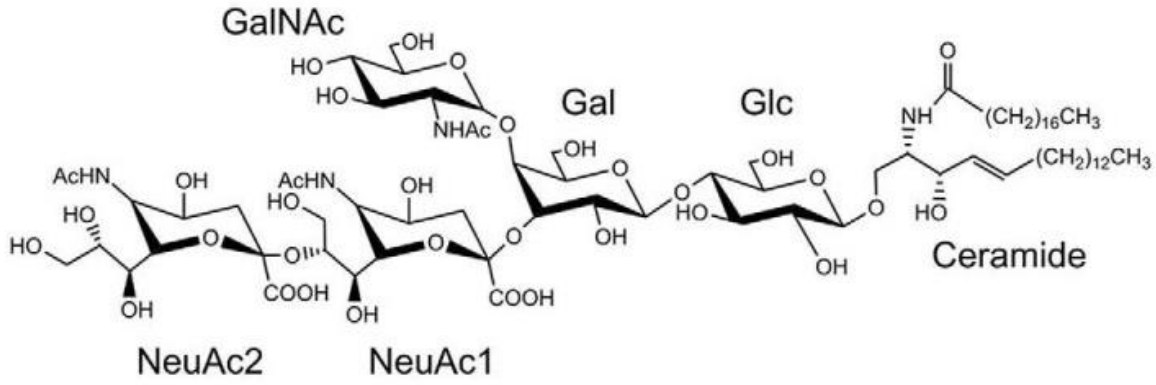

Figure 3. A molecule of the disialoganglioside GD2. Adapted from Horwacik et al. 2015 (152).

This step is thought to be the rate-limiting step of GD2 synthesis (153,154). GD3 is then converted to GD2 through the addition of a N-acetyl galactosamine molecule by GM2/GD2 synthase.

GD2 is ubiquitously and highly expressed on all human neuroblastoma samples evaluated so far. GD2 expression is also restricted on normal tissues, typically only found on the cerebellum and peripheral nerves (155–158). In addition to NB, GD2 expression has been detected on other cancers such as, but not limited to, osteosarcoma (159), glioblastoma (160,161), breast cancer (162,163), melanoma (164,165), and those of neuroectodermal origin (166,167). Interestingly, some studies suggest that GD2 is a cancer stem cell marker that promotes tumorigenesis in glioblastoma and breast cancer (162,168,169). These investigations found that GD2 expression correlated with other cancer stem cell markers, like CD133, and that expression of GD2 was more common on aggressive cancer subtypes (168). The inhibition of GD3S, a proposed rate limiting step to GD2 synthesis, had an anti-tumour effect and decreased metastasis in a MDA-MB-231 breast cancer tumour model (153,162). Similarly, high GD2 expression and high metastatic events are characteristic of NB cases. Furthermore, ‘b-type’ gangliosides, such as GD2, were seen to promote tumour angiogenesis in an oncogene-transformed mouse cell tumour model (170) However, GD2 expression was not found to be a prognostic marker for NB patients (171).

In 2015, dinutuximab was approved for therapeutic use to treat high-risk neuroblastoma patients (149,150). Dinutuximab is a chimeric antibody with mouse variable regions and a human IgG1 constant domain. Dinutuximab is also known as ch14.18. This antibody was chimerized from 14.G2a, an IgG2a class switch variant of the antibody 14.18 (94,172). The clone 14.G2a was designed to reduce human anti-mouse antibody (HAMA) syndrome responses seen when treating with the clone 14.18. Additional clones of αGD2 antibodies are currently being studied, such as

3F8 (173) and ME361-S2a (174). The clone ME361-S2a is produced by the mouse hybridoma HB-9326 and has a mouse IgG2a domain.

Dinutuximab mediates its anti-tumour effect of ADCC and CDC mechanisms with its Fc domain (149,175). Studies found that the effector cells mediating dinutuximab-ADCC to be neutrophils and NK cells. Thus, to improve the therapeutic efficacy, dinutuximab is given to patients in combination with immune-activating cytokines IL-2 and GM-CSF (176). GM-CSF activates neutrophils while IL-2 induces activation and proliferation of NK cells (177,178).

There has been a disputed additional mechanism of action for αGD2 therapy. Some studies have shown that αGD2 antibodies can mediate a direct cytotoxic function against $GD2^+$ cell lines from various cancers. A study proposed that this mechanism was dependent on isotype class, where the IgM class αGD2 antibody was non-cytotoxic (164) However, another study contested that the Fab fragments are capable of mediating cell death (174). Studies have reported that the αGD2 antibody-mediated cytotoxicity had characteristics of both apoptosis and necroptosis (164,179,180). The human melanoma cell line, HTB63, had increased levels of poly (ADP-ribose) polymerase (PARP) cleavage after 3F8 treatment *in vitro* (164). In support, cell death of IMR-32 cells occurred after treatment with the 14G2a antibody, which could be partially rescued by the pan-caspase inhibitor Z-VAD-FMK. Cells treated with the 14G2a antibody also had increased levels of caspase-3 cleavage (180). *In vitro* sensitivity to six chemotherapeutics (doxorubicin, etoposide, SN-38, paclitaxel, vinorelbine, and cixplatin) was enhanced by αGD2 antibody treatment in D18 cells transfected to express GD2 (181). However, it was proposed that αGD2 antibody cytotoxicity was mediated through anoikis, a detachment-induced cell death mechanism (179,182). Early work demonstrated that GD2 is important in cell adhesion (183). Furthermore, some studies used very high antibody concentrations (>20 μg/mL) of αGD2 antibody to achieve cell death. However,

antibody-mediated cytotoxicity in suspension lymphoma cell lines using typical antibody concentrations (<10 μg/mL) was also shown (179). Thus, more investigation is required to fully understand αGD2-mediated cell death.

1.4.5 Neuroblastoma and angiogenesis

Targeting tumour vascularization is another approach that is being investigated for treating NB patients. NB is a tumour that is highly vascularized, which is represented in the mouse models as well (184–186). Despite having no effect on cell proliferation *in vitro* and no change in vascular endothelial growth factor (VEGF) production, B-type gangliosides, which are overexpressed in NB, promote tumour vascularization in transformed cell tumour models (170). Furthermore, it was shown that the *MYCN* oncogene could down-regulate inhibitors of angiogenesis, such as activin A, and promote tumour vascularization in human NB cells (187,188). VEGF is a well-studied pro-angiogenic protein in tumours. Numerous studies have reported VEGF expression in NB, but there is contention of it being a prognostic marker for favorable or poor survival outcomes (189–191). However, NB tumour xenograft growth was inhibited when VEGF signalling was blocked with an antibody (192). Success has also been reported in using an anti-angiogenic small molecule inhibitor, sunitinib, to treat preclinical models of NB tumours. Sunitinib is an inhibitor of receptor tyrosine kinases, such as VEGF receptor and platelet-derived growth factor (PDGF) receptors, that are important in tumour angiogenesis, (193,194). Preclinical studies have reported that sunitinib can inhibit NB tumour growth and metastasis by targeting tumour vascularization and causing degradation of N-Myc protein (195–197). Currently, anti-vascular therapies (such as the αVEGF antibody bevacizumab or the anti-angiogenic chemotherapy lenalidomide (198)) are in clinical trials to determine whether therapies targeting tumour angiogenesis are efficacious in treating NB

patients. These studies support that targeting tumour angiogenesis is a viable option to be investigated for treating NB tumours.

1.5 Rationale and hypothesis

1.5.1 Hypothesis

I sought to improve the efficacy of αGD2 immunotherapy against NB. The approved αGD2 therapy, dinutuximab, increases survival by 20% for high-risk NB patients, yet five-year event free survival still sits around 40-66% (176). Furthermore, studies have shown that NB tumour microenvironments are suppressive to αGD2 treatment, which could be overcome with a combination immunotherapy approach with ICIs (109). IAP proteins, which are a resistant factor to cell death and ADCC (64), are expressed in NB samples and cell lines (5,6). As well, there is support for combining αGD2 therapy and anti-vascular therapy, evidenced by a clinical trial investigating dinutuximab and lenalidomide.

Antagonizing the IAPs with SMCs is a treatment approach that has shown synergy with immunotherapies such as ICIs in treating preclinical cancer models (43). SMCs can improve NK cytotoxicity (61,62), a main effector cell for αGD2 therapy, and antagonize the ADCC-resistant factor XIAP. Also, reports have shown that SMCs can sensitize tumour endothelium to TNFα-induced apoptosis and induce vascular shutdown in the tumour microenvironment (54,55).

I hypothesize that LCL161 will synergize with αGD2 immunotherapy against NB, and that this combination could be further potentiated by combining with a third therapeutic agent, such as a PD-1 axis-targeting ICI.

1.5.2 Objectives

To test my hypothesis, I have investigated the following objectives:

1. *Determine whether LCL161 monotherapy is effective in treating NXS2 and N2a cells*

   To test whether the SMC monotherapy is effective against NB, I treated the murine NB cell lines, NXS2 and N2a, with LCL161 and various cytokines and cytotoxic agents *in vitro.* I established *in vivo* models to test if NB tumour models are sensitive to LCL161 monotherapy. I also explored the combinations of LCL161 and anti-vascular drugs to potentiate anti-angiogenic effect.

2. *Evaluate if LCL161 and αGD2 antibody synergize to treat NXS2 cells*

   After testing LCL161 as a monotherapy, I evaluated if the SMC and an αGD2 antibody would synergize *in vivo* against the $GD2^+$ cell line, NXS2. I also acquired the antibody through gravity isolation from hybridoma supernatant. I then validated that the antibody was pure, specific, and functional before proceeding with *in vivo* experimentation.

3. *Potentiate the LCL161 and αGD2 combination with an immunotherapy that targets the PD-1 signalling axis*

   Following completion of the LCL161 and αGD2 combination survival study, I then investigated if the addition of an ICI would further potentiate the therapeutic efficacy. The ICI used was determined with a series of survival study screens.

These studies can be used to further examine the combination of LCL161 and αGD2 treatment in NB. With optimization, there is potential for a LCL161 and αGD2 antibody therapy combination to improve survival in high-risk NB patients.

2.0 MATERIALS AND METHODS

1.6 Reagents

The SMC, LCL161, was kindly provided by Novartis (Basel, Switzerland).

1.7 Antibodies & Stains

Table 2. Western Blot Antibodies

Target	Clone	Source	Species
cIAP1/2	RIAP1	(4)	Rabbit
XIAP	RIAP3	(4)	Rabbit
PARP	9542	Cell Signalling Technology	Rabbit
TNFR1	ADI-CSA-815	Enzo Life Sciences	Rabbit
TRADD	3694	New England Bio	Rabbit
Caspase 8	IG12	Enzo Life Sciences	Rat
cFlip	D5J1E	Cell Signalling Technology	Rabbit

Table 3. Immunohistochemistry antibodies and stains

Target	Fluorophore	Clone	Company	Species
GD2	N/A	14G2a	Biolegend	Mouse
Hoescht stain	DAPI			N/A
Anti-mouse	Alexa Fluor 488		Abcam	

Table 4. Flow cytometry antibodies and stains

Target	Fluorophore	Clone

MHC 1 (H-2Kd/H-2Dd)	Alexa Fluor 647	34-1-2S
PD-L1 (CD274)	PE-Cy7	19F.962
CD45	PerCP-Cy5.5	30-F11
CD3	APC/Cy7	17A2
CD49b	DX5	PE
Zombie Violet	Brilliant Violet 421	
GFP	Alexa Fluor 488	FM264G
GD2	PE	14G2a

All flow antibodies are of mouse species and were purchased from Biolegend (San Diego, California, USA).

1.8 Cell culture

1.8.1 Cancer cell lines

Cancer cell lines were grown at 37°C and 5% CO_2 in Dulbecco's Modified Eagle Medium (DMEM) or Roswell Park Memorial Institute (RPMI)-1640 media supplemented with 10% heat-inactivated fetal calf serum (FCS), 1% penicillin streptomycin, 1% glutamine and 1% nonessential amino acids (Invitrogen Life Technologies, Burlington, ON, Canada). Mouse mammary carcinoma (EMT6) cells and αGD2 antibody-producing hybridoma (ME361-S2a/HB-9326) were obtained from ATCC (Manassas, Virginia, USA) Murine neuroblastoma cell lines, NXS2 and Neuro2a (N2a) were provided by Dr. Paul Sondel (University of Wisconsin-Madison, Madison, Wisconsin, USA) and ATCC, respectively. The murine lymphoma cell line Yac-1 was kindly provided by Dr. Seung-Hwan Lee, while RMA and RMA-S cell lines were kindly provided by Dr. Michele Ardolino (University of Ottawa, Ottawa, ON, Canada).

1.8.2 NK isolation and LAK growth protocol

Spleens were recovered from A/J, C57BL/6J, or FVB/N mice that were >8 weeks old (Charles River, Wilmington, Massachusetts, USA) homogenized, and passed through a 200 μm mesh (Elko Filtering, Miami Gardens, Florida). Erythrocyte lysis was performed on the cell suspension with a 1 min incubation in 1 mL of ammonium-chloride-potassium lysis buffer (0.15 M NH4Cl, 10 mM KHCO3, 0.1 mM Na2EDTA, pH 7.2-7.4). NK cell enrichment of splenocyte population was then performed by immunomagnetic selection using either the EasySep™ Mouse CD49b Positive Selection Kit or the EasySep™ Mouse NK Cell Isolation Kit (Stemcell, Vancouver, BC, Canada). NK-rich splenocyte populations were then cultured in RPMI-1640 media supplemented with 10% FCS, 10 μM beta-mercaptoethanol, 1 % penicillin streptomycin, 1% Non-essential amino acids (Invitrogen), 20 mM 4-(2-hydroxyethyl)-1-piperazineethanesulfonic acid (HEPES), and 1000 U/mL recombinant human interleukin 2 (rh-IL2, Peprotech, Rocky Hill, New Jersey, USA) and maintained at 37°C and 5% CO_2. Cells were plated with a starting density of 0.5 x 10^6 to 1 x 10^6 cells/mL, with passaging performed on days 4, 6, and 7. Flow cytometry was used to confirm cell populations of >75% NK cells after 7 days with >95% viability.

1.9 αGD2 antibody isolation from ME361-S2a hybridoma

1.9.1 Supernatant collection

ME361-S2a hybridoma was cultured following ATCC guidelines. First, the cells were seeded at a density of approximately 2 x 10^5 cells/mL. Fresh media was added to double the culture volume every second day until the final volume exceeded 2 L. Once the desired volume was achieved, the culture was further incubated for up to two weeks or until four days after the media turned yellow to maximize antibody yield. The media was then collected and spun at 1000 xg for

30 min to pellet cells. The supernatant was passed through a 0.2 μm vacuum filter cup to remove cell debris.

1.9.2 Antibody isolation

Days prior to isolation, a gravity column was assembled using 500 mL media bottles and 50 mL Falcon tubes. A 10 mL centrifuge column (Thermofisher, Waltham, Massachusetts, USA) was packed with 10 mL of Protein G agarose beads (Exalpha, Shirley, Massachusetts, USA) and fastened at the bottom of the column. Filtered media supernatant was then diluted 1:1 with borate buffer (50mM sodium borate, 290mM boric acid, pH 8) and separated into 2 L fractions corresponding to the column volume capacity. Prior to isolation, the beads were washed with 100 mL of borate buffer. The diluted media was then added to the column, passed through the beads, and collected to be re-passed. The column was washed with 50 mL of borate buffer before 12 mL of elution buffer (46mM citric acid, 4mM sodium citrate, pH 2.6) was added and collected into a Falcon tube containing 3 mL of neutralization buffer (2M Tris, pH 9.5). The beads were once again washed with 50 mL borate buffer before another round of antibody isolation. This process was repeated four times for each 2 L fraction of diluted media collected.

Eluted antibody solution was then concentrated using Amicon Ultra-15 Centrifugal Filter columns with a 100 kDa molecular weight cut-off (MilliporeSigma, Burlington, Massachusetts, USA). After all antibody solution was passed through the columns, an additional spin with PBS was performed to desalt the isolated antibody. Antibody was then resuspended in sterile PBS, and quantified with a nanodrop reader. Antibody was then diluted to a concentration of 1.5-2 mg/mL in PBS, aliquoted and then froze at -20 ^{o}C. Antibody purity was analyzed via a SDS-PAGE, and functionality was tested with immunofluorescence and a LDH-based ADCC cytotoxicity assay.

1.10 Immunofluorescence

1.10.1 Fixed-cell immunofluorescence

Cells were plated 24-48 h prior in a Falcon Black/Clear 384 well microplate (BD Bioscience, San Jose, California, USA) at a density of 6 x 10^3 cells/well. They were fixed with 4% paraformaldehyde for 20 min. After washing with PBS, the cells were then permeabilized with 0.2% Triton X-100 for 5 min. Cells were again washed before incubating with primary antibody at a concentration of 5 μg/mL for 1 hr. Cells were then washed with PBS then incubated with the secondary antibody at a concentration of 5 μg/mL for 1-2 h. DAPI was added in the last 5 min of incubation to a final concentration of 1 ug/mL. After a final washing, 100 μL of PBS was added to each well and plate was sealed to prevent evaporation before reading. Plate was analyzed by the Opera QEHS high throughput instrument (PerkinElmer, Waltham, Massachusetts, USA) kindly operated by Dr. Stephen Baird (CHEO Research Institute, Ottawa, Ontario, Canada). Data was then uploaded to Columbus for image hosting (www.columbus.med.uottawa.ca).

1.10.2 Live-cell immunofluorescence

Live cell immunofluorescence was also performed where the setup was identical to fixed-cell immunofluorescence, but the staining procedure differed. The media was removed from the plate, and the primary antibody, diluted in cell media with 2% FCS, was then added. The cells were incubated on ice for 30 min. Next, the primary was removed, the secondary antibody, diluted in media with 2% FCS, was then added and cells were incubated on ice for 30 min. Cell nuclei were stained using 1μg/mL Hoescht 33342 (Thermo Fisher). Plate analysis then followed the fixed-cell immunofluorescence procedure.

1.11 Protein analysis

1.11.1 Protein acquisition

Cells were grown in 6-well plates. After overnight or 24 h of treatment, cells were scraped over ice in PBS and collected before cell lysis in radioimmunoprecipitation assay (RIPA) buffer containing protease inhibitor cocktail (Roche, Mississauga, Ontario, Canada). Protein samples were then quantified using a Bradford protein assay (Biorad, Hercules, California, USA). Samples were frozen at -80^{o}C.

1.11.2 SDS-PAGE

Protein samples were loaded at equivalent concentrations into a 10% polyacrylamide gel. The gels were run at 120V for ~1 h. Gels could then be used for Western blotting or Coomassie staining. For Coomassie staining, gels were incubated in 0.25% Coomassie Blue solution (50% methanol, 10% acetic acid, 40% water) for 2-4 h until blue. Gels were then exposed to destaining solution (5% methanol, 7.5% acetic acid, 87.5% water) for 4-24 h until background was clear. Gels were then scanned.

1.11.3 Western blotting

Gels were transferred to nitrocellulose membranes and blocked in Odyssey blocking buffer (Licor, Lincoln, Nebraska, USA). Membranes were then blotted with primary antibody overnight before being washed and blotted with secondary antibody for 2 h. Membranes were then scanned using an Odyssey infrared imaging system and ImageStudio program ver4.0 (Licor).

1.12 Cell viability assays

1.12.1 AlamarBlue viability assay

Cells were typically plated 24 h prior to treatment in a 96 well plate at densities ranging form 1-2 x 10^4 cells/well. Cells were then treated with: LCL161 (Novartis), TNFα (R&D Systems, Minneapolis, Minnesota, USA), IFNγ (Peprotech), IFNβ (PBL Assay Science, Piscataway, New Jersey, USA), TRAIL (R&D), Bcl-2 inhibitors ABT-199 and ABT-263 (sampled from SelleckChem, Houston, Texas, USA), caspase inhibitor Z-VAD-FMK and necroptosis inhibitor Necrostatin-1 (MilliporeSigma), or DMSO as vehicle control. A 7X alamarBlue solution was prepared by creating a 0.1% resazurin sodium salt solution in PBS (MilliporeSigma). After 24-48 h incubation, alamarBlue was added to a 1X concentration on to wells. Cells were further incubated for 2-6 h until average reading was 10x that of background well. Fluorescence of plates were read using a Synergy HTX plate reader using Gen5 software (Biotek, Winooski, Vermont, USA). Calculations for % viability were performed as follows:

$$\%\ viability = \frac{experimental\ signal - background}{control\ signal - background} * 100\%$$

% viability is calculated by normalizing experimental signal to the signal of the control condition, after correcting for background readings.

1.12.2 Cytotoxicity assay using LDH release kit

Cell cytotoxicity assays were completed using a lactate dehydrogenase (LDH) release kit (Takara Bio, Kusatsu, Shiga Prefecture, Japan) to measure LDH released from dead cells, following the suggested protocol. Typically, LAKs were grown for 7-8 days prior to experiment.

Target cells plated day of or day prior to assay at 1 x 10^4 cells/well in a 96-well flat bottom or v-bottom plate. Conditions were typically plated as quadruplicates and include:

- Spontaneous target cell release of LDH
- Spontaneous effector cells release of LDH at each ratio
- Maximum target cell release of LDH
- Effector cells at different ratios to target cells
- Media wells to measure baseline LDH in media.

Day of assay, LAKs were washed and counted, their viability confirmed to be >90%, then added at the denoted ratios. In each well, media had a final serum concentration of 2.5% to minimize signal saturation from background LDH. Plate was spun down at 300 xg for 1 min, then incubated for 4-6 h in the incubator. 15-30 min prior to end of incubation, Triton X-100 was added at a final concentration of 2% to lyse all cells in control wells for maximum LDH release from target cells. At the end of incubation, the plate was spun at 300 xg for 5 min to collect cell and debris, then 50 µL supernatant from each well was transferred to a new plate and 75 µL of reaction mixture was added to each well. The plate was incubated for 30 min in the dark at room temperature. The plate was then read at 490 nm (reaction signal) and 620 nm (accounts for signal interference by debris). Calculations for % cytotoxicity were performed in two steps as follows:

$$Well\ Signal = (490nm\ reading - 620nm\ reading) - Blank\ media\ signal$$

Here, interference from cell and cell debris is accounted for in every well, and corrected for baseline LDH readings in the media.

$$\%\ cytotoxicity = \frac{Expeirmental\ signal - (Target\ Spontaneous\ signal + Effector\ Spontaneous\ signal)}{Target\ Maximum\ signal - Target\ Spontnaeous\ signal} * 100\%$$

Next, % cytotoxicity is calculated by subtracting the spontaneous LDH releases of each cell compartment then normalizing to the corrected maximum target LDH release.

1.13 In vivo models

1.13.1 Establishing in vivo models

All animal studies were performed following protocols approved by the Animal Care and Veterinary Service (ACVS, University of Ottawa). Three syngeneic models were established for two cell lines, NXS2 and N2a, in A/J strain of female mice that are 4-5 weeks old (Charles River). Cell lines were tagged with firefly luciferase (Fluc) for visualization via IVIS. For *in vivo* preparation, cells were prepared by typical lifting with trypsin. Cells were then washed once with PBS, counted, and resuspended in DPBS at the desired concentration. Subcutaneous (S.c.) models were established by injection of 100 μL of cells into the right flank of the mouse. A metastatic model was established by intravenous (I.v.) injection of 100 μL via the tail vein. An orthotopic model was established by injection into the adrenal gland, following the protocol published by Khanna et al. (2002), described as follows. Buprenorphine is administered four to six hours before surgery and the following morning. Mice are put under anesthesia with 2% isofluorane for the duration of procedure. Surgical site is prepared by shaving and disinfecting using chlorohexidine and 70% sterile alcohol. A 1 cm incision was made left side high paracostal to the abdomen to allow visualization of the caudal border of the spleen and the cranial tip of the left kidney. The spleen was displaced cranially allowing exposure of the left adrenal gland. A 27-gauge needle was then used to inject 10 μL of cells into the adrenal gland. Stitches and staples were used to close the wound, with staples being removed approximately one week later. Topical bupivacaine was applied to the incision site at closure and again four to six hours later.

Treatments commenced once tumours were palpable for the s.c. model (>100 mm^3) or one week after tumour implantation for the orthotopic model. LCL161 was given by oral gavage (p.o.) at a concentration of 50-75 mg/kg. The αPD-1 clone J43 and RMP1-14, αPD-L1 clone 10F.9G2, αCTLA-4 clone 9H10, and αGD2 clone ME361-S2a antibodies or there isotypes were given by interperitoneal injection (i.p.) at 200-250 μg. Except for the αGD2 antibody which was isolated from the hybridoma, antibodies were purchased from Bio X Cell (Lebanon, New Hampshire, USA) or Leinco Technologies (Fenton, Missouri, USA). Sunitinib (SelleckChem). was given i.p. at a concentration of 35 mg/kg.

In-vivo imaging was used to monitor tumour growth, performed by Spectrum In vivo Imaging System (IVIS (PerkinElmer, Waltham, Massachusetts, USA)) at the Pre-Clinical Imaging Core (University of Ottawa) following a 10 min incubation after s.c. injection of 50 - 200 μl luciferin.

1.13.2 Survival studies

Survival studies were performed with endpoints determined alongside ACVS guidelines. S.c. tumours were measured every 2-3 days by calipers. Mice bearing s.c. tumours were deemed at endpoint if tumour volumes exceeded 2000 mm^3 using the following equation:

$$Volume = \frac{\pi}{4}(width^2 * length)$$

or if they displayed characteristics of moribund or their tumours developed lesions. Endpoints for the i.v. and orthotopic models were displays of moribund characteristics, lesions, and/or internal bleeding. Upon endpoint, animals were euthanized by anaesthesia and cervical dislocation.

1.13.3 Tumour vasculature

A necropsy evaluation was performed for most survival studies when the mice reached endpoint. A blind observer would evaluate the degree of angiogenesis present in the tumour, assessed by visible vasculature, overall blood content, and if the tumour was pressurized. This data was collected to estimate the therapeutic anti-vascular effect from each treatment group.

To further examine the anti-vascular effect, ultrasound imaging was performed to evaluate rate of blood flow in the tumour compared to regular tissue. A Vevo 2100 Ultra High Frequency ultrasound (VisualSonics, Toronto, Ontario, Canada) at the Pre-Clinical Imaging Core (University of Ottawa) was used to visualize the rate of non-targeted microbubble (VisualSonics) flow entry into the tumour using nonlinear contrast imaging.

1.14 Flow cytometry

1.14.1 Flow cytometry preparation

Cells were first collected and washed with phosphate buffered saline (PBS). If required, a Zombie viability stain was then added to cells at a 1/200 – 1/400 dilution and incubated for 20 min at room temperature in the dark, as per the manufacturer protocol. Cells were then washed and resuspended in PBS + 1% bovine serum albumin (BSA). If target cells contained an Fc region, Fc block was added at a 1/100 dilution and incubated for 7 min in the dark. Immediately following Fc block, the surface marker-targeting antibodies were added, typically at a 1/100 dilution, and incubated for up to 30 min at 4^{o}C. Cells were then washed and resuspended in PBS + 1% BSA. If internal staining was desired, cells were fixed and permeabilized by following the FOXP3 Fix/Perm Buffer kit (Biolegend). After permeabilization, the cells were then washed and resuspended in the appropriate buffer containing antibody targeting the internal markers. Cells were again incubated at 4^{o}C in the dark for up to 30 min before being washed and resuspended in

PBS + 1% BSA, now prepared for analysis. A Fortessa flow cytometer was used to run the samples, with data acquired by the BD FACSDiva software (BD, San Jose, CA, USA). Data was then analyzed using the FlowJo software (Tree Star, Ashland, OR, USA).

1.15 Statistical analysis

Statistical analysis for alamarBlue results was performed using a non-parametric Kruskal-Wallis test. If deemed significant, then multiple comparisons were performed using a Dunn's test (Graphpad). Kaplan-Meier survival curves were analyzed using a logrank test. If deemed significant, group-to-group comparison with a Holm-Sidak analysis was performed (Sigmaplot).

2.0 RESULTS

2.1 Testing murine NB cell lines *in vitro* sensitivity to LCL161

SMCs have been developed to treat cancers that have a mutated apoptotic pathway. SMCs function by antagonizing proteins from the IAP family to promote apoptosis and activate non-canonical NF-κB signalling (1,60,199). These traits have allowed SMCs to reach several clinical trials (200). SMCs often moderate their effects through TNFα and TRAIL signalling, molecules which bind death receptors leading to promotion of a death signalling pathway (1,137). SMCs have also been found to synergize with compounds or molecules which promote cell death. Studies have shown SMCs synergizing with both type 1 and type 2 interferons to kill cancer cell lines (41,201,202). Another class of small molecule inhibitors which promote apoptosis, Bcl-2 inhibitors, was shown to synergize with SMCs even in SMC-resistant hepatocellular carcinoma cell lines (37). Furthermore, SMCs have been found to sensitize NB cancer cells to chemotherapeutic agents (5) and IAP expression has been correlated to chemotherapy resistance (203).

SMCs have found limited success against NB cell lines. Most efficacy is seen when high concentrations of LCL161 (>10 μM) were combined with chemotherapeutics to kill human NB cell lines (134,204). In accordance with these results, NB cell lines have been found to silence expression of proteins in the apoptosis pathway (205). An example is caspase 8, which is a common site for promotor methylation in NB (206). However, there are means to prevent apoptosis other than silencing expression of required proteins. The protein cellular FADD-like IL-1β-converting enzyme inhibitor protein (cFlip), a caspase 8 homolog which inhibits caspase activation by preventing death-inducing signalling complex (DISC) formation, is commonly upregulated in cancer cells. Studies have shown that silencing of cFlip can sensitize cancer cells, such as the NB cell lines GI-ME-N and SK-N-AS, to SMC treatment (205).

I will determine if the NB cell lines, NXS2 and N2a, are susceptible *in vitro* to a SMC, LCL161, with or without various combinations of drugs or cytotoxic cytokines. Afterwards, I will confirm the expression of proteins involved in apoptosis signalling.

2.1.1 Murine NB cell lines are resistant to LCL161 and TNFα

Both murine NB cell lines, NXS2 and N2a, were tested for their sensitivity to LCL161 with or without TNFα. EMT6, a murine mammary carcinoma cell line which is sensitive to LCL161 and TNFα, was used as a positive control. An alamarBlue assay was used to determine cell viability after a 24 h incubation. Using the viability assay, I observed that only the EMT6 line is sensitive to LCL161 and TNFα *in vitro*. Both NXS2 and N2a cell lines had a maximum of 15% ($p<0.001$) and 20% ($p<0.0001$) cell death, respectively, when treated with 5μM LCL161 and 10ng/mL TNFα (Figure 4), while 80% ($p<0.0001$) cell death was seen with EMT6.

2.1.2 Murine NB cell lines are resistant to LCL161 with other cytotoxic compounds

Due to the limited response of the murine NB cell lines to LCL161, I tried treating the cell lines with other compounds in combination to render the cell lines sensitive to SMCs. The compounds I tested with LCL161 were: IFNγ and IFNβ, TRAIL, chemotherapy compounds SN-38, topotecan and irinotecan, and Bcl-2 inhibitors ABT-199 and ABT-263. Again, an alamarBlue assay was used to determine cell viability 24 h after treatment. Both combinations of LCL161 and IFNβ or TRAIL killed 14-17% of either NXS2 (not significant (n.s.) and $p<0.01$) and N2a cells (n.s. and n.s.) (Figure 5A). This is a similar rate of cell death to that of LCL161 and TNFα combination. Overall, the cytotoxic compounds I tested were not very effective at killing either NXS2 or N2a cell lines, but LCL61 could sensitize both cells significantly to IFNβ-induced cell death ($p<0.001$). I did not observe killing of NXS2 or N2a cells by the Bcl-2 inhibitors ABT-199 and ABT-263. I only observed cell death responses of NXS2 and N2a to Bcl-2 inhibition at a high and clinically

irrelevant concentration of 20μM (Figure 5B) (207). At 20μM, ABT-199 killed 85% of NXS2 cells but only 15% of N2a cells, and no synergy was seen when combined with LCL161. The viability assay shows ABT-263 was effective against both cell lines at a concentration of 20μM. Oddly, when treated with a combination of ABT-263 and LCL161, NXS2 responded synergistically (97% cell death, $p<0.05$) while N2a responded antagonistically (67% cell death, $p<0.05$). I also examined using common chemotherapeutic compounds that inhibit topoisomerases with LCL161, and even at high concentrations little efficacy was seen in killing the NB cell lines (Figure 5B). Topotecan was more effective against NXS2 cells (48% cell death) than N2a cells but had decreased toxicity with LCL161 (20%). NXS2 had moderate sensitivity to irinotecan (25%), and no synergy with LCL161 was seen. The SN-38 compound was the most effective chemotherapy against both cell lines (NXS2 48%, N2a 15%), but reacted antagonistically in combination with LCL161 (37%, 8% respectively).

Due to the limited response of NXS2 and N2a cell lines to LCL161 treatment with cytotoxic compounds, I questioned whether the apoptosis signalling pathway was intact. NB cell lines have been reported to downregulate expression of necessary apoptotic proteins, such as TNFR type 1 associated death domain (TRADD), caspase-8, or TNFR1 (205) . I confirmed expression of relevant apoptosis proteins with a Western blot. Protein samples were collected from cells incubated for overnight or 24 h with LCL161, TNFα, or staurosporine. EMT6, the LCL161-sensitive cancer cell line, was used as a control. First, I confirmed expression of the IAP proteins, cIAP1/2 and XIAP, in the murine NB cell lines (Figure 6). Oddly, XIAP was detected at a smaller weight in the EMT6 cell line. TRADD, TNFR1, and caspase-8, proteins which are commonly silenced in NB cell lines, were found to be expressed in both NB cell lines (Figure 6). Expression of the caspase-8 inhibitor, cFlip, was also detected in NXS2, N2a, and EMT6 cell lines.

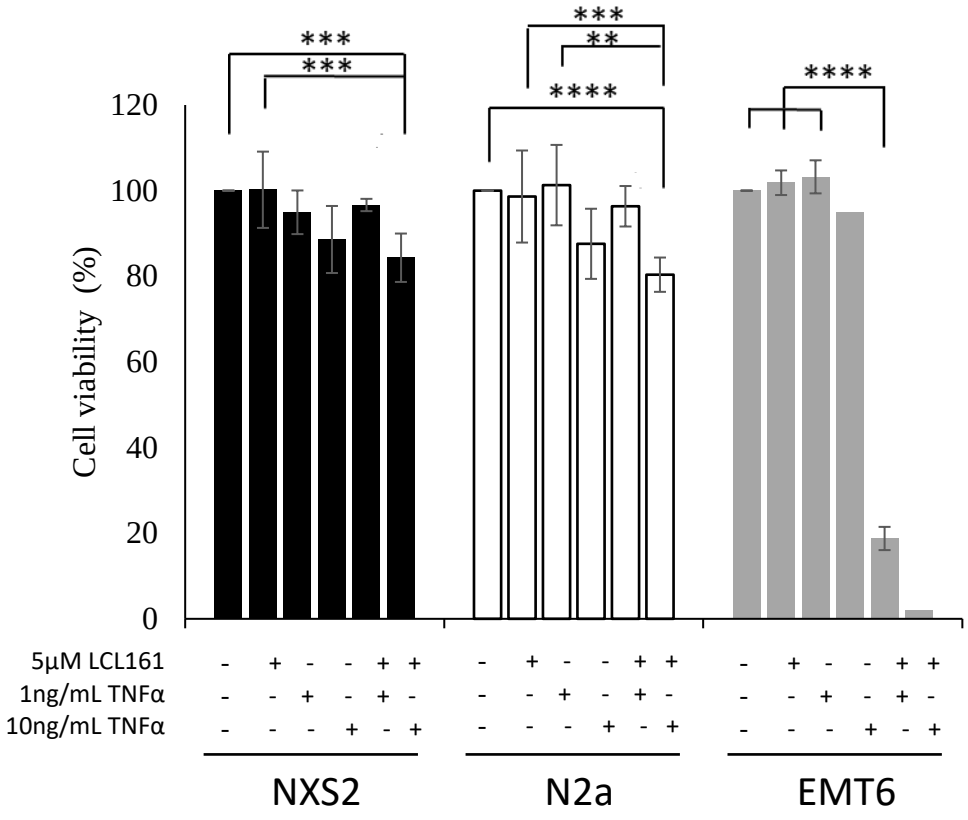
***
***
***
**
****
****
120
100
80
60
40
20
0
Cell viability (%)
5μM LCL161
1ng/mL TNFα
10ng/mL TNFα
NXS2
N2a
EMT6

Figure 4. Murine NB cell lines are not sensitive to LCL161 and TNFa. Cells were treated for 24 h with 5μM LCL161 and 1-10ng/mL TNFα for 24 h. Viability measured with an alamarBlue assay. DMSO was used as a vehicle control. Only $p<0.01$ is shown; ** = $p<0.01$; *** = $p<0.001$; **** = $p<0.0001$ (n=2-3; Mean±SD). Cell death is only seen in the EMT6 cell line with LCL161 and TNFα combination.

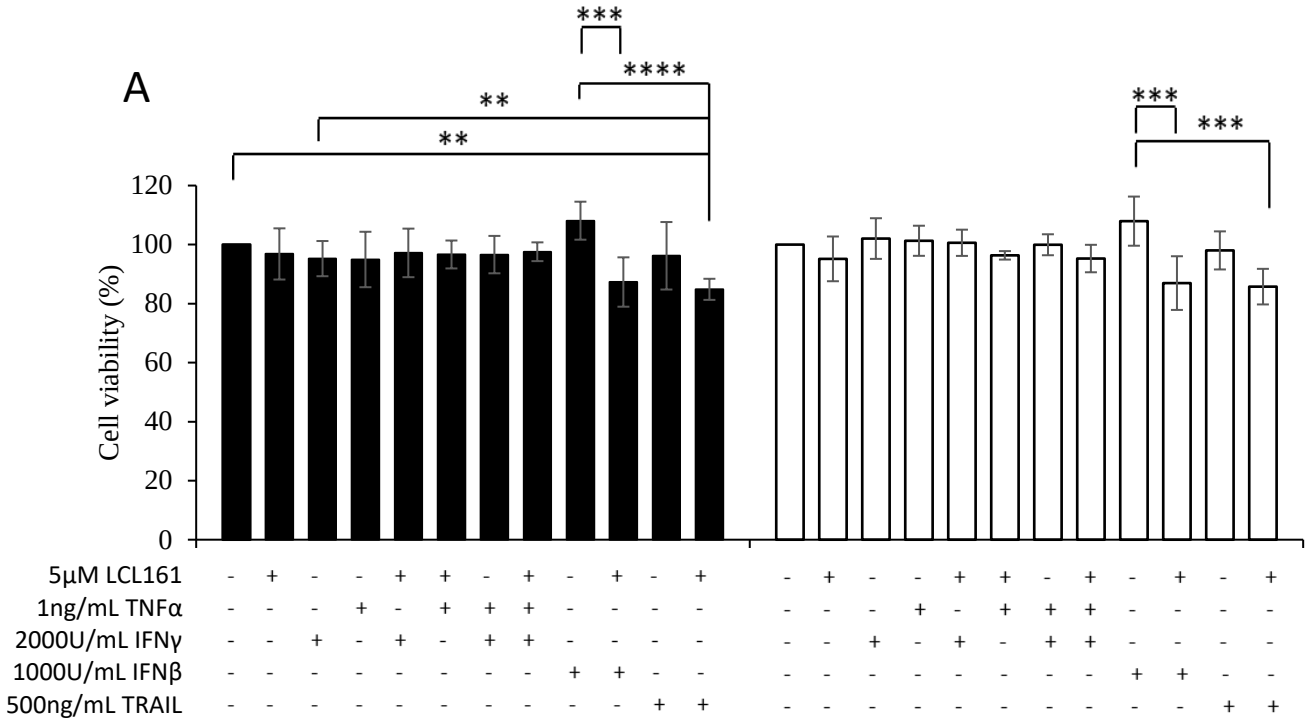
A
***
****
**
**
***
***
Cell viability (%)
120
100
80
60
40
20
0
5μM LCL161
1ng/mL TNFα
2000U/mL IFNγ
1000U/mL IFNβ
500ng/mL TRAIL

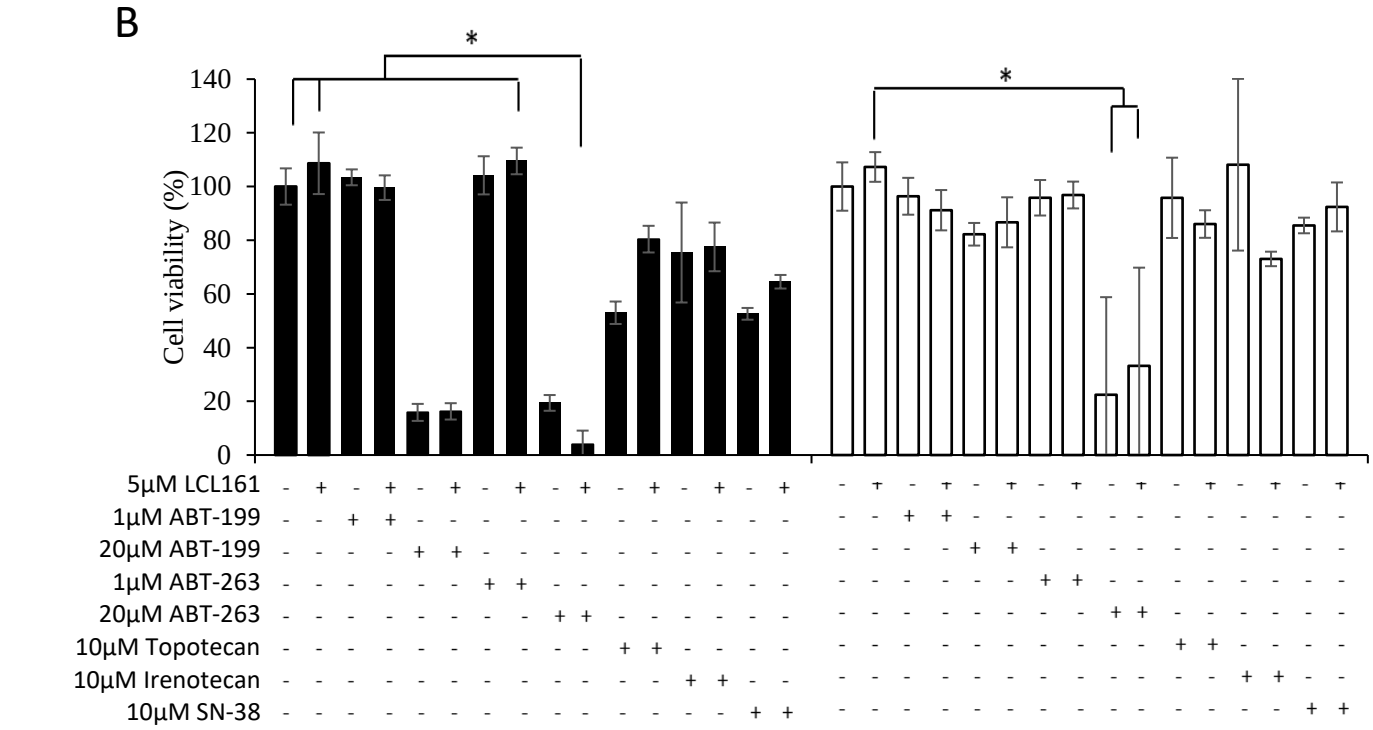
B
*
*
Cell viability (%)
140
120
100
80
60
40
20
0
5μM LCL161
1μM ABT-199
20μM ABT-199
1μM ABT-263
20μM ABT-263
10μM Topotecan
10μM Irenotecan
10μM SN-38

Figure 5. Cytotoxic cytokines and compounds do not sensitize murine NB cell lines to LCL161. Viability measured by alamarBlue assay. DMSO was used as a vehicle control. A) Plated NB cells were treated for 24 h with cytokines at denoted concentrations with or without LCL161. Only $p<0.01$ is shown; ** = $p<0.01$; *** = $p<0.001$; **** = $p<0.0001$ (n=2-3; Mean±SD). B) Plated NB cells were treated for 24 h with cytotoxic compounds at denoted concentrations with or without LCL161. * = $p<0.05$. (n=1-2; Mean±SD).

In response to LCL161 treatment, cells typically degrade cIAP1/2 and, if cell death is induced, reduce expression of XIAP. In response to LCL161, NXS2 and EMT6 were seen to reduce cIAP1/2 levels while N2a did not. Interestingly, cIAP1/2 downregulation did not lead to apoptotic cell death in NXS2. A decrease in XIAP expression was only found in the EMT6 cell line after treatment with LCL161 and TNFα, which coincides with the alamarBlue results showing cell death. Loss of full length caspase-8 was also seen in this EMT6 condition.

Since the NXS2 and N2a cell lines were resistant to various cytotoxic compounds yet expressed proteins that are often silenced in NB, I questioned whether these cells could undergo apoptotic cell death. Staurosporine, a protein kinase inhibitor, was used as a positive control (208) to induce apoptosis. PARP cleavage, a hallmark of apoptosis (209), was used to detect apoptotic cell death. PARP cleavage was present in NXS2 and N2a samples treated with staurosporine but not LCL161 (Figure 7).

2.2 Testing murine NB cell lines *in vivo* sensitivity to LCL161

Next, I explored the NXS2 and N2a cell lines sensitivity to LCL161 *in vivo.* With the *in vitro* viability assays and Western blots, I observed that the murine NB cell lines express IAP proteins but do not undergo apoptotic cell death in response to SMCs. However, some cell lines have different responses to SMC when tested *in vitro* and *in vivo* (39,132). This variable sensitivity to SMCs is presumably due to the range of effects SMCs could have on the tumour microenvironment. Reports have shown that SMCs can have various effects on immune cells like frequency, cytotoxicity, and activation (38,56,57,60,79,80). but also are capable of inhibiting angiogenesis in the tumour (55,210). Studies have shown that SMCs can reduce vascularization in EMT6 and B16 tumour

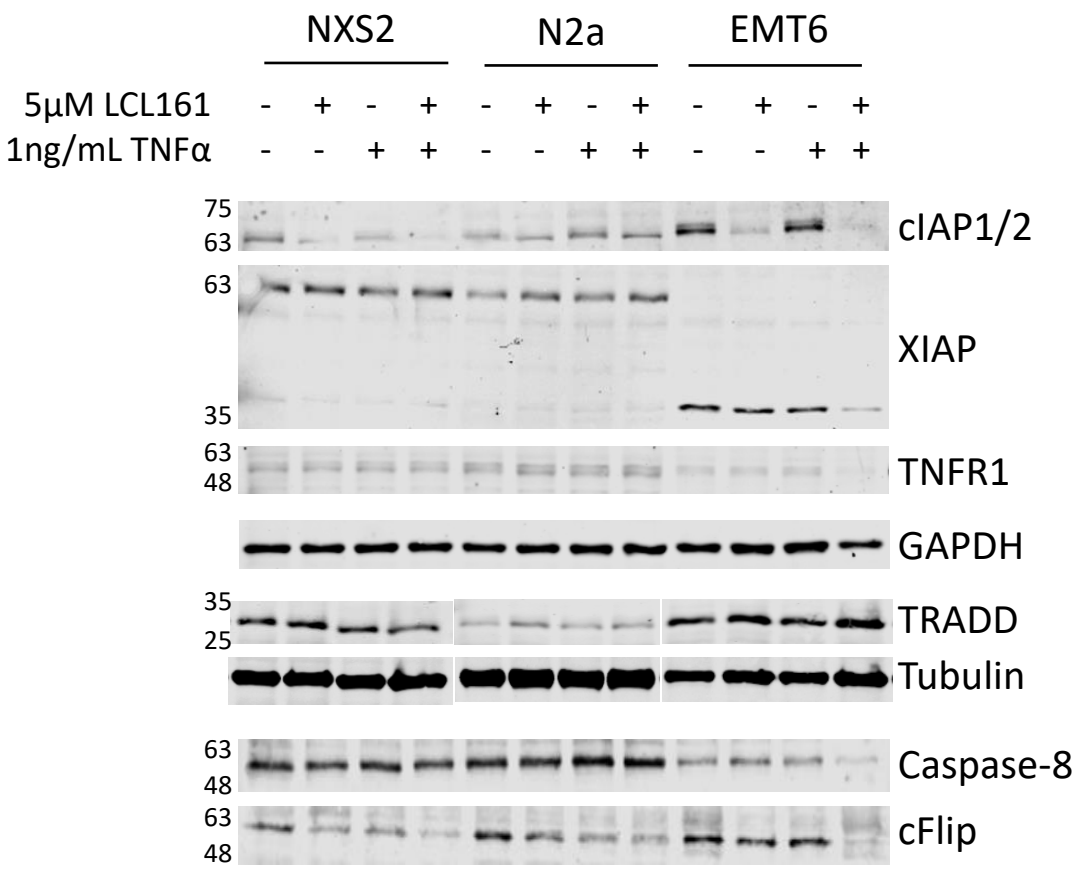
NXS2
N2a
EMT6
5μM LCL161 - + - + - + - + - + - +
1ng/mL TNFα - - + + - - + + - - + +
75
63
cIAP1/2
63
XIAP
35
63
48
TNFR1
GAPDH
35
25
TRADD
Tubulin
63
48
Caspase-8
63
48
cFlip

Figure 6. Apoptotic pathway components are expressed in murine NB cell lines. Western blots of proteins involved in the apoptotic pathway. NB cells were treated for 24 h with or without LCL161 and TNFα. E7 tubulin or GAPDH proteins or total protein content used as control. EMT6 was used as a positive control. Relevant weights in kDa are included on the left side. Cell death is only seen in the EMT6 cell line with LCL161 and TNFα combination, as expected.

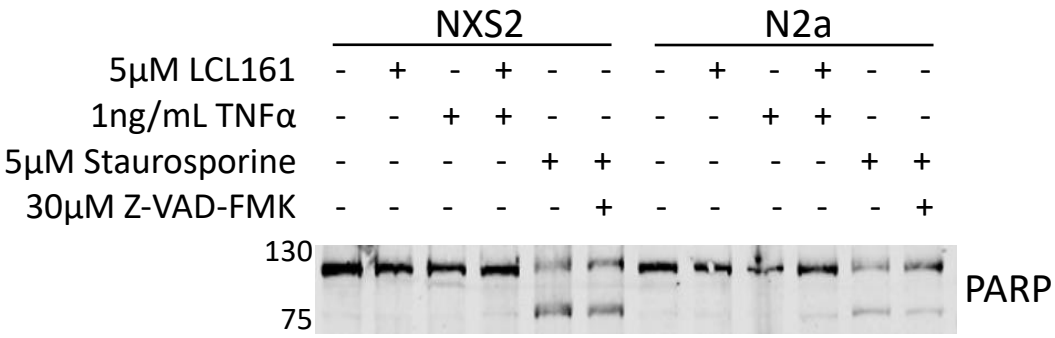
NXS2
N2a
5µM LCL161 - + - + - - - + - + - -
1ng/mL TNFα - - + + - - - - + + - -
5µM Staurosporine - - - - + + - - - - + +
30µM Z-VAD-FMK - - - - - + - - - - - +
130
75
PARP

Figure 7. PARP cleavage in murine NB cell lines occurs with staurosporine but not LCL161. Western blot assessing PARP cleavage in NXS2 and N2a cell lines. Cells were treated overnight with LCL161, TNFα, staurosporine or Z-VAD-FMK. Total protein content used as a control. Relevant weights in kDa are included on the left side.

models by rendering tumour endothelial cells sensitive to TNFα signalling. This reduction in tumour vasculature resulted in tumour growth inhibition. Thus, I proceeded with *in vivo* testing NXS2 and N2a cells to fully understand the susceptibility of NB cell lines to SMCs. As well, establishing *in vivo* models of NB enables me to test potential combination treatments of SMCs with other compounds which act by modulating the tumour microenvironment, such as immunotherapies. Studies have reported that NB tumours are highly vascularized and that this feature could be responsible for the high metastatic rates in NB (184,185,211). Reports have been successful in targeting angiogenesis to extend mouse survival or kill cancer cells in preclinical NB models (192,195,196). As well, there are several current clinical trials testing anti-vascular therapy, such as the αVEGF antibody, bevacizumab, against NB (198). I will investigate whether NB cell lines are sensitive to LCL161 treatment *in vivo* and will monitor the state of vascularization of SMC-treated NB tumours. If LCL161 promotes vascular shutdown in the NB *in vivo* models, then I will try to potentiate this effect by combining LCL161 with an anti-vascular agent to use against NXS2 cells.

2.2.1 Establishing s.c., i.v., orthotopic tumour models of NXS2 and N2a cell lines

Before studying NB in an *in vivo* setting, I first had to establish tumour models that could be consistently reproduced and also were representative of the NB disease. I established three tumour models for each murine NB cell line (Figure 8). A subcutaneous (s.c.) model, which permits better monitoring of tumour growth, was established with cells injected into the fatpad on the right flank of the mouse. An intravenous (i.v.) model, which acts as a substitute metastasis model, was established with cells injected through the tail vein. The orthotopic model, which best represents the typical NB primary tumour, was established with cells injected directly into the adrenal gland according to the protocol from Khanna et al. 2002 (185).

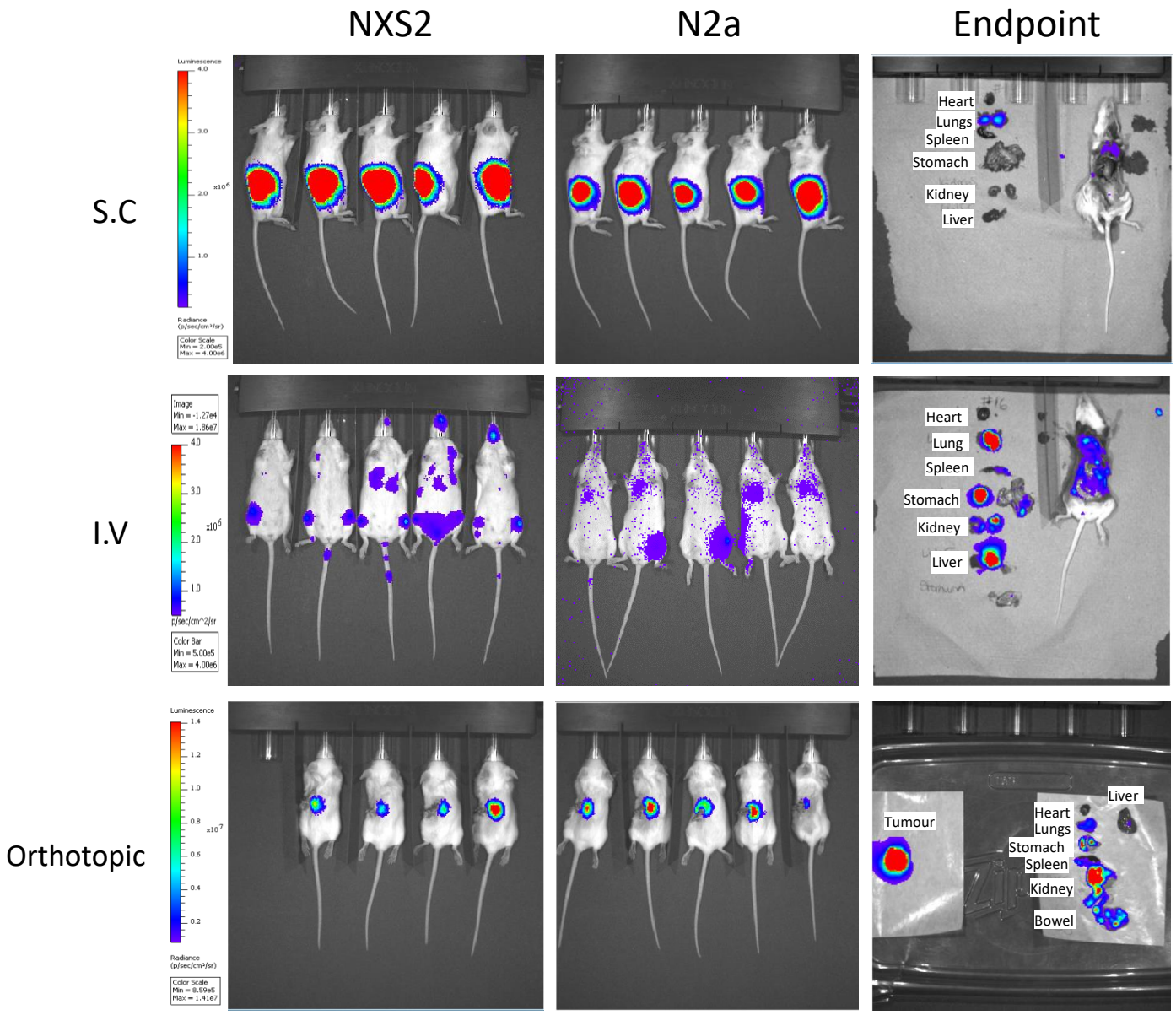
NXS2
N2a
Endpoint
S.C
I.V
Orthotopic
Heart
Lungs
Spleen
Stomach
Kidney
Liver
Lung
Tumour
Bowel

Figure 8.NXS2 and N2a syngeneic tumours established in s.c., i.v., and orthotopic mouse models. IVIS images were taken using a 1s exposure on mice incubated for 10min after a s.c. injection of 1.6mg of luciferin. Tumours were imaged 7d after injection of Fluc-tagged tumour cells. 5 $x10^5$ cells injected for s.c. model and i.v. models. 5 $x10^4$ cells were injected for the orthotopic model. Necropsies were performed at endpoint. Organs were prepared 7min into 10min incubation. Scale: p/sec/cm2/sr

Each model was established successfully and consistently across mice (Figure 8). NB tumours have a high incidence of metastasis, so I performed a necropsy evaluation complemented with IVIS imaging to look for cancer cells in other organs. I observed minimal metastatic events in the s.c. tumour model, with the most common secondary site being lungs. The i.v. model, a substitute metastatic model, had a very high incidence of metastasis, with cancer cells present in most organs tested. However, the limitation of this model is that it lacks a primary tumour site. I found the orthotopic model to be most realistic of the NB disease. This model begins with a primary tumour in the adrenal gland which then metastasizes at a high rate to numerous organs. This is similar to a true NB case where the majority of tumours originate in the adrenal gland and then metastasize.

2.2.2 NXS2 s.c. tumour growth responds to LCL161 with a minor delay in growth

After establishing the *in vivo* tumour models for both murine NB cell lines, I next examined their sensitivity to SMC monotherapy *in vivo.* Tumours were established in a s.c. or orthotopic model, then given 50 mg/kg or 75 mg/kg LCL161 p.o. four times, respectively. I observed that four treatments of LCL161 monotherapy was capable of slightly extending survival in mice bearing NXS2 tumour models. Interestingly, LCL161 monotherapy was most effective in delaying tumour growth in the s.c. NXS2 model (Figure 9A, $p<0.07$) which was also seen as the most vascularized tumour model. I also observed that LCL161 monotherapy was ineffective at extending survival of mice bearing N2a orthotopic tumours (Figure 9B), which are the least vascularized NB tumour model studied in my project.

2.2.3 Anti-vascular effect of LCL161 reduces NB tumour angiogenesis

Since mice bearing the most vascular tumour model, the NXS2 s.c. model, had the best response to LCL161, I performed an observational experiment to monitor any potential LCL161-mediated

A

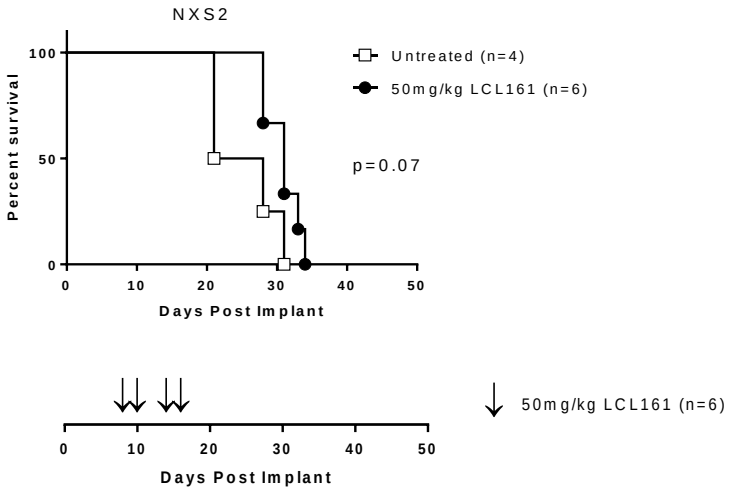
NXS2
Untreated (n=4)
50mg/kg LCL161 (n=6)
p=0.07
Percent survival
Days Post Implant
50mg/kg LCL161 (n=6)
Days Post Implant

B

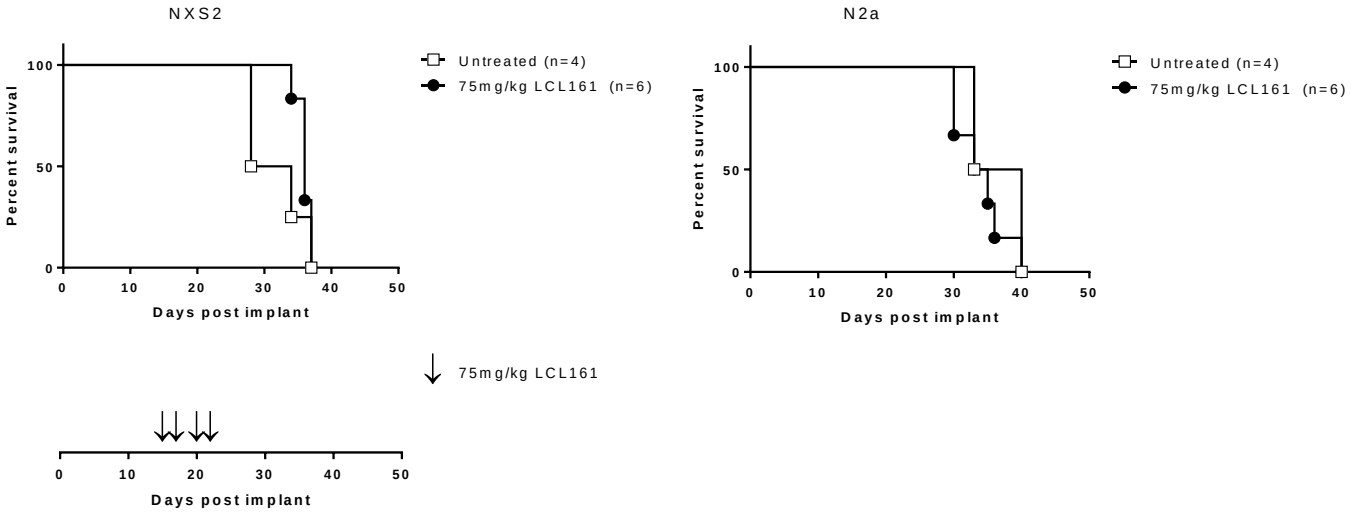
NXS2
Untreated (n=4)
75mg/kg LCL161 (n=6)
Percent survival
Days post implant
75mg/kg LCL161
Days post implant
N2a
Untreated (n=4)
75mg/kg LCL161 (n=6)
Percent survival
Days post implant

Figure 9. LCL161 monotherapy slightly delays NXS2 s.c tumour growth. A) 5 x 10^5 NXS2-Fluc cells injected s.c. Mice were treated four times with 50mg/kg LCL161 p.o. after tumours were palpable. Tumour volumes were measured three times a week until endpoint. B) 5 x 10^4 NXS2 and N2a Fluc-tagged cells injected into the adrenal gland. Mice were treated four times with 75mg/kg LCL161 p.o.

anti-angiogenic effects. I examined NXS2 s.c. tumours at endpoint with a necropsy performed by a blind observer for most of my *in vivo* experiments. Results from these necropsy examinations show that LCL161-treated mice had tumours with a reduced degree of angiogenesis, including decreased visible vasculature and reduced overall blood content in the tumours. These observations support that LCL161 could have anti-vascular effects on NXS2 s.c. tumours. Interestingly, I even observed this vascular effect by LCL161 in tumours treated in with ICIs as well.

Since I observed LCL161 decrease tumour angiogenesis through necropsy evaluation, I proceeded to confirm vasculature shutdown of LCL161 by using ultrasound imaging. Using a Vevo 2100 ultrasound, the rate of non-targeted microbubble flow entry into the tumour was measured using contrast imaging in a control and a LCL161-treated mouse with a NXS2 s.c. tumour. I can model the perfusion rate of the selected tissue by measuring the rate of non-targeted microbubble flow entry.

Using ultrasound imaging, I found that LCL161 treatment, even 24 h after given once at 75 mg/kg, can shut down tumour vasculature (data not shown). Although, it should be noted that only one mouse in each group was examined and further experimentation is required.

2.2.4 LCL161 and sunitinib combine to delay tumour growth of NXS2 s.c. model.

With the ultrasound imaging experiment and necropsy evaluation, I found that LCL161 treatment of mice bearing NXS2 s.c. tumours induced tumour vascular shutdown. Thus, I investigated whether I could potentiate this anti-angiogenic effect of LCL161 by combining LCL161 with sunitinib, an anti-vascular agent. Sunitinib is a clinically approved small molecule inhibitor of receptor tyrosine kinases, such as PDGF-receptor and VEGF-receptor (193,194,212). These two receptors are relevant in promoting tumour angiogenesis and growth. Following treatment schedules of other preclinical studies (196,213), which also considered toxicity, sunitinib was given i.p. for fourteen days at 35 mg/kg. LCL161 was given p.o. four times at 75 mg/kg to mice with NXS2 s.c. tumours.

Here, I see that the combination of LCL161 and sunitinib is effective in delaying tumour growth of the NXS2 s.c. model (Figure 10). This combination significantly delayed tumour growth, as determined by a logrank analysis. (Figure 10B, $p<0.05$). However, further group-to-group analysis with a Holm-Sidak test proved no significance. I observed no signs of toxicity in mice receiving the combination treatment. The tumour growth curves best display the ability of the combination to elicit a delay in tumour growth. I observed minor differences in the monotherapy growth curves vs the control condition, with few subjects undergoing a drug response. However, all mice receiving the combination of LCL161 and sunitinib have right-shifted tumour volume growth curves, indicating a combination effect (Figure 10A).

2.3 Testing *in vivo* sensitivity of NXS2 s.c. tumour model to LCL161 in combination with αGD2 antibody

I have shown that NXS2 and N2A cells are resistant to LCL161 *in vitro* and had minimal delays in tumour growth *in vivo* This delay in tumour growth was increased by combining LCL161 with

A

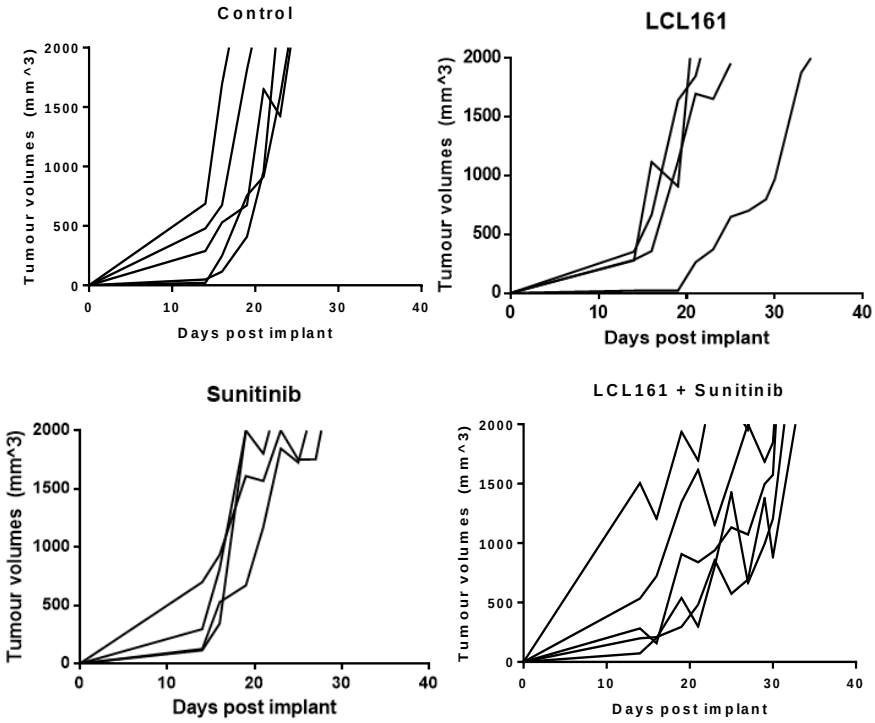
Control
LCL161
Sunitinib
LCL161 + Sunitinib
Tumour volumes (mm^3)
Days post implant
0
500
1000
1500
2000
0
10
20
30
40

B

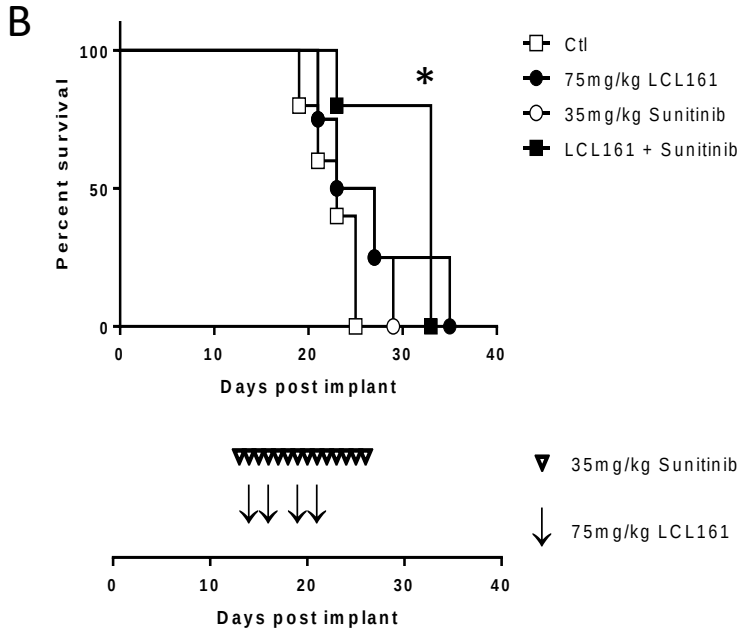
Percent survival
Days post implant
Ctl
75mg/kg LCL161
35mg/kg Sunitinib
LCL161 + Sunitinib
*
0
50
100
0
10
20
30
40
35mg/kg Sunitinib
75mg/kg LCL161

Figure 10. LCL161 and sunitinib combine to delay tumour growth in NXS2 s.c. tumour model. 5×10^5 NXS2-fluc cells were injected s.c. with measurements performed three times a week. Once tumours were palpable, 75mg/kg LCL161 was given four times p.o. and 35mg/kg sunitinib was given fourteen times i.p. N=5 mice for control and combination group, while N=4 for monotherapy groups. A) Individual tumour volume growth curves B) Kaplan-Meier curve depicting mouse survival with associated treatment schedule. * = $p<0.05$.

the anti-vascular agent, sunitinib. However, I wanted to further explore SMCs against NB using a combination which is more clinically relevant. The most recently approved immunotherapy for NB is an αGD2 antibody with a reported mechanism of action of ADCC and CDC (149,150). This therapy led to a 20% overall increase in survival for high-risk group patients but is still being investigated for improvements. Some αGD2 antibody combination strategies used in clinical and pre-clinical studies are immune-activating cytokines (214,215), anti-vascular agents (216), and ICIs (109).

I have shown that LCL161 has an anti-angiogenic role in my NXS2 tumour model, which is corroborated by studies reporting LCL161 can shutdown tumour vasculature. Furthermore, reports indicate that SMCs increase NK cytotoxicity against NK-susceptible cell lines (61,62). A study demonstrated that XIAP is a resistant factor used by cancer cells to inhibit ADCC (64). Thus, I examined whether an αGD2 antibody could synergize with LCL161 to delay tumour growth and increase mouse survival of an *in vivo* $GD2^+$ NXS2 s.c. model.

To study the combination of αGD2 antibody with LCL161, I first had to acquire a GD2-targeting antibody. The hybridoma HB-9326, which produces the mouse IgG2a αGD2 clone ME361-S2a, was obtained from ATCC. I had to first isolate the antibody, then verify purity and binding ability, then determine if it was ADCC capable. I also had to establish protocols for isolation and maintenance of an effector cell population that could mediate ADCC. Since it is difficult to acquire a suitable number of murine NK cells for experimentation, I used lymphokine activated killer cells (LAKs) as a substitute.

2.3.1 SDS-PAGE of samples from antibody isolation

I grew the ME361-S2a hybridoma to 2 L of media, then incubated for one-to-two weeks to maximize antibody production. The αGD2 antibody of IgG2a isotype was isolated using a gravity

column packed with Protein G beads. I passed the media a total of four times through the isolation column to maximize yield. I then took aliquots from the following steps of the isolation and purification process: starting media, media after column pass 1-4, wash from spin column, and final antibody solution. I than loaded these samples onto a polyacrylamide gel and ran sodium dodecyl sulfate-polyacrylamide gel electrophoresis (SDS-PAGE) to visualize the antibody content and purity at each stage of the isolation (Figure 11).

I performed SDS-PAGE on the antibody samples and then stained them with Coomassie Blue. The gel shows three distinct bands appearing at 50-55 kDa, 25kDa, and 20-25kDa (Figure 11, lanes 13 and 14). These three sizes correspond to expected kDa weights of heavy and light chains. Importantly, there are no other bands significantly present in the antibody sample lanes, indicating the sample is pure. Furthermore, both the first and second batch of isolated antibody have identical band patterns indicating consistent antibody sample was produced. Post-translational modifications, such as glycosylation, could account for the presence of two light chain bands.

2.3.2 Staining positive and negative murine NB cell lines using isolated antibody

After verifying the purity of the antibody isolation with SDS-PAGE, I wanted to confirm the capability of the antibody to bind to its target, GD2. I performed high throughput immunofluorescence assay on the $GD2^+$ (NXS2) and $GD2^-$ (N2a) NB cell lines hoping to validate the sensitivity and specificity of the antibody. I used the commercially available 14G2a clone as a positive control for these experiments. First, I attempted fixed-cell immunofluorescence. Both the negative and positive cell lines stained positive with both clones of αGD2 antibody (Figure 12A).

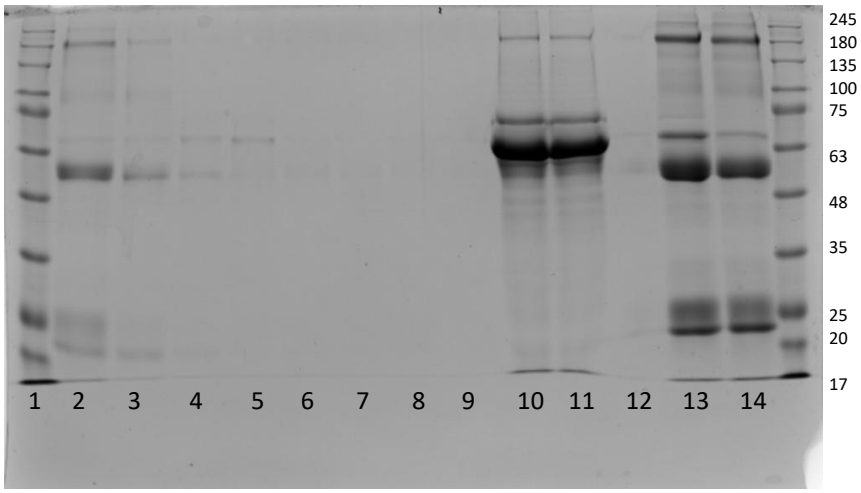
245
180
135
100
75
63
48
35
25
20
17
1 2 3 4 5 6 7 8 9 10 11 12 13 14

Figure 11. Validating purity of gravity column antibody isolation of ME361-S2a antibody by SDS-PAGE. Coomassie blue staining of SDS-PAGE containing samples from each fraction of antibody isolation and purification process. Supernatant from HB-9326 was passed through a Protein G gravity column four times to isolate antibody. 20μL aliquots were loaded into each well from the samples. 3μL of protein ladder was loaded, with kDa band sizes labelled on the right of gel. Lanes: 1. Protein ladder, 2. First isolation from media, 3. Second isolation from media, 4. Third isolation from media, 5. Fourth isolation from media, 6. Flow through from spin column from first pass, 7. Flow through from second pass, 8. Flow through from third pass, 9. Flow through from fourth pass, 10. Hybridoma media before isolation, 11. Media after isolation, 12. Flow through from PBS wash of antibody isolation, 13. First attempt of antibody isolation, 14. Second attempt of antibody isolation. Post-translational modifications, such as glycosylation, could account for the presence of two light chain bands.

Next, I performed live-cell immunofluorescence to stain live, untouched cells. Here, only the $GD2^+$ cell line stained positive, however it was at an unexpectedly low rate (Figure 12B).

Due to the unexpected results form immunofluorescence staining, I also tried using the unconjugated ME361-S2a antibody for preparation in flow cytometry staining. The pre-conjugated and unconjugated 14G2a clones were used as a positive control. Again, the antibody was sensitive to only the $GD2^+$ cell line, NXS2, and minimal N2a cells stained positive (Figure 13). Both 14G2a and ME361-S2a antibodies conjugated with Alexafluor-488 produced similar positive population sizes of about 8%. The pre-conjugated antibody stained an 18% positive population.

Although the isolated antibody performed similar to the commercially available clone, the overall low rate of $GD2^+$ cells in the cell line NXS2 was surprising. Upon repeating flow cytometry staining for GD2, $GD2^+$ cells for NXS2 ranged from 10-80% of cells (data not shown). Thus, I attempted to optimize flow cytometry staining for GD2. A previous study suggested that GD2 molecules were involved in anoikis and cell adhesion (183,217), so I hypothesized that the antigen is being destroyed or masked by staining preparation. I attempted to lift the adherent NB cell lines in different manners, using scraping, or low and high levels of trypsin and enzyme-free cell dissociation buffer, to try and minimize any potential damage of the GD2 molecule. Following lifting of the cells, the typical flow staining protocol was followed. Here, I observed that the manner of preparing cells for staining does affect the $GD2^+$ population (Figure 14). Trypsin, being most harsh, seemed to damage or reduce GD2 antigen on the cell surface. The enzyme free dissociation buffer, regarded as a gentler approach to lifting cells, conserved more GD2 antigen on the cell surface. Gentle scraping with a cell scraper was also tested, which produced a high expression of GD2 retained on the $GD2^+$ cell line. This trend is depicted by the histograms shifting more positive with the different lifting techniques.

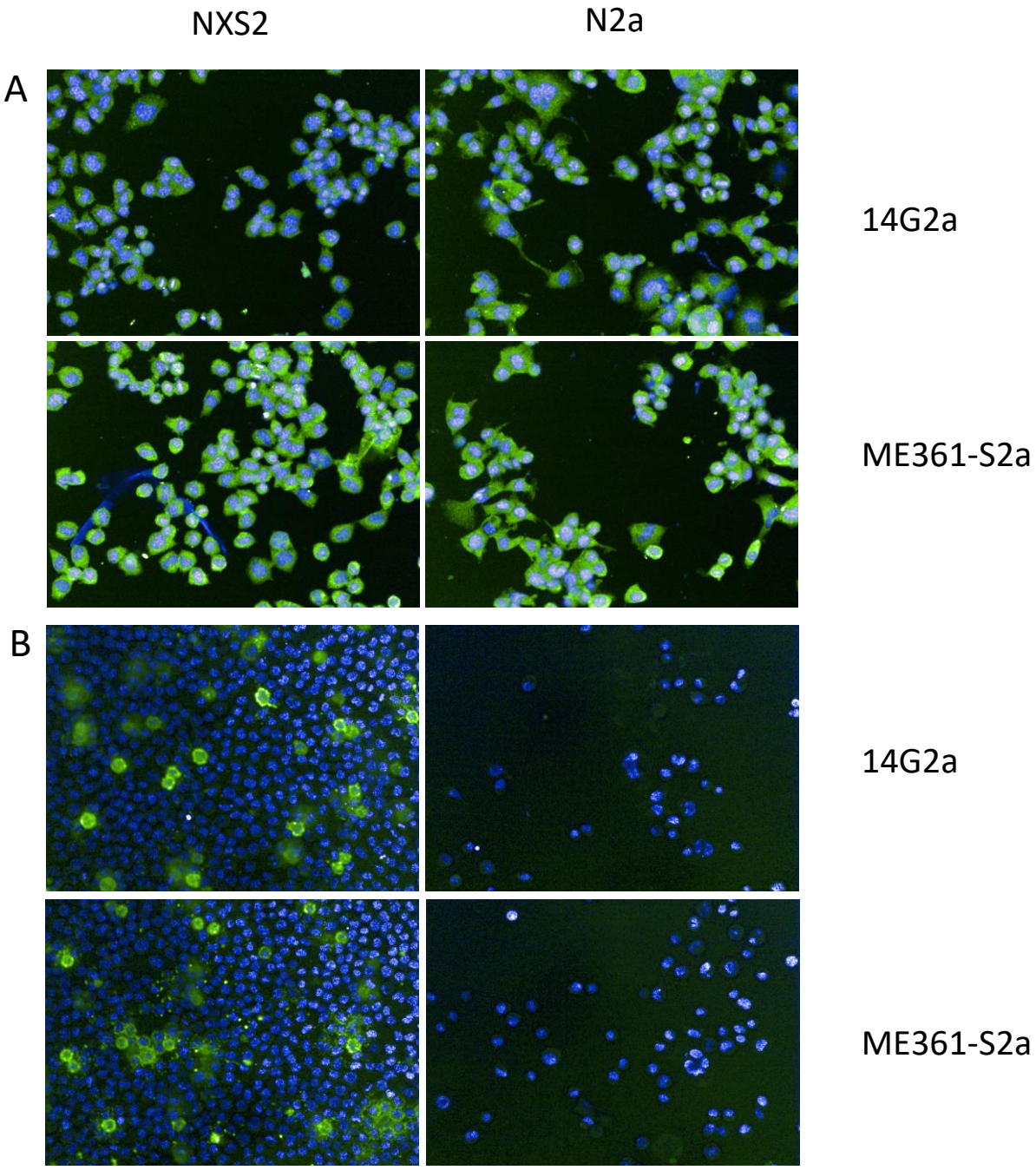
NXS2
N2a
A
14G2a
ME361-S2a
B
14G2a
ME361-S2a

Figure 12. Isolated and commercial αGD2 antibody staining are comparable by Immunofluorescence. High throughput immunofluorescence was performed with 5 μg/mL isolated ME361-S2a or commercially available 14G2a clones of GD2 specific antibody, 5 μg/mL Alexafluor-488 secondary, and 1 μg/mL Dapi (for fixed cell) or Hoescht 33342 (for live cell) nuclei stain. Images were taken by Dr. Baird using an Opera QEHS high throughput scanner. A) Fixed-cell immunofluorescence of NXS2 and N2a cells. B) Live cell immunofluorescence of NXS2 and N2a cells. Cells were cultured for 24 h prior to staining. Representative images are shown.

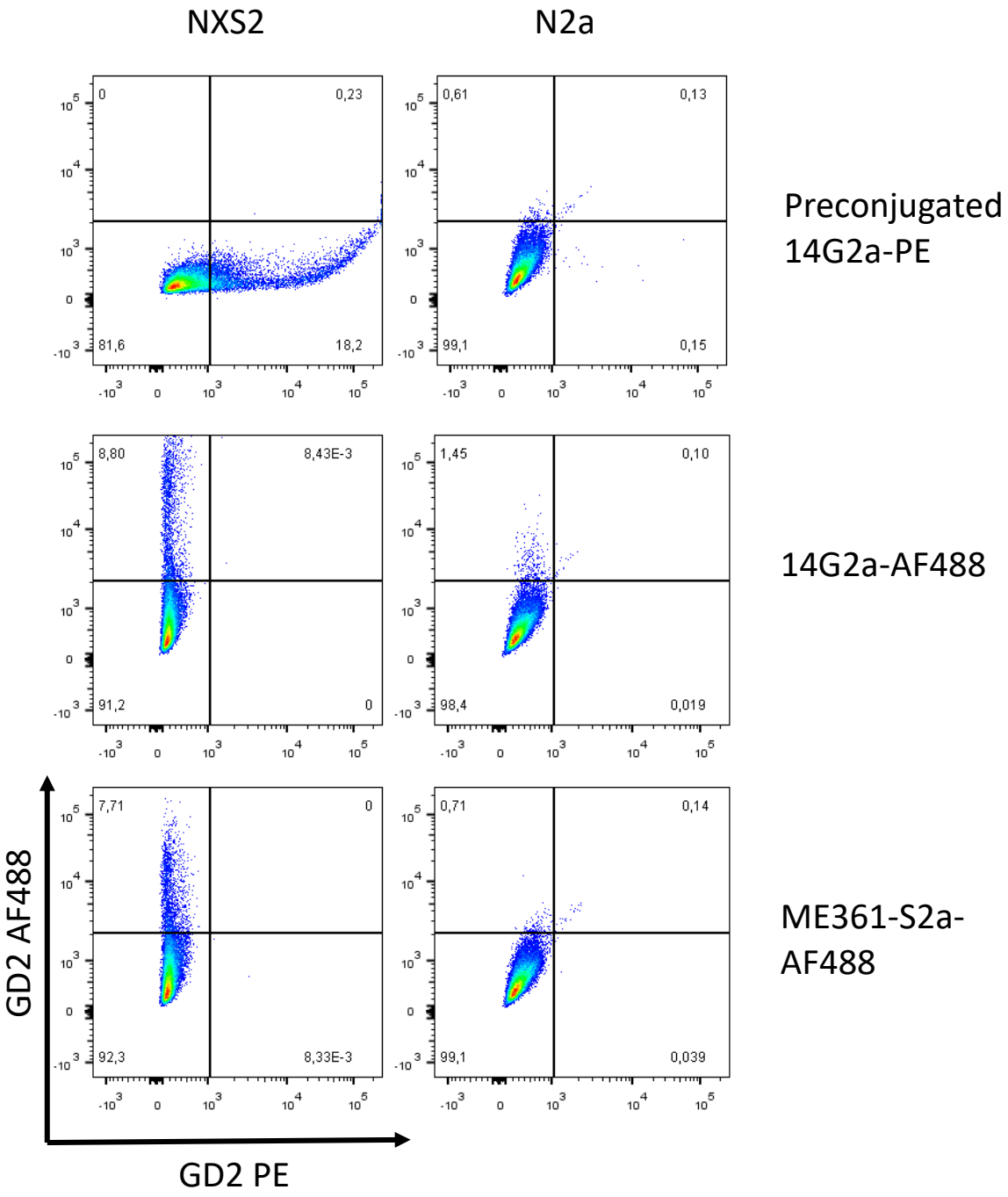
NXS2
N2a
0
0,23
81,6
18,2
0,61
0,13
99,1
0,15
Preconjugated 14G2a-PE
8,80
8,43E-3
91,2
0
1,45
0,10
98,4
0,019
14G2a-AF488
7,71
0
92,3
8,33E-3
0,71
0,14
99,1
0,039
ME361-S2a-AF488
GD2 AF488
GD2 PE

Figure 13. Isolated and commercial αGD2 antibody staining are comparable by flow cytometry. NXS2 and N2a cells were cultured for 24 h prior to staining. Cells were stained with either a flow cytometry 14G2a antibody, preconjugated to PE fluorophore, or incubated for 30min on ice with 5ug/mL 14G2a unconjugated or ME361-S2a antibody, then incubated for another 30min on ice with Alexafluor488 secondary. Representative flow plots show staining profile for each antibody.

I also tested intracellular staining for GD2. Often in flow cytometry, intracellular staining is used against antigens that are either inconsistent or difficult to stain on the cell surface. The intracellular staining for GD2 was positive for both NXS2 and N2a (Figure 15A), which supports the fixed-cell immunofluorescence results (Figure 12A). Thus, I tested for specificity of the intracellular GD2 staining with trying to block the binding by adding the unconjugated antibody clones 14G2a (isoclonal) and ME361-S2a (non-clonal). Interestingly, both unconjugated clones of αGD2 antibody reduced the overall percent of $GD2^+$ cells for both the NXS2 and N2a cell line (Figure 15B). The NXS2 cell line had an original $GD2^+$ population of 68%, which fell to 55% and 48% using the 14G2a and ME361-S2a clone, respectively. For this experiment, intracellular staining of the N2a cell line had a 32% positive population which fell to 24% and 19%.

2.3.3 New cell model to reliably measure GD2 expression: LCL161 does not affect expression of GD2 on lymphoma cells when cell death is rescued

My previous work with validating the ME361-S2a antibody and optimizing GD2 staining has shown that: staining GD2 is inconsistent extracellularly, GD2 antigen is sensitive to cell preparation, and αGD2 antibodies are not specific to GD2 for intracellular staining. However, I was able to confirm that the isolated antibody, ME361-S2a, was staining similarly to the commercially available 14G2a clone. Before using a LCL161 and αGD2 antibody combination *in vivo,* I wanted to investigate if LCL161 would modulate GD2 expression in the $GD2^+$ NXS2 cell line, but I was unable to accurately measure changes in GD2 expression. To avoid the GD2 staining limitations, which are related to preparation of the adherent NB cell lines, I introduced a new cancer model which was $GD2^+$ but also suspension cells. RMA and RMA/S cells are murine lymphoma cell lines which have been reported to express GD2 molecules (218). Using flow cytometry, I confirmed that these cell lines express GD2 and that I could consistently stain for

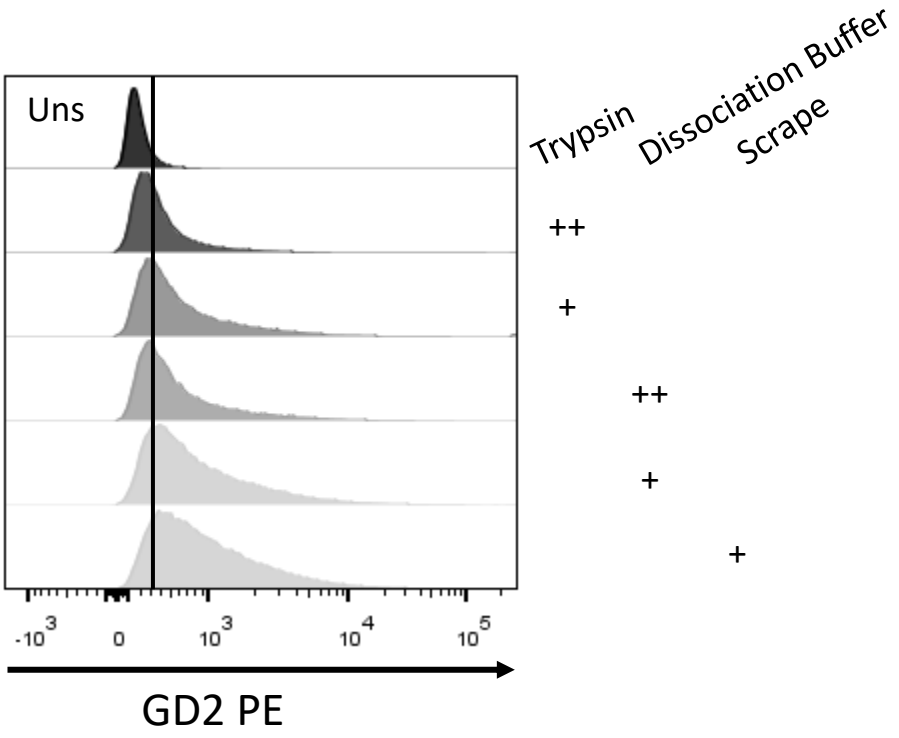
Uns
Trypsin
Dissociation Buffer
Scrape
++
+
++
+
+
-10^3
0
10^3
10^4
10^5
GD2 PE

Figure 14. Variability in GD2 staining on flow cytometry. GD2 staining is affected by different techniques used to lift adherent cells. After 24 h, NXS2 cells were lifted using various amounts of trypsin, dissociation buffer, or a scraping method. Cells were stained using a pre-conjugated 14G2a-PE clone. The top histogram is the unstained sample, while the bar represents the positive population gate. The histograms underneath are NXS2 cells lifted with various methods, listed on the right, before staining.

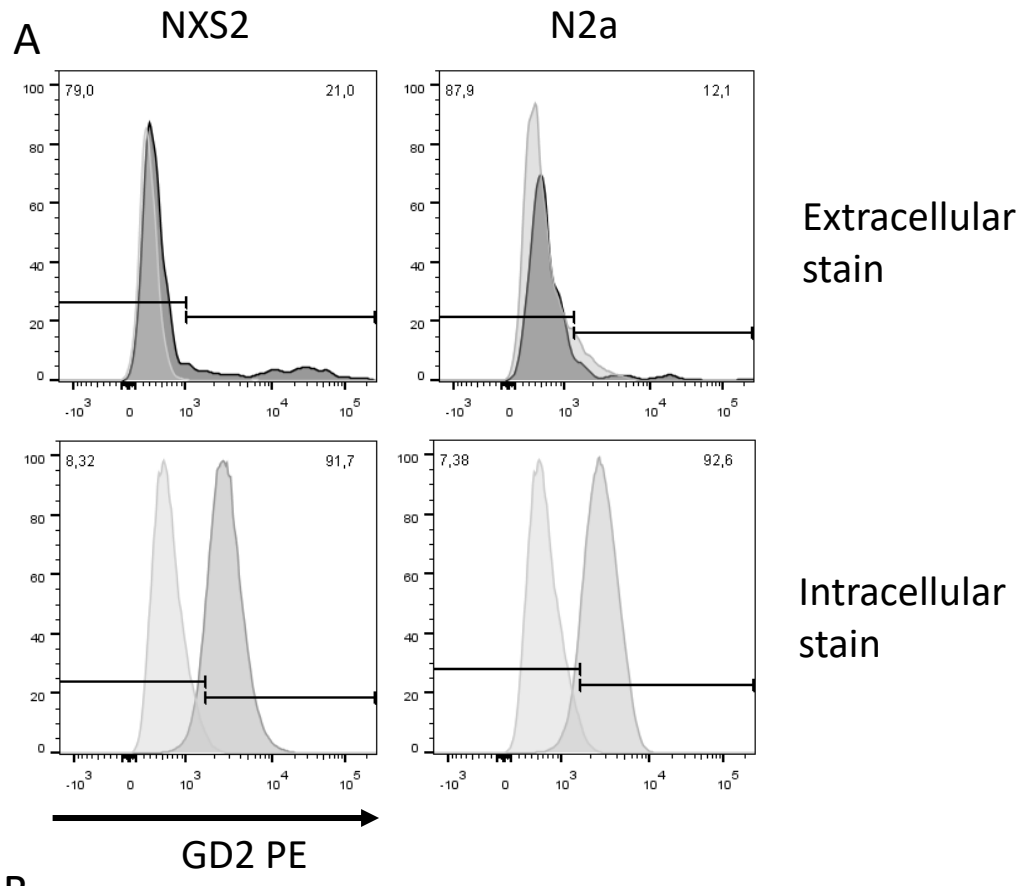
A
NXS2
N2a
79,0
21,0
87,9
12,1
8,32
91,7
7,38
92,6
Extracellular stain
Intracellular stain
GD2 PE

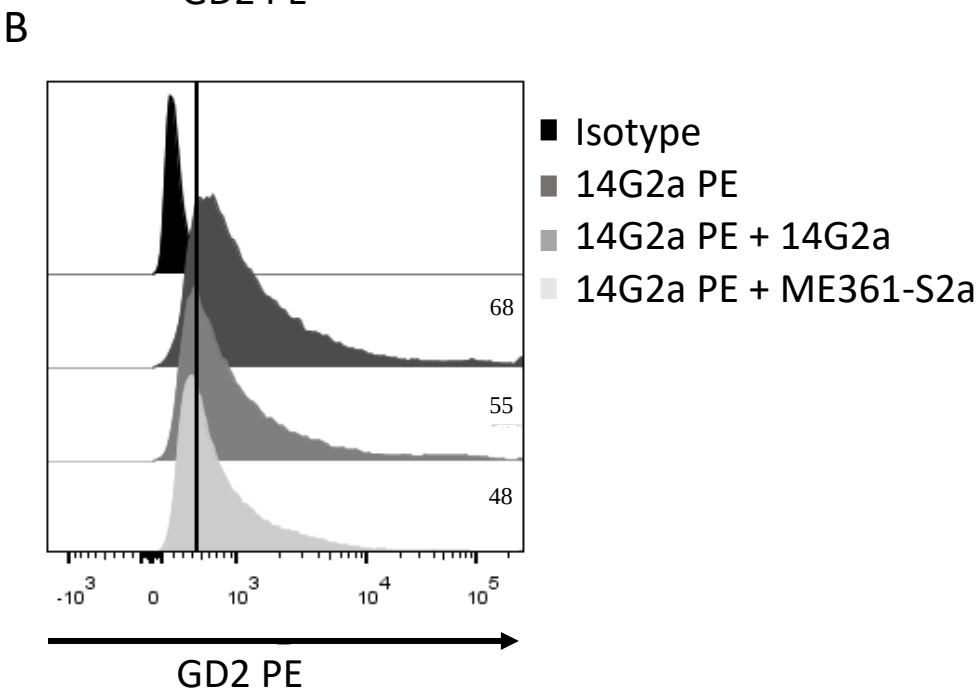
B
Isotype
14G2a PE
14G2a PE + 14G2a
14G2a PE + ME361-S2a
68
55
48
GD2 PE

Figure 15. Intracellular staining of GD2 specifically stains $GD2^+$ and $GD2^-$ cell lines. Intracellular positive population can be reduced by unconjugated antibody addition. A) Both extra- and intracellular staining of GD2 on NXS2 and N2a cells with the preconjugated 14G2a-PE antibody and analyzed by flow cytometry. Gates were set by isotype control sample, seen as lighter shade sample in histograms. B) Blocking of intracellular staining by unconjugated antibody clones. Cells were stained with preconjugated 14G2a-PE antibody after incubation with unconjugated 14G2a and ME361-S2a clones. Percent positive population listed on right. Black bar represents positive signal. Representative histograms are shown for each experiment.

GD2 expression (data not shown). Thus, these cell lines could act as a model to investigate modulating GD2 expression by LCL161.

The expression of GD2 was measured by flow cytometry 24 h after treatment with 5 μM LCL161. GD2 expression was increased and decreased in the RMA and RMA/S cell lines, respectively, (Figure 16A). However, unlike the NB cell lines, I observed that these lymphoma cell lines were sensitive to LCL161 with and without TNFα, as determined by an alamarBlue assay (Figure 16B). Thus, I rescued cell death using Necrostatin-1 and found that the change in GD2 expression mediated by LCL161 was negated (Figure 16A).

2.3.4 Analysis of LAK isolation, purity, and functionality.

I have shown the isolated αGD2 antibody, ME36-S2a, is pure and capable of specifically binding GD2. Before using the antibody for *in* vivo experiments, I must also validate if it is capable of mediating ADCC. To perform an ADCC experiment, I must first introduce and optimize a protocol for generating ADCC-capable effector cells and measuring cytotoxicity. LAKs were chosen as the effector population due to the ability to generate sufficient cell numbers for testing and their ability to mediate ADCC (219).

I produced LAKs by growing NK cells in 1000 U/mL recombinant human-IL2. NK cells were isolated by magnetic separation from a homogenized mouse spleen. After seven days of culture, these cells were confirmed to be majority $CD45^{+}CD49b^{+}CD3^{-}$ and viable (zombie violet negative) by flow cytometry, as shown with representative flow diagrams (Figure 17A). Furthermore, the cells were capable of mediating cell cytotoxicity against the NK sensitive cell line, Yac-1, as measured by an LDH release assay (Figure 17B).

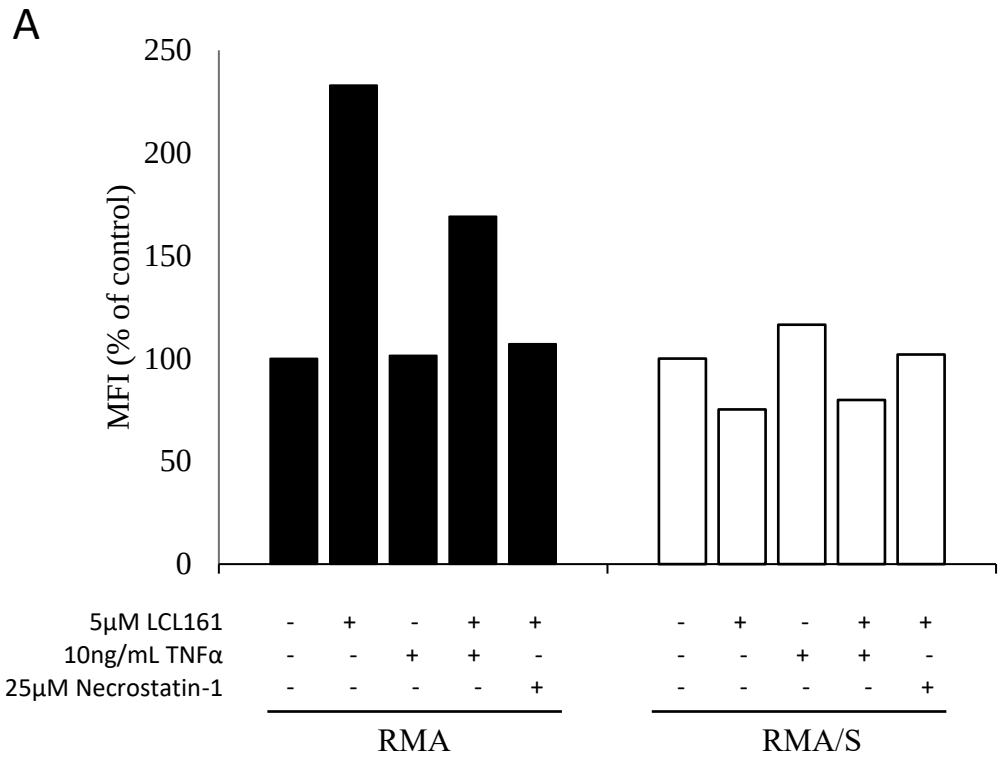
A
250
200
150
100
50
0
MFI (% of control)
5μM LCL161 - + - + + - + - + +
10ng/mL TNFα - - + + - - - + + -
25μM Necrostatin-1 - - - - + - - - - +
RMA
RMA/S

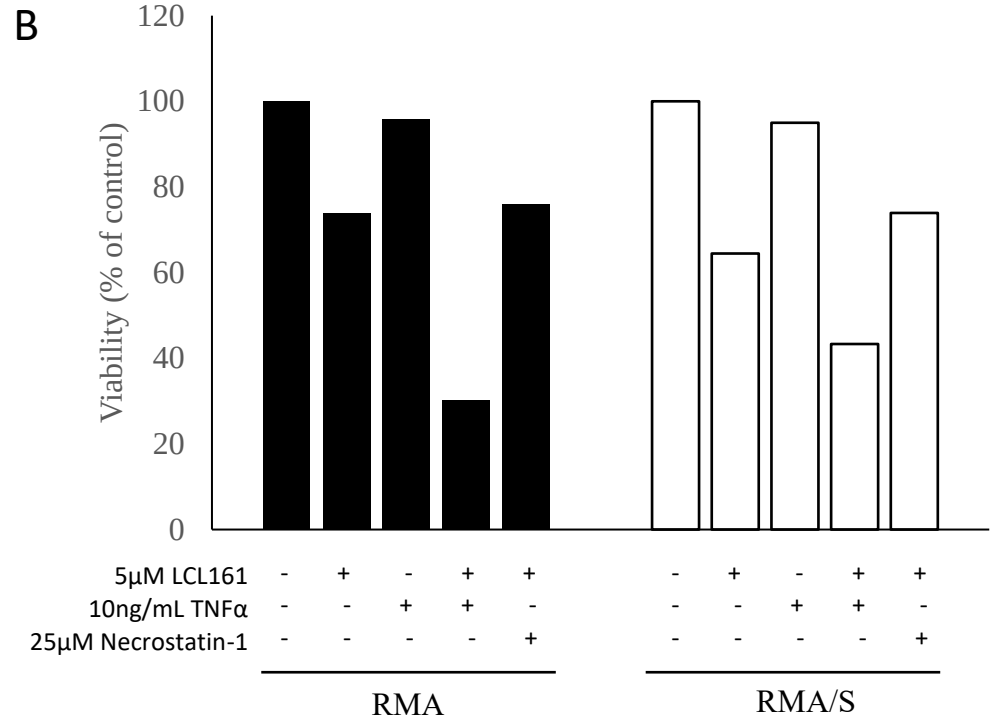
B
120
100
80
60
40
20
0
Viability (% of control)
5μM LCL161 - + - + + - + - + +
10ng/mL TNFα - - + + - - - + + -
25μM Necrostatin-1 - - - - + - - - - +
RMA
RMA/S

Figure 16. In vitro impact of LCL161 on GD2 expression modelled in RMA and RMA/S cell lines. A) Normalized MFI of GD2-PE expression on RMA and RMA/S Alive (Zombie Violet negative) cells after 24 h of treatment (n=1; Mean±SD). B) Viability was measured using an alamarBlue assay after 24 h of treatment before preparation for flow cytometry. Associated alamarBlue results shown and is representative (n=3; Mean).

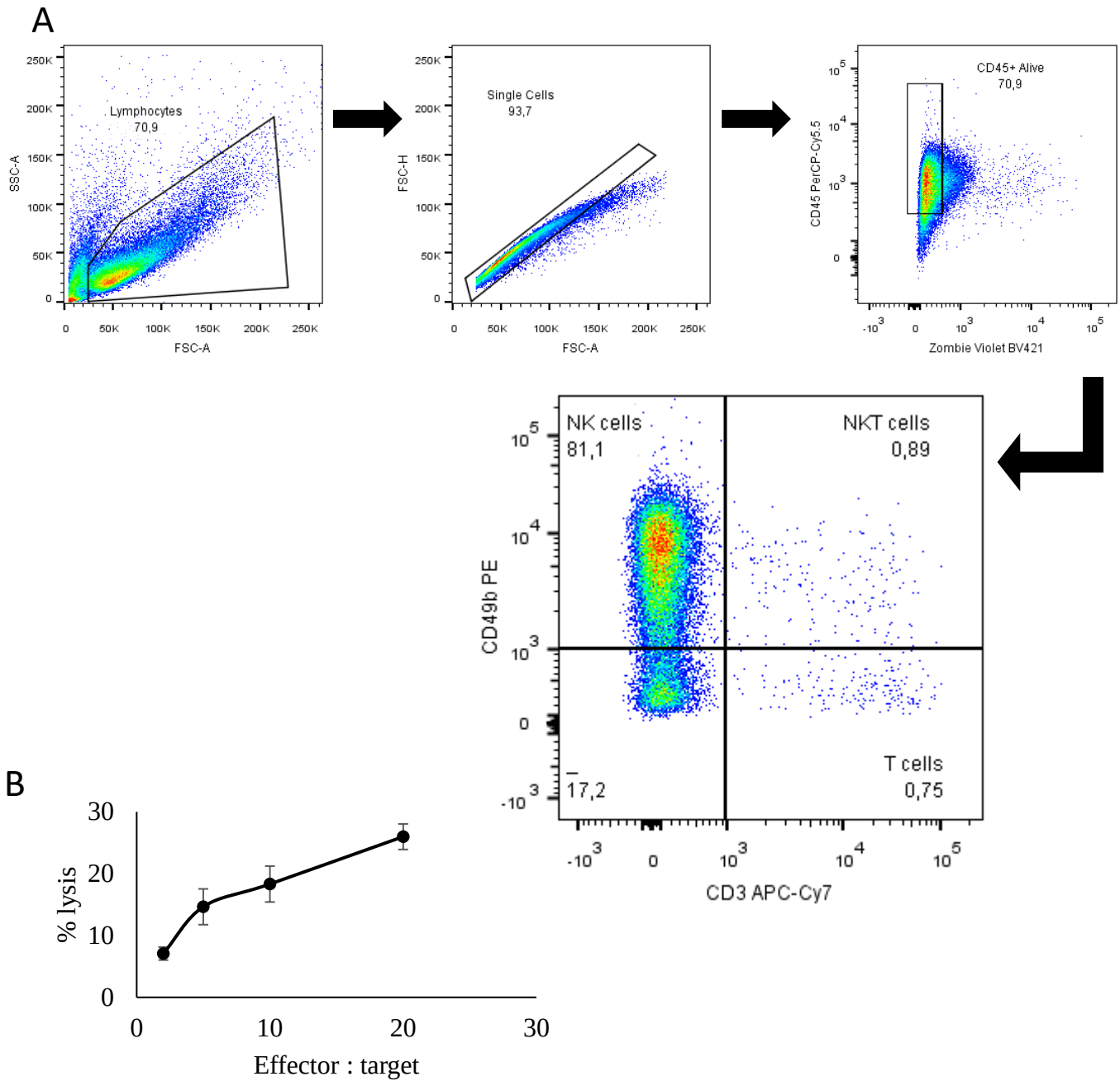
A
Lymphocytes
70,9
SSC-A
FSC-A
Single Cells
93,7
FSC-H
FSC-A
CD45+ Alive
70,9
CD45 PerCP-Cy5.5
Zombie Violet BV421
NK cells
81,1
NKT cells
0,89
T cells
0,75
17,2
CD49b PE
CD3 APC-Cy7
B
% lysis
Effector : target

Figure 17. LAK population is viable, of high purity, and capable of lysing cells. Splenocytes cultured in 1000 U/mL rh-IL2 for seven days after a negative NK cell magnetic isolation. A) Representative flow diagrams showing a viable LAK population of high purity. B) Killing assay with LAKs cocultured for four hours with Yac-1 cells. % lysis measured by an LDH release assay.

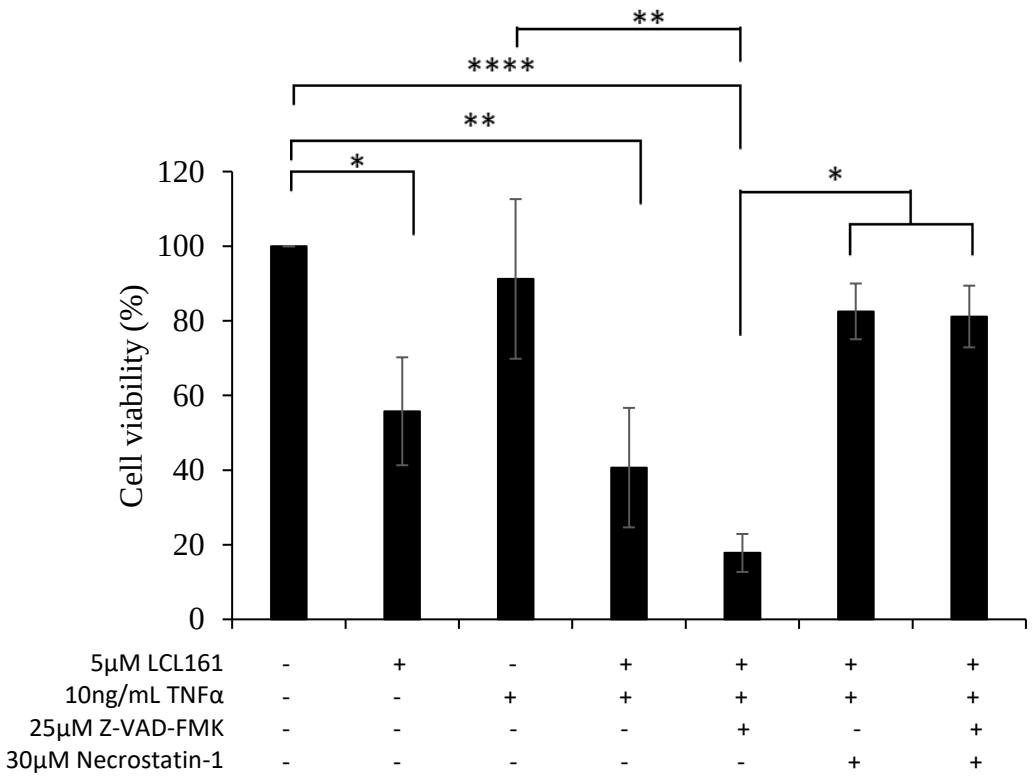
**
****
**
*
*
120
100
80
60
40
20
0
Cell viability (%)
5μM LCL161 - + - + + + +
10ng/mL TNFα - - + + + + +
25μM Z-VAD-FMK - - - - + - +
30μM Necrostatin-1 - - - - - + +

Figure 18. LAKs are sensitive to necroptosis with LCL161. Day seven cultured LAKs in 1000U/mL rh-IL2 were treated with 5μM LCL161 and 10ng/mL TNFa for 24 h. Viability measured with an alamarBlue assay. Cell death rescue attempted by adding 25μM Z-VAD-FMK and 30 μM Necrostatin-1. * = $p<0.05$; ** = $p<0.01$; *** = $p<0.001$; **** = $p<0.0001$.

2.3.5 LAKs are sensitive to LCL161 in vitro

Next, I wanted to assess if the LAK population was sensitive to LCL161 treatment *in vitro*. If sensitive, it would prevent testing the anti-tumour efficacy of the LCL161 and αGD2 antibody combination *in vitro*. LAKs were treated with LCL161 with TNFα for 24 h, and Z-VAD-FMK or Necrostatin-1 was added to rescue cell death. The viability assay was performed using alamarBlue. LAKs were sensitive to LCL161 *in vitro*, undergoing necroptosis when treated with LCL161 and TNFα for 24 h, inducing 58% cell death (Figure 18, $p<0.01$). Cell death could be rescued by Necrostatin-1 but was further promoted by caspase inhibition using Z-VAD-FMK. Thus, I cannot test the *in vitro* efficacy of the LCL161 and αGD2 antibody combination with this model.

2.3.6 Isolated antibody can mediate ADCC but is not directly cytotoxic.

After verifying the capability of the antibody to bind GD2 in a specific and sensitive manner, and generating a suitable effector cell population, I wanted to ensure the antibody was functional and could also mediate ADCC. I added the isolated antibody to a final concentration of 10 μg/mL to LAKs in a coculture of NXS2 cells. The cells were incubated for 4 h then ADCC was measured using an LDH release kit. A 15% and 12% increase in cell lysis was noted in the 10:1 and 20:1 effector to target cell conditions which had ME361-S2a isolated antibody, respectively (Figure 20A). Unexpectedly, the cell lysis decreased to that of the control condition at the higher ratio of 40:1. Both batches of antibody isolation, denoted αGD2 Ab 1 and 2, produced identical rates of cell lysis in this assay.

Furthermore, in the literature, it has been contested that αGD2 antibodies are able to mediate apoptosis directly on numerous cancer types, including the NB cell line iMR-32 (149,164,174,179,180,217,220). Thus, I investigated whether a combination of SMC and αGD2

A

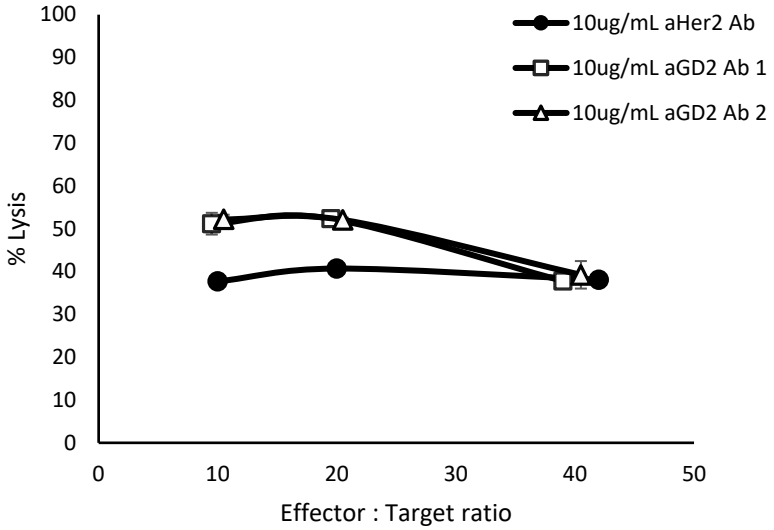
100
90
80
70
60
50
40
30
20
10
0
% Lysis
0
10
20
30
40
50
Effector : Target ratio
10ug/mL aHer2 Ab
10ug/mL aGD2 Ab 1
10ug/mL aGD2 Ab 2

B

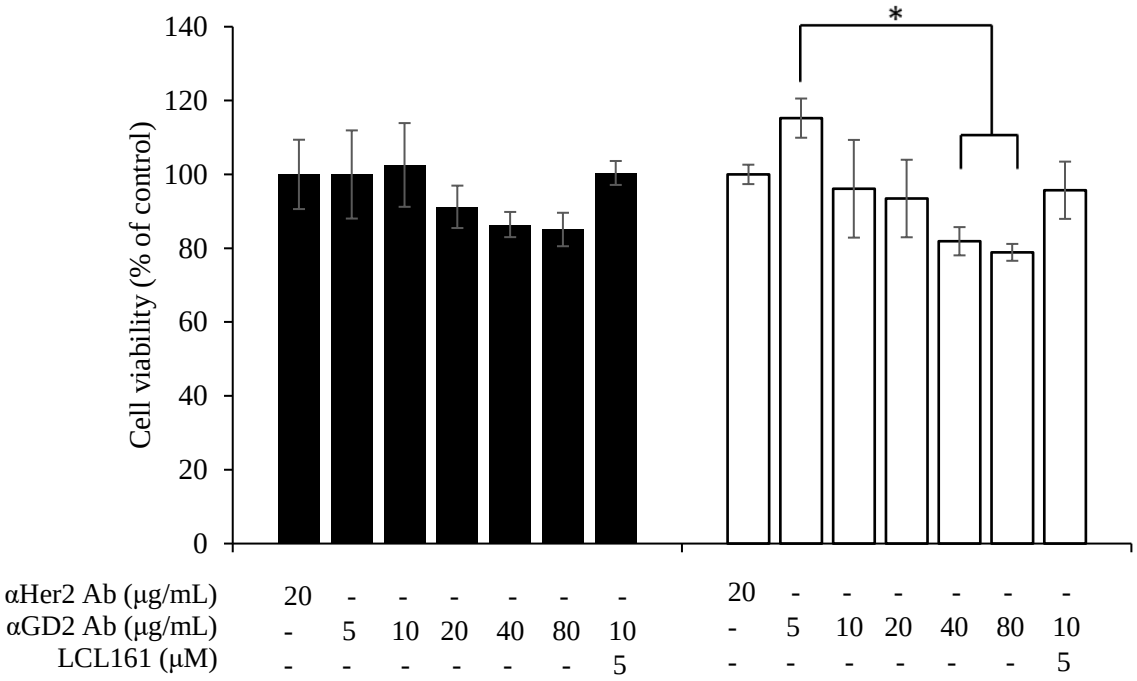
140
120
100
80
60
40
20
0
Cell viability (% of control)
*
αHer2 Ab (μg/mL) 20 - - - - - - 20 - - - - - -
αGD2 Ab (μg/mL) - 5 10 20 40 80 10 - 5 10 20 40 80 10
LCL161 (μM) - - - - - - 5 - - - - - - 5

Figure 19. ME361-S2a antibody is capable of mediating ADCC but is not directly cytotoxic. A) LAKs and NXS2 cells cocultured for 4 h with or without 10ug/mL ME361-S2a antibody. Cytotoxicity was measured using an LDH release kit. aGD2 Ab 1 and 2 conditions use isolated ME361-S2a antibody from batches 1 and 2, respectively. Representative experiment shown (n=3; Mean±SD). B) NXS2 and N2a cell lines were treated for 24-48 h with a range of ME361-S2a concentrations. Viability was measured using an alamarBlue assay. * = $p<0.05$ (n=2; Mean±SD).

antibody treatment could synergize and cause apoptosis directly to NB cells. The cells were treated with ME361-S2a and LCL161, with cell viability measured after 24 h using an alamarBlue assay.

I observed minimal cell death with the αGD2 antibody, even when used in combination with the apoptosis-promoting LCL161 (Figure 19B). At the highest antibody concentrations of 40 and 80 μg/mL, some NXS2 cell death was seen (15%). However, the $GD2^-$ cell line N2a experienced 20% cell death ($p<0.05$), indicating it was probably due to reasons unspecific to GD2 binding.

2.3.7 Dual combination of LCL161 and αGD2 antibody delays tumour growth of NXS2 in vivo

I have shown that the antibody is of high purity, can bind GD2 specifically, and is able to mediate ADCC with LAKs against a $GD2^+$ NXS2 cell line. Next, I sought to determine if the combination of LCL161 and αGD2 antibody would synergize *in vivo* against a NXS2 tumour model. NXS2-Fluc cells were implanted s.c. and treatments were started after tumours became palpable. Mice received LCL161 p.o. at 75 mg/kg four times and αGD2 antibody i.p. 200 μg six times. Tumour volumes were measured three times a week until endpoint. I observed that the combination was effective in delaying tumour growth (Figure 20B). Here, the approved treatment for NB, αGD2 immunotherapy, was the least effective treatment in delaying tumour growth against the NXS2 s.c. model and seemed to create a bimodal group of responders and non-responders (Figure 20A). The tumour volume growth curves show that the combination group is consistently right-shifted compared to the control group (Figure 20A).

2.4 Testing a triple combination to try and further potentiate αGD2 antibody and LCL161 combination-mediated delay in NXS2 tumour growth

The combination of ME361-S2a and LCL161 had some effect in delaying NXS2 s.c. tumour growth, however it was not deemed significant upon logrank analysis. I thought to combine a third

A

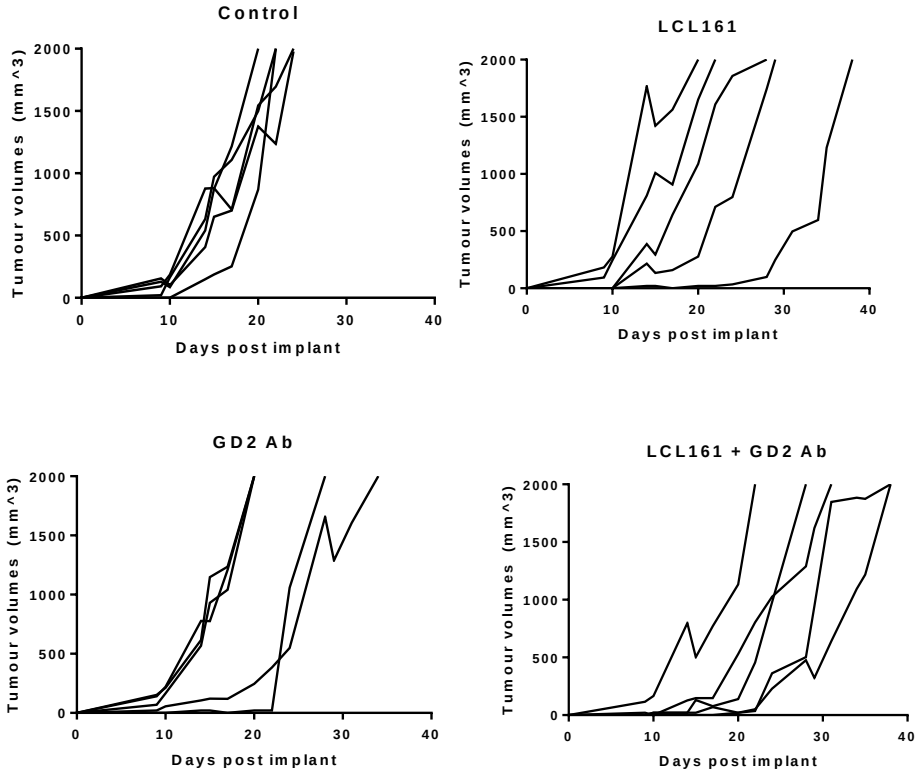
Control
LCL161
GD2 Ab
LCL161 + GD2 Ab
Tumour volumes (mm^3)
Days post implant
0
500
1000
1500
2000
0
10
20
30
40

B

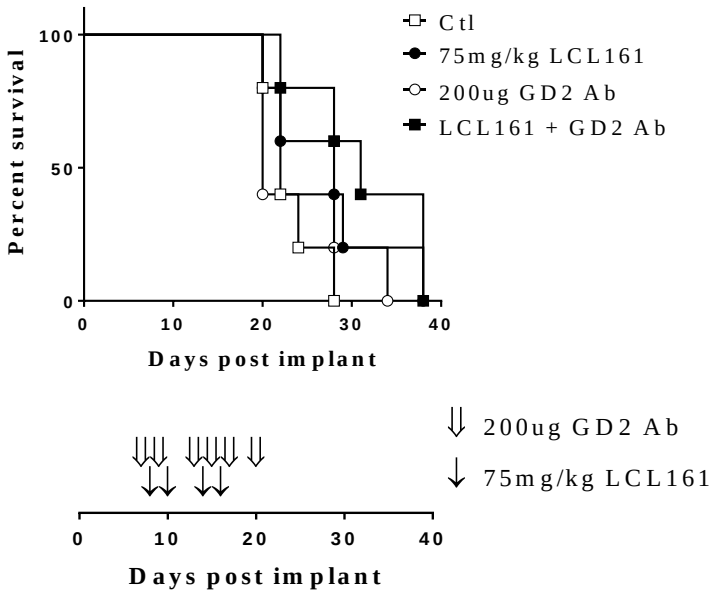
Ctl
75mg/kg LCL161
200ug GD2 Ab
LCL161 + GD2 Ab
Percent survival
Days post implant
0
50
100
0
10
20
30
40

⇓ 200ug GD2 Ab
↓ 75mg/kg LCL161
0
10
20
30
40
Days post implant

Figure 20. LCL161 and aGD2 antibody combine to delay tumour growth in NXS2 s.c. tumour model. 5 x10^5 NXS2-fluc cells were injected s.c. with measurements performed three times a week. Once tumours were palpable, 75mg/kg LCL161 was given four times p.o. and 200μg αGD2 or IgG isotype antibody was given six times i.p. N=5 mice for all groups. A) Individual tumour volume growth curves. B) Kaplan-Meier curve depicting mouse survival with associated treatment schedule.

agent to further potentiate the anti-tumour effect of this combination. Currently, there is only one approved immunotherapy for NB, the GD2-targeting dinutuximab. However, recent success occurred with combining an αGD2 antibody and an antibody targeting the PD-1 signalling axis in a preclinical setting (109). This study led to establishing a clinical trial for an αPD-1 and αGD2 combination immunotherapy (148). Studies have been successful with using αCTLA-4 and αPD-1 antibodies against NB in preclinical models (147,221). Other reports have also shown that SMCs synergize with αCTLA-4 and αPD-1 immunotherapies in glioblastoma and bladder cancer models (38,43,222). Additionally, depletion of the cIAP1 gene increased the efficacy of αPD-1 antibody treatments in melanoma tumour models (223).

Here, I investigated whether LCL161 can synergize with ICIs to treat NXS2 tumour models. The ICI with the best anti-tumour response will be used in a triple combination with LCL161 and an αGD2 antibody to treat a NXS2 s.c. tumour model.

2.4.1 LCL161 does not affect expression of MHC 1 or PD-L1 in vitro

Since I wanted to test the potential synergy of LCL161 and other immunotherapies in treating murine NB cells, I first examined whether SMCs would modulate the expression of MHC 1 and PD-L1 on NXS2 and N2a cell lines. MHC 1 is essential for presenting antigen to stimulate an immune response (29). PD-L1 inhibits the action of effector immune cells (103). Both proteins play an important part in responding to immunotherapies. The protein expression was measured by flow cytometry 24 h after treating with 5 μM LCL161 and 1 ng/mL TNFα. I also treated with 1000 U/mL IFNγ to for a control to upregulate PD-L1 and MHC 1 expression. There was no modulation of PD-L1 expression in NXS2 or N2a cells with LCL161 or TNFα (Figure 21A). For NXS2 cells, TNFα increased MHC 1 mean fluorescence intensity (MFI) by 116%, over DMSO

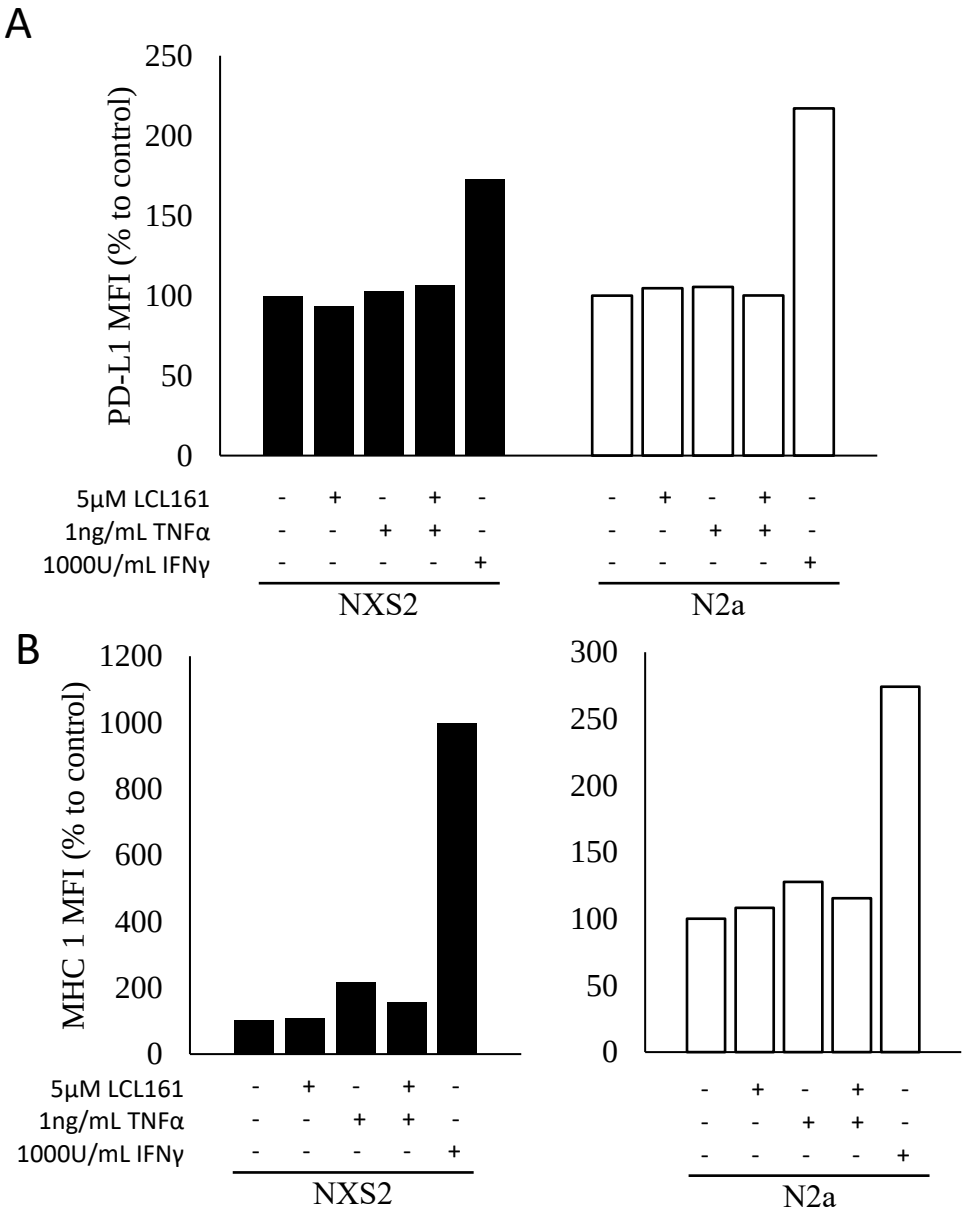
A
PD-L1 MFI (% to control)
250
200
150
100
50
0
5μM LCL161 - + - + - - + - + -
1ng/mL TNFα - - + + - - - + + -
1000U/mL IFNγ - - - - + - - - - +
NXS2
N2a
B
MHC 1 MFI (% to control)
1200
1000
800
600
400
200
0
300
250
200
150
100
50
0
5μM LCL161 - + - + - - + - + -
1ng/mL TNFα - - + + - - - + + -
1000U/mL IFNγ - - - - + - - - - +
NXS2
N2a

Figure 21. Expression of PD-L1 and MHC 1 on NXS2 and N2a cell lines responding to LCL161 in vitro. A) Normalized MFI of PD-L1-BV711 expression on NXS2 and N2a cells after 24 h of treatment (n=1; Mean). B) Normalized MFI of MHC 1-PE expression on NXS2 and N2a cells after 24 h of treatment (n=1; Mean).

control, and then the combination with LCL161 increased MHC 1 MFI by 57%. For N2a cells, a similar trend was observed where TNFα increased MHC 1 MFI by 27%, over DMSO control, and by 15% with a LCL161 combination (Figure 21B). Both cell lines responded to IFNγ by drastically increasing MHC 1 and PD-L1 MFI

2.4.2 αPD-L1 antibody is the most effective ICI in combination with LCL161 against NXS2 s.c. model

After confirmation that LCL161 would not impact MHC 1 or PD-L1 expression, I sought to determine which ICI would be most effective with LCL161 to treat the NXS2 s.c. tumour model. Delays in growth of NXS2 and N2a tumours has been reported with αPD-1 (109,147), αCTLA-4 (140,221), and αPD-L1 (147,221) antibody treatments in other preclinical studies. As well, SMCs have been found to synergize with these immunotherapies (39,43,222). Thus, I used survival studies to determine which combination of ICI and LCL161 was most effective at delaying murine NB tumour growth. NXS2 cells were implanted s.c. and treatments were started after tumours became palpable. I treated with LCL161 at 50 or 75 mg/kg p.o. four times and αPD-1, αCTLA4, αPD-L1 antibodies at 250 μg i.p. six times. The first survival study had treatments of 50 mg/kg LCL161, and since responses were marginal, I increased the LCL161 concentration to 75 mg/kg for the second study. Tumour volumes were measured three times a week until endpoint. The first survival study examined αCTLA-4 clone 9H10 and αPD-1 clone J43 antibody with LCL161 against NXS2 s.c. model. Treatments were stopped early when it was apparent that both combination groups were ineffective in delaying tumour growth (Figure 22A). Using a second survival study, I then examined the anti-tumour effect of αPD-L1 clone 10F.9G2 and αPD-1 clone RMP114 antibodies in combination with LCL161 against NXS2 s.c. tumours. Here, slightly

A

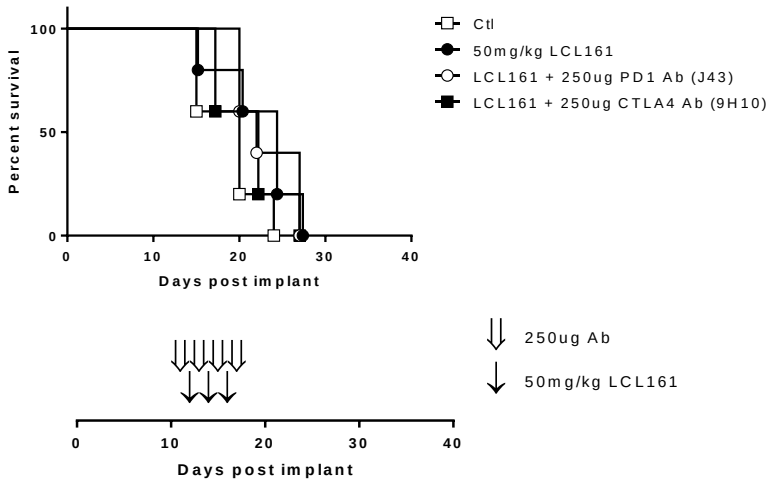
Percent survival
100
50
0
0
10
20
30
40
Days post implant
Ctl
50mg/kg LCL161
LCL161 + 250ug PD1 Ab (J43)
LCL161 + 250ug CTLA4 Ab (9H10)

0
10
20
30
40
Days post implant
250ug Ab
50mg/kg LCL161

B

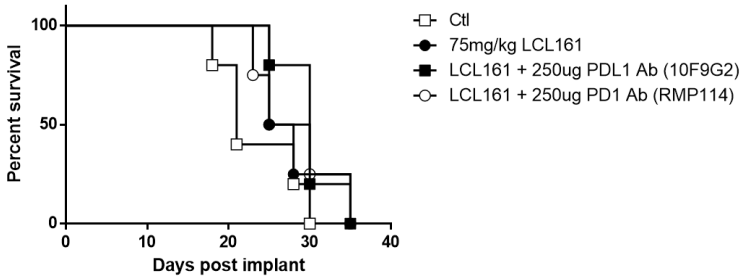
Percent survival
100
50
0
0
10
20
30
40
Days post implant
Ctl
75mg/kg LCL161
LCL161 + 250ug PDL1 Ab (10F9G2)
LCL161 + 250ug PD1 Ab (RMP114)

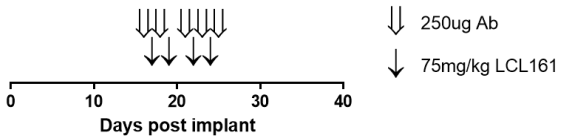
0
10
20
30
40
Days post implant
250ug Ab
75mg/kg LCL161

Figure 22. αPD-L1 antibody is the most effective ICI with LCL161 against NXS2 s.c. tumour model. 5 x10^5 NXS2-fluc cells were injected s.c. with measurements performed three times a week. Kaplan-Meier curve depicting mouse survival with associated treatment schedule. Treatments started once tumours were palpable. A) 50mg/kg LCL161 was given four times p.o. and 250μg of αPD1 (clone J43), αCTLA-4, or hamster IgG antibody per injection was given six times i.p. N=5 mice for all groups. B) 75mg/kg LCL161 was given four times p.o. and 250ug of αPD1 (clone RMP114), αPD-L1, or rat IgG antibody was given six times i.p. N=5 mice for control and αPD-L1 + LCL161 groups. N=4 mice for LCL161 and αPD-1+LCL161 groups.

improved responses were observed for both αPD1 clone RMP114 and αPD-L1 clone 10F.9G2 combinations with LCL161 compared to the untreated condition (Figure 22B). The αPD-L1 antibody with LCL161 combination was the most effective of the ICIs tested, and thus it was followed up with a survival study using monotherapy control groups.

2.4.3 Further examination of αPD-L1 antibody and LCL161 combination in delaying NXS2 tumour growth

The αPD-L1 antibody was the most effective ICI in combination with LCL161 to treat the NXS2 s.c. model. I wanted to further examine how more effective the combination was in comparison to either αPD-L1 or LCL161 monotherapies. I implanted the NXS2 cells orthotopically and began giving treatments a week later to allow tumour establishment. I gave LCL161 at 75 mg/kg p.o. four times and αPD-L1 antibodies at 250 μg i.p. six times. Mice were observed for moribund characteristics for designation of humane endpoints. I found that the combination group delayed tumour growth and increased mouse survival (Figure 23, p=0.07). Furthermore, the combination treatment also cured one of five mice, which was confirmed with IVIS imaging. I then rechallenged the mouse with N2a and NXS2 cells s.c. into right and left flank, respectively, and observed tumour growth only occur by N2a cells on the right flank (data not shown). Tumour cells used for rechallenge were not Fluc-tagged to avoid any immune memory response being non-tumour antigen specific.

2.4.4 Addition of αPD-L1 antibody slightly improves LCL161 and αGD2 antibody combination in delaying tumour growth against NXS2 s.c. model

I have shown delays in tumour growth with either αGD2 and αPD-L1 antibodies used in combination with LCL161 in treating NXS2 cells *in vivo*. I wanted to further potentiate the efficacy of these treatments by using a triple combination. Some studies have suggested that inhibiting the

PD-1 signalling axis is effective against preclinical NB (147), even showing synergy with αGD2 antibody against an NXS2 model (109). Further support for using a LCL161, αPD-1 antibody and αGD2 antibody combination is seen with: drugs targeting tumour angiogenesis are also currently being researched in combination with dinutuximab (216), LCL161 has shown to promote NK cytotoxicity (61,62), XIAP resists ADCC (64), and LCL161 synergizes with ICIs in delaying tumour growth (38,43). Thus, I tested the triple combination of LCL161 with both αGD2 and αPD-L1 antibodies. NXS2 cells were implanted s.c. and treatments were started after tumours were palpable. Each of 75 mg/kg LCL161 p.o., 200 μg αGD2 i.p., and 250 μg αPD-L1 i.p. were given four times. Tumour volumes were measured three times a week until endpoint. The triple combination was most successful at delaying tumour growth, deemed significant with a logrank comparison (Figure 24, $p=0.03$). However, a Holm-Sidak multiple comparison showed no significance amongst groups. The group receiving the triple combination treatment had the most right shifted growth curves versus the other treatment groups. One mouse receiving LCL161 and αGD2 antibody treatments had complete inhibition of tumour growth. Currently, I am rechallenging the mouse with NXS2 and N2a cells injected s.c. to determine if a memory immune response was formed.

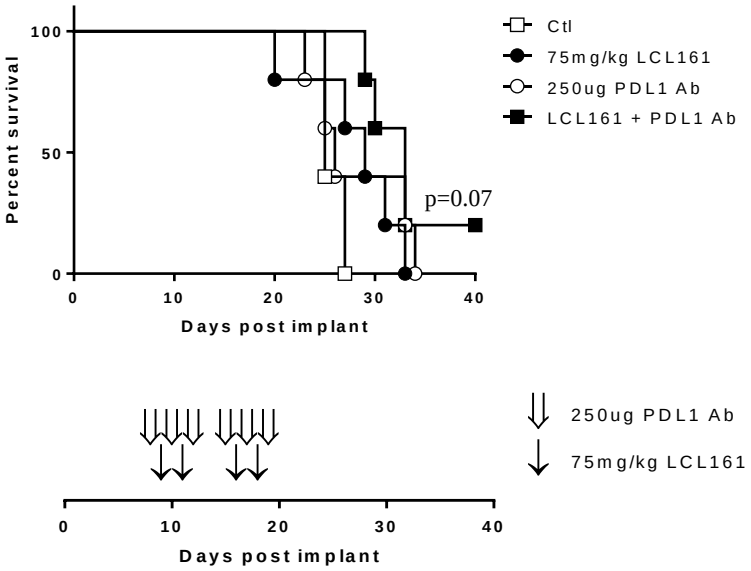
Percent survival
100
50
0
0
10
20
30
40
Days post implant
p=0.07
Ctl
75mg/kg LCL161
250ug PDL1 Ab
LCL161 + PDL1 Ab
250ug PDL1 Ab
75mg/kg LCL161
0
10
20
30
40
Days post implant

Figure 23. Combination of LCL161 and αPD-L1 antibody against NXS2 orthotopic tumour model slightly extends mouse survival. 5 x10^4 NXS2-fluc cells were injected into the adrenal gland and given 7 d to establish before treatments. 75mg/kg LCL161 was given four times p.o. and 250ug of αPD-L1 or rat IgG antibody was given six times i.p. N=5 mice for all groups. Kaplan-Meier curve depicting mouse survival with associated treatment schedule. * = $p<0.05$.

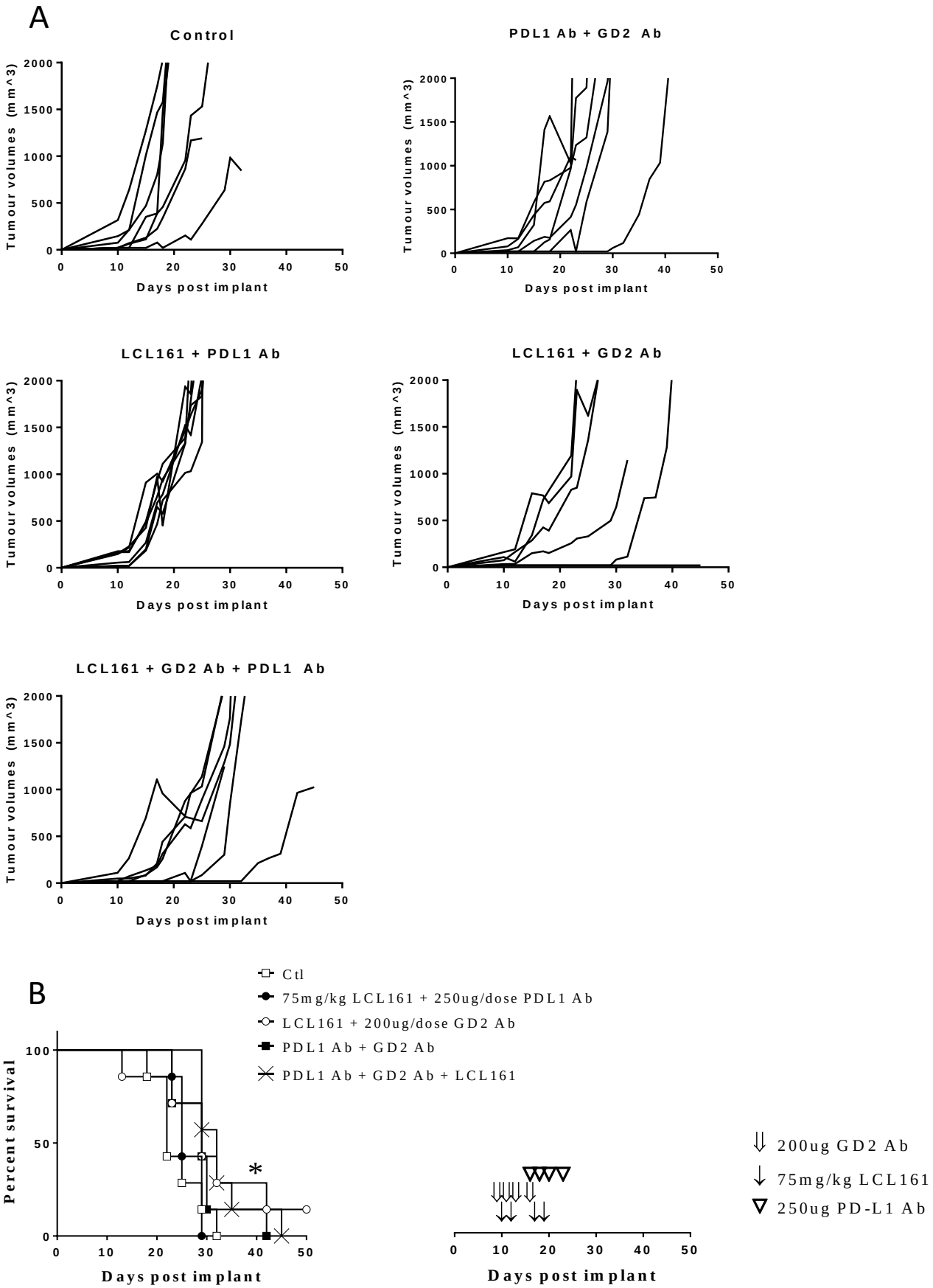
A
Control
PDL1 Ab + GD2 Ab
LCL161 + PDL1 Ab
LCL161 + GD2 Ab
LCL161 + GD2 Ab + PDL1 Ab
Tumour volumes (mm^3)
Days post implant
B
Ctl
75mg/kg LCL161 + 250ug/dose PDL1 Ab
LCL161 + 200ug/dose GD2 Ab
PDL1 Ab + GD2 Ab
PDL1 Ab + GD2 Ab + LCL161
Percent survival
*
200ug GD2 Ab
75mg/kg LCL161
250ug PD-L1 Ab

Figure 24. Triple combination of αGD2 antibody, αPD-L1 antibody. and LCL161 further delays NXS2 s.c. tumour growth. 5 x10^5 NXS2-fluc cells were injected s.c. with measurements performed three times a week. Once tumours were palpable, 75mg/kg LCL161 was given four times p.o., 200μg of αGD2 or mouse IgG antibody was given four times i.p., 250μg of αPD-L1 or rat IgG antibody was given four times i.p. N=7 mice for all groups. A) Individual tumour volume growth curves. B) Kaplan-Meier curve depicting mouse survival with associated treatment schedule. * = $p<0.05$.

3.0 DISCUSSION

3.1 Overview

There are approximately 800 new cases of neuroblastoma (NB) diagnosed each year in the United States, which accounts for 6% of pediatric cancers and 15% of all pediatric cancer deaths. This is despite aggressive treatment approaches including surgery, chemotherapy, radiation and immunotherapy. (130,224).

Immunotherapies are effective tools against cancer. Many immunotherapy strategies have already been investigated against NB such as: ICIs (109,140,141,221), tumour vaccinations (225), adoptive cell therapies (226,227), and monoclonal antibodies (156,176). In 2015, the biologic dinutuximab (United Therapeutics), which targets GD2, was approved for use against high-risk NB (149,150). However, this immunotherapy only leads to a 20% increase in two-year survival of high-risk patients despite having serious side effects due to the localization of GD2 on peripheral nerves. Preclinical and clinical studies have focused on ways to improve αGD2 therapy, such as combinations with anti-vascular drugs or other immunotherapies (109).

IAP proteins are found to be overexpressed in numerous cancer types, including some NB tumours and NB cell lines (5,204,205). The IAP protein family is capable of not only preventing apoptosis but also modulating NF-κB signalling (3,4,33). Antagonizing IAP proteins with a SMC has previously been found to be efficacious in combination with various immunotherapies (38,40,41). In the context of NB, however, SMCs have had minimal cytotoxicity (132). Here I investigated whether using a SMC could synergize with an approved immunotherapeutic for NB in a preclinical mouse model.

3.2 SMC as a monotherapy against NB

3.2.1 In vitro efficacy of SMC

I first investigated whether the SMC, LCL161, would be effective at killing murine NB cell lines *in vitro*. I found that both NXS2 and N2a cells were resistant to LCL161 and TNFα (Figure 4). Previous studies have investigated SMC cytotoxicity against NB cell lines and found some cell death responses only at a high concentration of 10 μM LCL161 (5,134). The SMC, LBW242, was minimally cytotoxic as a monotherapy, but LBW242, as well as other SMCs did synergize with various chemotherapeutics. For example, the combination of LCL161 and vincristine was able to abrogate vincristine-resistance in NB cell lines (CHLA-15 and CHLA-20) recovered from a patient (45). The Eschenburg lab also screened several chemotherapy drug classes to determine that the vinca alkaloid class was most effective in combination with LCL161 (204). The combination of LCL161 and vinca alkaloid killed the following human and *de novo* NB cell lines: Kelly, NB1691, SH-EOP, SK-N-AS, SK-NBE2-M17, SK-N-SH, HGW-1, and HGW-2 (6) Limited *in vitro* responses to two SMCs were also seen in the human NB cell lines SK-N-AS and CHP-212 (137). The cell lines GI-ME-N and SK-N-AS, were also found to have some sensitivity to the SMC AEG40730 (205). Interestingly, in this study, all NB cell lines (GI-LI-N, IMR-32, Lan-1, Lan-5, SHY-SY5Y, SK-NB2) that were completely resistant to the SMC AEG40730-mediated cell death were missing core components to the TNFα-mediated apoptosis pathway such as TNF-R1, caspase-8, and TRADD. The cell lines GI-ME-N, Lan-1, Lan-5, SK-N-AS, and SK-NB2 also expressed cFlip, a critical apoptotic resistance factor. The cell lines that showed some cell death in response to AEG40730 in combination with TNFα or TRAIL, GI-ME-N and SK-N-AS, were not missing any of the assessed apoptotic components. However, these cell lines could also be further sensitized to SMCs through silencing of cFlip by siRNA (205).

Next, I investigated whether other apoptosis-inducing cytokines or compounds could sensitize NXS2 and N2a cells to LCL161. A previous study showed that knockdown of Bcl-2 by siRNA sensitized SMC-resistant Huh-7 and SK-Hep1 hepatocellular carcinoma cells to LCL161 (228). IFNγ-induced expression of caspase-8 made the human NB cell line, IMR-32, sensitive to TRAIL-mediated apoptosis (229). As well, GI-ME-N and SK-N-AS were also susceptible to TRAIL and AEG40730 combination (205) When combined, chemotherapies and SMCs have been shown to kill several human NB cell lines *in vitro*, albeit when using the higher concentration of 10 μM LCL161 (6). My attempts at combining LCL161 with IFNγ, IFNβ, and TRAIL were unsuccessful at promoting cell death in NXS2 and N2a cell lines. Introducing a Bcl-2 inhibitor or various chemotherapies had limited response against these cell lines as well (Figure 5). This is not surprising as NB cell lines sensitive to Bcl-2 inhibitors are typically those with *MYCN* amplification, which is not seen in NXS2 and N2a cells. As well, the three chemotherapies that I tested (topotecan, irinotecan, and SN-38) were all topoisomerase inhibitors. It was observed that a screen of chemotherapy classes with LCL161 had marginal synergy in killing NB cell lines *in vitro* when using topoisomerase inhibitors in the human NB cell lines (6) – perhaps using vinca alkaloid chemotherapeutics would improve the drug responses.

Since the cells lines that I tested were poor responders to LCL161-mediated cell death, I investigated whether the core components to the apoptosis pathway were intact (Figure 6). By western blot analysis, I found that cIAP1/2 and XIAP were expressed in both cell lines, but at a lower level than that of the control murine breast mammary carcinoma cell line, EMT6. However, a previous study reported that the level of IAP expression does not correlate with response sensitivity to SMCs (205) The proteins TRADD, TNFR1, and caspase-8 were all expressed in both NXS2 and N2a cell lines. These components are essential for apoptosis signalling and were the

proteins most commonly silenced in human NB cell lines resistant to SMCs (205). Although the core components were expressed, no PARP cleavage was seen in response to LCL161 treatment by NXS2 or N2a cells. Moreover, N2a cells also did not degrade cIAP1/2 proteins after addition of LCL161. NXS2 cells did respond to LCL161 treatment with downregulation of cIAP1/2 proteins but still could not undergo apoptosis, as assessed by the lack of PARP cleavage, which only occurred in these cells following staurosporine treatment (Figure 7). PARP is a target for caspase cleavage and is used as an indicator for caspase activation and apoptosis (230). Staurosporine is capable of inducing both intrinsic and extrinsic apoptosis (208). If only the intrinsic apoptosis pathway is functional in these cell lines, it could account for PARP cleavage present in staurosporine conditions but not that of LCL161. The caspase inhibitor cFlip was also expressed by both murine NB cell lines and could account for the murine NB cell lines resistance to SMCs (205). Verification of cFlip as a resistant factor to SMCs could be achieved with specific knockdown by siRNA. In conclusion, the *in vitro* testing shows that NXS2 and N2a cells were resistant to induction of apoptosis by LCL161.

3.2.2 Potentiating the anti-vascular effect of LCL161

Next, I investigated the *in vivo* responses of NB to LCL161. Different sensitivities to SMCs have been found both *in vitro* and *in vivo* (39,132), results that have been previously published and seen by our lab as well. Durable cures have been achieved in transgenic multiple myeloma cell lines, which were resistant *in vitro* to LCL161 (39). The different sensitivities to LCL161 can be due to the reported ability of SMCs to modulate the tumour microenvironment, from the targeting of tumour vasculature (55,210) to the recruitment of tumour infiltrating lymphocytes (38,80,231). Interestingly, a study found a significant decrease in NXS2 tumour volume when the subcutaneous model was treated with LCL161, with or without the chemotherapeutic vincristine (5). However,

it should be noted that these treatments were started the day after cell injection. This could create a scenario of treating the cells before the tumour is fully established. In my project, the sub-cutaneous model of NXS2 was the most responsive to LCL161 monotherapy (Figure 9A). Interestingly, it was also the most vascularized NB tumour that was examined. The ability of SMCs to target tumour vasculature should not be overlooked. SMCs have been investigated for their ability to reduce the tumour vasculature, with studies showing SMC-induced destruction of vascular endothelium occurs in a TNFα-dependent manner (55,210). Thus, I decided to investigate if the ability of LCL161 to cause tumour vascular collapse could be responsible for the delay in tumour growth. I observed, by performing a necropsy on mice at endpoint, that tumours had decreased vasculature in response to LCL161 treatment. I was able to corroborate this finding with ultrasound imaging that showed a decreased rate of perfusion in the tumour of a mouse that received LCL161 (data not shown). I decided to further potentiate this anti-angiogenic effect of LCL161 by combining LCL161 with the anti-angiogenic drug, sunitinib. Although not currently being investigated against NB in the clinic, sunitinib has been approved for renal cell carcinoma and gastrointestinal stromal tumours (212,232). The combination of LCL161 and sunitinib was superior in delaying tumour growth in the NXS2 s.c. model than either treatment alone (Figure 10). Unfortunately, it was too costly for our lab to obtain αVEGF antibody, which would have been a more clinically relevant and specific tool for targeting NB tumour vasculature (190–192). One limitation of sunitinib is that, as a kinase inhibitor, it has a broad range of effects not related to targeting tumour vasculature. Sunitinib has been shown to decrease Treg cell levels, reduce production of tumour growth factor-β and IL-10 (233) and promote a type-1 immune response in models of murine hepatocellular carcinoma and renal cell carcinoma (234). Sunitinib is also able to deplete myeloid-derived suppressor cells in a human papillomavirus-induced cancer (213).

Thus, there is potential for the *in vivo* anti-tumour response of sunitinib to be due to the down-regulation of immunosuppressive populations (like Tregs and myeloid derived suppressor cells) and the promotion of anti-tumour type-1 responses. Coincidentally, SMCs have been shown to reduce Treg populations, with IAPs proving essential for suppressive ability of Tregs (80,235). Combining a SMC with αCTLA-4 antibody (a Treg-targeting therapy) has been found to be efficacious in delaying tumour growth by our lab (222). Thus, it should be investigated if LCL161 is synergizing with sunitinib by targeting tumour vasculature, by inhibiting immunosuppressive populations, or by both mechanisms.

Due to the vascularity of NB tumours, targeting angiogenesis is considered a viable therapeutic strategy (184,186,211). Currently, there are 18 clinical trials involving NB and angiogenesis targeting listed on the National Institute of Health website for clinical trials (198), with the most common agent being bevacizumab, an αVEGF antibody. *MYCN* amplification, a common mutation in NB, promotes an angiogenic tumour microenvironment (188) and induces down-regulation of endothelial growth inhibitors like activin A (187). Sunitinib has been used to counteract the pro-angiogenic environment produced from *MYCN* amplification by degrading N-myc (195). Sunitinib has also been shown to have anti-cancer effects *in vivo* and *in vitro* against NB by inhibiting cell proliferation and phosphorylation of VEGF-receptors (196).

Overall, LCL161 can impair angiogenesis in the NXS2 s.c. tumour model and the combination with sunitinib can further delay tumour growth. However, sunitinib is not currently approved for NB nor is it in clinical trials. Thus, I decided to explore more clinically relevant therapy combinations with LCL161 to treat NB cells.

3.3 LCL161 and αGD2 antibody combination against NXS2 s.c.

The most recent approved therapy for NB is αGD2 immunotherapy using the monoclonal antibody dinutuximab (149,150). This biologic has a reported mechanism of action of ADCC and CDC. Studies have shown that LCL161 can promote human NK cytotoxicity against rhabdomyosarcoma and Hodgkin's lymphoma cell lines (61,62). XIAP was also found to be a resistant factor to αHer2-targeting ADCC in cancer cells (64). Thus, I decided to explore the combination of LCL161 and αGD2 antibody against NB.

3.3.1 Isolation and validation of GD2-targeting antibody

I was unable to obtain the clinical grade αGD2 antibody, ch14.18 (United Therapeutics) due to its proprietary nature. Other hybridomas producing 14G2a or 3F8 were also unobtainable during my project due to proprietary constraints. However, I acquired the hybridoma HB-9326 (from ATCC) which produces the αGD2 antibody clone ME361-S2a of mouse isotype IgG2a. I validated the purity of the antibody using SDS-PAGE, with three specific bands appearing in the expected regions for the heavy and light chains (Figure 11).

Interestingly, I found that the GD2 epitope for antibody staining is impacted by how the cell is prepared for staining. Different techniques and intensities used to lift cells modified the proportion of the cells positive for GD2, with trypsin being most harsh having the lowest yield and an enzyme-free dissociation buffer or light scraping having the highest $GD2^+$ population (Figure 14). Coincidentally, a study found that GD2 is involved in cell adhesion, with αGD2 antibodies able to prevent cell attachment or induce cell-lifting of adherent melanoma cells and the human NB cell line SK-N-AS (183). Interestingly, the GD2-targeting antibody, 3F8, was also found to bind the glycoprotein neural cell adhesion molecule (NCAM), which is involved in cell adhesion (236). Knockdown of the GM2-GD2 synthase, impairing GD2 synthesis, also led to increased anoikis

(detachment-induced apoptosis) in renal adenocarcinoma cells (182). I then tried intracellular staining of GD2 since extracellular staining of GD2 was affected by cell preparation. However, here I found the $GD2^-$ cell line, N2a, stained positive with either isolated or commercial αGD2 antibodies (Figure 15). Interestingly, by adding unconjugated iso-clonal or non-clonal antibodies before intracellular staining, I could decrease the proportion of the $GD2^+$ positive population in both the NXS2 and N2a cell lines. This suggests that although the αGD2 antibodies are staining a non-GD2 epitope incorrectly inside the cell, they are still staining a target specifically. Studies have stated that extracellular staining of the antibody clone 14G2a could bind to CD166/activated leukocyte cell adhesion molecule (ALCAM), or 3F8 could bind NCAM (179,237,238). Although those targets are transmembrane proteins, one source has suggested that ganglioside antibodies can also recognize cytosolic proteins, such as carbonic anhydrous II (239). Thus, numerous studies have reported αGD2 antibodies bind targets that are not GD2. This could explain the occurrence of a $GD2^+$ population in the $GD2^-$ N2a cell line only during intracellular GD2 staining. Therefore, staining for GD2 should be thoroughly planned. One should have consideration for adherent cell preparation and fixation of cells or tissue, and caution should be taken to account for false-positive signals. Studies have reported very high rates of $GD2^+$ cells when staining with fixed-cell immunohistochemistry (240,241), and very low rates of extracellular stained $GD2^+$ cells in the NXS2 cell line (109). Without appropriate precautions for GD2 staining, results could be misleading. However, my isolated ME361-S2a antibody stained similarly to that of the commercially available 14G2a clone, suggesting the antibodies were equivalent in specificity and sensitivity.

Next, I verified if the antibody was capable of mediating ADCC. Here, I observed that different batches of isolated ME361-S2a antibodies increase the LAK mediated-cytotoxicity compared to

controls (Figure 19A). The elevated cytotoxicity measurements observed when the antibody is present in the coculture indicates that the isolated ME361-S2a antibody is in proper conformation to mediate ADCC. However, αGD2 antibodies have been suggested to have other functions, which has been debated in the literature. Some papers claim that αGD2 antibodies, such as the ME361-S2a clone, could directly induce apoptotic effects in cancer cells. One study found that αGD2 antibody-mediated apoptosis to be dependent on focal adhesion kinase (FAK) dephosphorylation, p38 activation, and anoikis in $GD2^+$ small cell lung cancer cell lines (SCLC) (242). The same group found that SCLC cell lines transfected with a GD3 synthase gene had higher expression of GD2 and GD3 gangliosides and increased proliferation. This increase in proliferation could then be abrogated by their αGD2 antibody (181). Another group found the αGD2 antibody clone 14G2a could produce 20% and 50% cell death at 5μg/mL and 40μg/mL respectively, in the human NB cell line, IMR32 (180). They observed a significant decrease in cell attachment and an increase in caspase-3 after antibody treatment. Also, the tumoricidal effect of 14G2a synergized with various chemotherapeutics in killing IMR-32 cells The ME361-S2a clone killed 15-18% of cells *in vitro* at 5μg/mL after 24 h in a mouse lymphoma (EL-4), human NB (IMR-32), and human melanoma (mS) cell line (179). Interestingly, the ME361-S2a clone Fab fragments were reported to reduce cell proliferation and induce apoptosis in EL-4 cells after 24 h (174). However, the patent for ME361-S2a does not mention a mechanism of direct cell cytotoxicity (220), and the FDA approval for dinutuximab specifically states that there was no evidence of tumour inhibition in the absence of effector cells or complement proteins (149). I found that the ME361-S2a antibody was not capable of promoting cell death in both the N2a and NXS2 cell lines, even when used with the apoptotic agent LCL161 (Figure 19B). I also attempted the assay in IMR-32 cells and observed no response (data not shown). To confirm that the isolated ME361-S2a clone cannot promote cell

death, I should repeat the experiment but with using the EL-4 cell line. EL-4 cells are supposedly the most responsive $GD2^+$ cell line to αGD2 antibody cytotoxicity in the literature. Thus, although I had isolated a pure and specific antibody that was capable of mediating ADCC, apoptosis could not be induced in the available $GD2^+$ cell models.

3.3.2 Treating NXS2 s.c. model with a dual combination of LCL161 and αGD2 antibody.

After successfully isolating a pure and functional αGD2 antibody, I investigated its ability to synergize with LCL161 in treating mice bearing NXS2 tumours. Prior to the survival study, I examined whether LCL161 would modulate GD2 expression on cancer cells. I used a model of suspension cell lines, RMA and RMA/S, to avoid the problematic staining limitations of the adherent NB cell lines. These murine lymphoma cell lines, RMA and RMA/S, were previously reported to express GD2 (218). I confirmed that these cells expressed GD2 and that the GD2 staining was consistent (data not shown). The GD2 expression of RMA and RMA/S cell lines was increased and decreased, respectively, *in vitro* by LCL161 treatment (Figure 16A). However, I showed with a viability assay that these cells were sensitive to SMCs, which is not seen in NXS2 and N2a cell lines (Figure 16B). I used Necrostatin-1 to rescue cell death and observed that the increase and decrease in GD2 expression modulated by LCL161 was negated. This suggests that the change in GD2 expression might be a response to cell death and not direct modulation by LCL161.

Regulation of GD2 expression has been studied in breast cancer stem cells and cell lines. These studies have reported NF-κB as an activator for GD3 synthase expression through the transcription factor forkhead box protein C2 (FOXC2) (153,243). GD3 synthase synthesizes the GD2 precursor GD3 and was suggested to be a rate limiting step in the GD2 synthesis process (244). One paper inhibited NF-κB signalling by silencing IKKα expression or by treating with BMS-345541 and

found significant decreases in the expression of GD3 synthase and GD2 in breast cancer stem cells (245). Due to their methods, however, no conclusion can be made if it is canonical, alternative, or both NF-κB pathways involved in modulating GD2 expression. IKKα is involved in both NF-κB pathways (32) and BMS-345541 targets both IKKα and IKKβ (246). However, recently it was seen that TNFα could increase GD2 expression in some, but not all, breast cancer cell lines (247). Thus, more investigation is required to determine the true impact of SMC-mediated modulation of GD2 expression. Analysis of GD3 synthase expression and NF-κB activation in the RMA, RMA/S, NXS2 and N2a cell lines would complement my results. As well, I could repeat the previous studies that used a breast cancer model with a NB model to validate their findings.

Next, I used the dual combination of αGD2 antibody and LCL161 to treat mice bearing NXS2 s.c. tumours. The combination treatment delayed tumour growth more than either monotherapy, but it was not deemed significant using logrank analysis (Figure 20). However, there is opportunity for SMCs and αGD2 antibody to synergize in treating NB tumours. XIAP, a target for SMCs, is a resistant factor to κHer2-ADCC. XIAP inhibits activation of caspases-3, -7, and -9 and suppresses reactive oxygen species accumulation (64). The SMC used in my project, LCL161, can antagonize XIAP but preferentially targets cIAP1/2. Perhaps using a SMC which better targets XIAP would further potentiate the combination efficacy in killing NB tumours. Additionally, the αVEGF antibody, bevacizumab, was found to remodel tumour vasculature and promote the anti-tumour effects of GD2-chimeric antigen receptor (CAR) T-cells against IMR-32 and HTLA-230 xenograft models (248). CAR T-cells are T-cells with an engineered antigen receptor that recognizes a designated antigen (249). In support, there is also currently a clinical trial investigating dinutuximab and lenalidomide, which is an anti-angiogenic compound (216). These studies support the use of an αGD2 antibody combination with LCL161 due to the anti-vascular ability of

SMCs. Also, dinutuximab therapy includes a combination with IL-2, GM-CSF and retinoic acid (149,176). IL-2 and GM-CSF are used to stimulate NK cell and neutrophil populations. Studies have shown that SMCs improve target cell sensitivity to NK-mediated cytotoxicity and, in combination with IL-2, increase NK cytotoxicity potential *in vitro* using rhabdomyosarcoma and hepatocellular carcinoma models (61,62). As well, it was reported that neutrophil cytotoxicity and recruitment was promoted with the addition of a SMC against a bladder and ovarian cancer model, respectively (231,250). Despite the complementary features of LCL161 and αGD2 therapies, further work is required for the combination to create significant delays in tumour growth.

3.4 Treating the NXS2 s.c. model with a triple combination of LCL161, αGD2 antibody, and αPD-L1 antibody

3.4.1 NXS2 tumour models treated with dual combination of LCL161 and ICIs

I investigated if I could further improve the efficacy of the LCL161 and αGD2 antibody combination by addition of an ICI. First, I explored if SMCs would impact the expression of MHC or PD-L1, two molecules vital for mediating sensitivity to immunotherapies. MHC presents antigen to immune cells (29), while PD-L1 binds the immune checkpoint PD-1 (103). The NF-κB pathway regulates expression of important immune molecules such as MHC (28–30,251). Literature has also reported that the cytokine TNFα is capable of modulating expression of MHC molecules, albeit independently from NF-κB signalling (252). However, SMCs, capable of modulating NF-κB signalling and inducing TNFα expression, were not found to promote MHC expression in a rhabdomyosarcoma cell line (61). Similarly, I observed TNFα promote expression of MHC on the murine NB cell lines *in vitro*, while LCL161 had no effect or even dampened the MHC expression response to TNFα (Figure 21B). NF-κB and TNFα have also been shown to promote PD-L1 stabilization and expression on cancer and immune cells (107,253,254). However,

no change in PD-L1 expression was seen on murine NB cell lines from LCL161 and TNFα treatment *in vitro* (Figure 21A). This may be because both NXS2 and N2a cell lines were found to express PD-L1 even when untreated, and the PD-L1 stabilization may not impact overall expression. However, IFNγ treatment increased expression levels of MHC 1 and PD-L1 on both NXS2 and N2a cell lines, indicating that the MHC 1 and PD-L1 expression could be induced in these cell lines. This indicates that LCL161 does not modulate the expression of MHC 1 or PD-L1 on NXS2 and N2a cells.

I then determined which ICI (αCTLA-4, αPD-1, or αPD-L1 antibody) synergized best with LCL161 in treating NXS2 s.c. tumours. The first survival study examined NXS2 tumour growth in mice treated with αCTLA-4 (clone 9H10) antibody or αPD-1 (clone J43) antibody in combination with LCL161. I observed minor delays in tumour growth (Figure 22A). The next survival study examined αPD-1 (clone RMP114) antibody or αPD-L1 (clone 10F.9G2) antibody in combination with LCL161. The RMP114 clone of αPD-1 antibody was used because it was found to better target NK cells than the J43 clone (Dr, Michele Ardolino, oral communication, January 2017). There were improved delays in tumour growth for both combinations relative to the first survival study. The combination of αPD-L1 antibody and LCL161 was the most efficacious ICI and SMC combination tested (Figure 22B). I re-examined the αPD-L1 antibody with LCL161 combination in treating an orthotopic NXS2 model and included the proper monotherapy control groups. Here, I found the combination increased mouse survival relative to either monotherapy or untreated groups, however it was not deemed significant by logrank analysis (Figure 23). Additionally, one of the five mice in the group receiving the combination treatment was cured. The cured mouse was rechallenged with both NXS2 and N2a s.c. tumours and only the N2a tumour grew, indicating an immune memory response was established.

Studies are investigating ICIs as a potential therapy for NB patients. Several studies report expressions of PD-L1 and PD-1 molecules in NB patient tumour microenvironments and that the presence of these molecules correlate with poor survival (142,255). Five clinical trials are currently studying the use of ipillimumab (αCTLA-4) or nivolumab (αPD-1) therapy in patients with NB (256). Previous preclinical studies have treated NXS2 and N2a tumour models with ICIs in combination with histone deacetylase inhibitors (257), other ICIs (221), αCD4 depletion (147) or αGD2 antibody (109). However, it is not surprising that I observed a limited response to a single ICI and LCL161. One study reported responses in both NXS2 and N2a models only when an αPD-1/PD-L1 antibody and αCD4 antibody combination treatment was used. They deduced that inhibition of the PD-1 signalling axis and all $CD4^+$ suppressive subpopulations was required for achieving optimal survival responses with using ICIs against the NB tumour models. Even a combination of αPD-1 antibody with αCD25 antibody, an approach targets Tregs, was ineffective in extending mouse survival (147).

3.4.2 NXS2 s.c. tumours treated with a triple combination of αPD-L1, αGD2 antibodies and LCL161

I proceeded to use the αPD-L1 antibody to further potentiate the anti-tumour effects of the dual combination treatment of αGD2 antibody and LCL161. I observed the triple combination improve the delay in NXS2 s.c. tumour growth relative to all dual combinations tried (Figure 24). However, in the LCL161 and αGD2 combination treatment group, one of the seven mice did respond with a cure which is currently being tested for a memory response. Although the triple combination was not deemed to significantly extend mouse survival and delay tumour growth by multiple group comparison using a Holm-Sidak analysis, there is literature support to further investigate this combination. One study that used the anti-angiogenic biologic, bevacizumab, to improve αGD2-

CAR T-cell efficacy in killing NB tumours also found that this combination increased the PD-L1 expression on xenograft NB tumour cell. They suggested a third agent inhibiting the PD-1 axis could further improve the response (248). In support, αGD2 antibody was further improved by αPD-1 antibody in a NXS2 tumour model (109). Similarly, there is a current clinical trial using dinutuximab with nivolumab, an αPD-1 antibody, which further suggests that the approved αGD2 immunotherapy should be combined with an ICI (148).

3.5 Future Directions

There are several directions that my project can take. First, more investigation into the resistance of NB cell lines to SMC is required. More extensive analyses of apoptosis pathways could be examined for the repression of existence of associated proteins in NXS2 and N2a cells. I only examined the components previously reported silenced in human NB cell lines which may not correspond to that of the murine NB cell lines. Furthermore, there could also be mutations in the expressed proteins which render them dysfunctional and nonresponsive to apoptotic stimuli. An example would be if N2a cells had a mutated cIAP1/2 protein, preventing auto-ubiquitination and subsequent degradation of cIAP1/2 in response to LCL161. Next, the anti-vascular mechanism of LCL161 should be determined. One study found LCL161 treatment of a B16 tumour model made endothelial cells sensitive to TNFα-induced cell death (210). We will have to verify if the same mechanism is occurring in the NB model and determine the major source of TNFα production. One interesting combination would be to try a triple combination of sunitinib, LCL161, and αGD2 antibody against the NXS2 tumour model. Either drug in combination with LCL161 produced moderate delays in NXS2 tumour growth, so a triple combination of LCL161, sunitinib, and αGD2 antibody could be tested. Moreover, additional investigation of the dual combination of LCL161 and αGD2 immunotherapy is required. I found that this combination was more efficacious than

either monotherapy in delaying tumour growth, but still not significant. Similarly, the triple combination, with the addition of αPD-L1, further increased the delay in tumour growth of all dual combinations but was still not significant. The mechanism of action for αGD2 therapy is reported as CDC and NK and neutrophil-mediated ADCC (149). LAKs, *in vitro* NK substitutes, were sensitive to LCL161 treatment. Thus, the other mechanisms of action could be more relevant for dissecting the complementary interaction of LCL161 and αGD2 therapies in murine models. Also, I should point out that papers showing NK and SMC synergy were using human models of cancer. Perhaps exploring this combination using human models would be more efficacious. Furthermore, the αGD2 immunotherapy, although approved for NB, was not very effective against the NXS2 s.c. model as a monotherapy. This may be due to a variety of reasons such as the use of a different antibody clone, the absence of activating cytokine combinations, or the small sample sizes. My experimental approach could be repeated with a more clinically relevant αGD2 clone. As well, I could repeat the survival study with the activating cytokines such as IL-2 and GM-CSF. Some research has even investigated using an αGD2 antibody-IL-2 fusion immunokine against NB (258). A combination with LCL161 in this approach may be informative. I could also investigate response factors instead of additional therapeutic combinations. The αGD2 monotherapy group seemed to produce two populations of responders and non-responders which might refer to a certain immunological event occurring. By determining the immunological event responsible for the responder and non-responder groups, one could isolate a population form the treatment group which would better respond to the αGD2 antibody treatments. Similarly, it was found that clinical outcome to dinutuximab therapy was dependent on killer immunoglobulin-like receptor (KIR) and KIR ligand genotypes of patients (259).

3.6 Conclusion

In summary, my work has established a broad foundation for this project to advance. I examined the use of LCL161 monotherapy against NB, concluding it as ineffective against murine NB cell lines *in vitro*. I demonstrated moderate delays in tumour growth in the NXS2 s.c. model using a combination of LCL161 and sunitinib. This finding is consistent with the known anti-vascular effects of LCL161. I established protocols for LAK culturing, cytotoxicity assays, and antibody isolation. I then tested this isolated αGD2 antibody with LCL161 against NXS2 and observed some efficacy in delaying tumour growth, which was further potentiated with αPD-L1 antibody. Subsequent work is warranted for the investigation underlying the mechanisms behind LCL161 and αGD2 antibody effects and how these agents modulate the tumour microenvironment. With the addition of the SMC, LCL161, I have further improved αGD2 antibody treatment in a NB model. With optimization, this could lead to a clinical trial with dinutuximab to treat $GD2^+$ cancers like NB and improve overall survival.

REFERENCES

1. Vince JE, Wong WW-L, Khan N, Feltham R, Chau D, Ahmed AU, et al. IAP Antagonists Target cIAP1 to Induce TNFα-Dependent Apoptosis. Cell [Internet]. 2007 Nov 16 [cited 2018 Jun 22];131(4):682–93. Available from: http://www.ncbi.nlm.nih.gov/pubmed/18022363

2. Listen P, Roy N, Tamai K, Lefebvre C, Baird S, Cherton-Horvat G, et al. Suppression of apoptosis in mammalian cells by NAIP and a related family of IAP genes. Nature [Internet]. 1996 Jan 25 [cited 2016 Nov 19];379(6563):349–53. Available from: http://www.nature.com/doifinder/10.1038/379349a0

3. Lu M, Lin S-C, Huang Y, Kang YJ, Rich R, Lo Y-C, et al. XIAP Induces NF-κB Activation via the BIR1/TAB1 Interaction and BIR1 Dimerization. Mol Cell [Internet]. 2007 Jun 8 [cited 2018 Mar 12];26(5):689–702. Available from: https://www.sciencedirect.com/science/article/pii/S1097276507002870

4. Mahoney DJ, Cheung HH, Mrad RL, Plenchette S, Simard C, Enwere E, et al. Both cIAP1 and cIAP2 regulate TNFalpha-mediated NF-kappaB activation. Proc Natl Acad Sci U S A [Internet]. 2008 Aug 19 [cited 2018 Jul 26];105(33):11778–83. Available from: http://www.ncbi.nlm.nih.gov/pubmed/18697935

5. Eschenburg G, Eggert A, Schramm A, Lode HN, Hundsdoerfer P. Smac mimetic LBW242 sensitizes XIAP-overexpressing neuroblastoma cells for TNF-α-independent apoptosis. Cancer Res [Internet]. 2012 May 15 [cited 2018 Feb 27];72(10):2645–56. Available from: http://www.ncbi.nlm.nih.gov/pubmed/22491673

6. Najem S, Langemann D, Appl B, Trochimiuk M, Hundsdoerfer P, Reinshagen K, et al. Smac mimetic LCL161 supports neuroblastoma chemotherapy in a drug class-dependent manner and synergistically interacts with ALK inhibitor TAE684 in cells with ALK mutation F1174L. Oncotarget [Internet]. 2016 Nov 7 [cited 2016 Nov 19]; Available from: http://www.oncotarget.com/abstract/12055

7. Crook NE, Clem RJ, Miller LK. An apoptosis-inhibiting baculovirus gene with a zinc finger-like motif. J Virol [Internet]. 1993 Apr [cited 2018 Jul 26];67(4):2168–74. Available from: http://www.ncbi.nlm.nih.gov/pubmed/8445726

8. Obexer P, Ausserlechner MJ. X-Linked Inhibitor of Apoptosis Protein â€“ A Critical Death Resistance Regulator and Therapeutic Target for Personalized Cancer Therapy. Front Oncol [Internet]. 2014 Jul 28 [cited 2018 Jul 26];4:197. Available from: http://journal.frontiersin.org/article/10.3389/fonc.2014.00197/abstract

9. Eckelman BP, Drag M, Snipas SJ, Salvesen GS. The mechanism of peptide-binding specificity of IAP BIR domains. Cell Death Differ [Internet]. 2008 May 1 [cited 2018 Aug 26];15(5):920–8. Available from: http://www.nature.com/articles/cdd20086

10. Mace PD, Linke K, Feltham R, Schumacher F-R, Smith CA, Vaux DL, et al. Structures of the cIAP2 RING Domain Reveal Conformational Changes Associated with Ubiquitin-conjugating Enzyme (E2) Recruitment * □ S and the. 2008 [cited 2018 Aug 26]; Available from: http://www.jbc.org/

11. Ni T, Li W, Zou F. Critical Review The Ubiquitin Ligase Ability of IAPs Regulates Apoptosis. [cited 2018 Aug 26]; Available from: https://iubmb.onlinelibrary.wiley.com/doi/pdf/10.1080/15216540500389013

12. Oberoi-Khanuja TK, Murali A, Rajalingam K. IAPs on the move: role of inhibitors of apoptosis proteins in cell migration. Cell Death Dis [Internet]. 2013 Sep 5 [cited 2018 Aug 26];4(9):e784. Available from: http://www.ncbi.nlm.nih.gov/pubmed/24008728

13. Rumble JM, Duckett CS. Diverse functions within the IAP family. J Cell Sci [Internet]. 2008 [cited 2018 Aug 26];121:3505–7. Available from: http://jcs.biologists.org/content/joces/121/21/3505.full.pdf

14. Wu H, Lo Y-C. Structures, Domains and Functions in Cell Death (DD, DED, CARD, PYD). In: Encyclopedia of Life Sciences [Internet]. Chichester, UK: John Wiley & Sons, Ltd; 2009 [cited 2018 Aug 26]. Available from: http://doi.wiley.com/10.1002/9780470015902.a0021579

15. Jang T, Kim SH, Jeong J-H, Kim S, Kim Y-G, Kim YG, et al. Crystal structure of caspase recruiting domain (CARD) of apoptosis repressor with CARD (ARC) and its implication in inhibition of apoptosis. Sci Rep [Internet]. 2015 Jun 3 [cited 2018 Aug 26];5:9847. Available from: http://www.ncbi.nlm.nih.gov/pubmed/26038885

16. Shi Y. Caspase activation, inhibition, and reactivation: a mechanistic view. Protein Sci [Internet]. 2004 Aug [cited 2018 Aug 26];13(8):1979–87. Available from: http://www.ncbi.nlm.nih.gov/pubmed/15273300

17. Chen M, Wang J. Initiator caspases in apoptosis signaling pathways. Apoptosis [Internet]. 2002 Aug [cited 2018 Aug 26];7(4):313–9. Available from: http://www.ncbi.nlm.nih.gov/pubmed/12101390

18. Slee EA, Adrain C, Martin SJ. Executioner caspase-3, -6, and -7 perform distinct, non-redundant roles during the demolition phase of apoptosis. J Biol Chem [Internet]. 2001 Mar 9 [cited 2018 Aug 19];276(10):7320–6. Available from: http://www.ncbi.nlm.nih.gov/pubmed/11058599

19. Bai L, Smith DC, Wang S. Small-molecule SMAC mimetics as new cancer therapeutics. Pharmacol Ther [Internet]. 2014 Oct [cited 2016 Nov 19];144(1):82–95. Available from: http://linkinghub.elsevier.com/retrieve/pii/S0163725814001028

20. Suzuki Y, Nakabayashi Y, Nakata K, Reed JC, Takahashi R. X-linked Inhibitor of Apoptosis Protein (XIAP) Inhibits Caspase-3 and -7 in Distinct Modes. J Biol Chem [Internet]. 2001 Jul 20 [cited 2018 Jul 30];276(29):27058–63. Available from: http://www.ncbi.nlm.nih.gov/pubmed/11359776

21. Shiozaki EN, Chai J, Rigotti DJ, Riedl SJ, Li P, Srinivasula SM, et al. Mechanism of XIAP-mediated inhibition of caspase-9. Mol Cell [Internet]. 2003 Feb [cited 2018 Aug 26];11(2):519–27. Available from: http://www.ncbi.nlm.nih.gov/pubmed/12620238

22. Eckelman BP, Salvesen GS. The Human Anti-apoptotic Proteins cIAP1 and cIAP2 Bind but Do Not Inhibit Caspases. J Biol Chem [Internet]. 2006 Feb 10 [cited 2018 Jul 26];281(6):3254–60. Available from: http://www.ncbi.nlm.nih.gov/pubmed/16339151

23. Choi YE, Butterworth M, Malladi S, Duckett CS, Cohen GM, Bratton SB. The E3 Ubiquitin Ligase cIAP1 Binds and Ubiquitinates Caspase-3 and -7 via Unique Mechanisms at Distinct Steps in Their Processing. J Biol Chem [Internet]. 2009 May 8 [cited 2018 Jul 26];284(19):12772–82. Available from: http://www.ncbi.nlm.nih.gov/pubmed/19258326

24. Lawrence T. The nuclear factor NF-kappaB pathway in inflammation. Cold Spring Harb Perspect Biol [Internet]. 2009 Dec [cited 2018 Aug 19];1(6):a001651. Available from: http://www.ncbi.nlm.nih.gov/pubmed/20457564

25. Zhang Q, Lenardo MJ, Baltimore D. Leading Edge Review 30 Years of NF-kB: A Blossoming of Relevance to Human Pathobiology. Cell [Internet]. 2017 [cited 2018 Aug 26];168:37–57. Available from: http://dx.doi.org/10.1016/j.cell.2016.12.012

26. Hayden MS, Ghosh S. NF-kB, the first quarter-century: remarkable progress and outstanding questions. [cited 2018 Aug 26]; Available from: http://www.genesdev.org/cgi/doi/10.1101/gad.183434.111.

27. Collart MA, Baeuerle P, Vassalli P. Regulation of tumor necrosis factor alpha transcription in macrophages: involvement of four kappa B-like motifs and of constitutive and inducible forms of NF-kappa B. Mol Cell Biol [Internet]. 1990 Apr [cited 2018 Aug 26];10(4):1498–506. Available from: http://www.ncbi.nlm.nih.gov/pubmed/2181276

28. Forloni M, Albini S, Limongi MZ, Cifaldi L, Boldrini R, Nicotra MR, et al. NF- B, and not MYCN, Regulates MHC Class I and Endoplasmic Reticulum Aminopeptidases in Human Neuroblastoma Cells. Cancer Res [Internet]. 2010 Feb 1 [cited 2018 Aug 26];70(3):916–24. Available from: http://www.ncbi.nlm.nih.gov/pubmed/20103633

29. Lorenzi S, Forloni M, Cifaldi L, Antonucci C, Citti A, Boldrini R, et al. IRF1 and NF-kB Restore MHC Class I-Restricted Tumor Antigen Processing and Presentation to Cytotoxic T Cells in Aggressive Neuroblastoma. Appel S, editor. PLoS One [Internet]. 2012 Oct 5 [cited 2018 Aug 26];7(10):e46928. Available from: http://dx.plos.org/10.1371/journal.pone.0046928

30. Israël A, Le Bail O, Hatat D, Piette J, Kieran M, Logeat F, et al. TNF stimulates expression of mouse MHC class I genes by inducing an NF kappa B-like enhancer binding activity which displaces constitutive factors. EMBO J [Internet]. 1989 Dec 1 [cited 2018 Aug 26];8(12):3793–800. Available from: http://www.ncbi.nlm.nih.gov/pubmed/2555174

31. LEE S, SEO S, KIM B, KIM C, LEE J, KANG J, et al. IFN-gamma regulates the

expression of B7-H1 in dermal fibroblast cells. J Dermatol Sci [Internet]. 2005 Nov [cited 2018 Aug 26];40(2):95–103. Available from: http://www.ncbi.nlm.nih.gov/pubmed/16085391

32. Sun S-C. Non-canonical NF-κB signaling pathway. Cell Res [Internet]. 2011 Jan [cited 2018 Aug 26];21(1):71–85. Available from: http://www.ncbi.nlm.nih.gov/pubmed/21173796

33. Varfolomeev E, Blankenship JW, Wayson SM, Fedorova A V, Kayagaki N, Garg P, et al. IAP antagonists induce autoubiquitination of c-IAPs, NF-kappaB activation, and TNFalpha-dependent apoptosis. Cell [Internet]. 2007 Nov 16 [cited 2018 Jul 26];131(4):669–81. Available from: http://www.ncbi.nlm.nih.gov/pubmed/18022362

34. Du C, Fang M, Li Y, Li L, Wang X. Smac, a mitochondrial protein that promotes cytochrome c-dependent caspase activation by eliminating IAP inhibition. Cell [Internet]. 2000 Jul 7 [cited 2018 Jul 26];102(1):33–42. Available from: http://www.ncbi.nlm.nih.gov/pubmed/10929711

35. Adrain C, Creagh EM, Martin SJ. Apoptosis-associated release of Smac/DIABLO from mitochondria requires active caspases and is blocked by Bcl-2. EMBO J [Internet]. 2001 Dec 3 [cited 2018 Aug 26];20(23):6627–36. Available from: http://www.ncbi.nlm.nih.gov/pubmed/11726499

36. Sun H, Nikolovska-Coleska Z, Yang C-Y, Qian D, Lu J, Qiu S, et al. Design of small-molecule peptidic and nonpeptidic Smac mimetics. Acc Chem Res [Internet]. 2008 Oct [cited 2018 Aug 26];41(10):1264–77. Available from: http://www.ncbi.nlm.nih.gov/pubmed/18937395

37. Chen K-F, Lin J-P, Shiau C-W, Tai W-T, Liu C-Y, Yu H-C, et al. Inhibition of Bcl-2 improves effect of LCL161, a SMAC mimetic, in hepatocellular carcinoma cells. Biochem Pharmacol [Internet]. 2012 Aug 1 [cited 2018 Jun 22];84(3):268–77. Available from: http://www.ncbi.nlm.nih.gov/pubmed/22580047

38. Kim D-S, Dastidar H, Zhang C, Zemp FJ, Lau K, Ernst M, et al. Smac mimetics and oncolytic viruses synergize in driving anticancer T-cell responses through complementary mechanisms. Nat Commun [Internet]. 2017 Dec 24 [cited 2018 Jul 30];8(1):344. Available from: http://www.nature.com/articles/s41467-017-00324-x

39. Chesi M, Mirza NN, Garbitt VM, Sharik ME, Dueck AC, Asmann YW, et al. IAP antagonists induce anti-tumor immunity in multiple myeloma. Nat Med [Internet]. 2016 [cited 2018 Jul 30];22(12):1411–20. Available from: http://www.ncbi.nlm.nih.gov/pubmed/27841872

40. Dobson CC, Naing T, Beug ST, Faye MD, Chabot J, St-Jean M, et al. Oncolytic virus synergizes with Smac mimetic compounds to induce rhabdomyosarcoma cell death in a syngeneic murine model. Oncotarget [Internet]. 2017 Jan 10 [cited 2018 Jul 31];8(2):3495–508. Available from: http://www.ncbi.nlm.nih.gov/pubmed/27966453

41. Beug ST, Tang VA, LaCasse EC, Cheung HH, Beauregard CE, Brun J, et al. Smac mimetics and innate immune stimuli synergize to promote tumor death. Nat Biotechnol [Internet]. 2014 Jan 26 [cited 2016 Nov 19];32(2):182–90. Available from: http://www.nature.com/doifinder/10.1038/nbt.2806

42. Cheung HH, Beug ST, St Jean M, Brewster A, Kelly NL, Wang S, et al. Smac mimetic compounds potentiate interleukin-1beta-mediated cell death. J Biol Chem [Internet]. 2010 Dec 24 [cited 2018 Jun 22];285(52):40612–23. Available from: http://www.ncbi.nlm.nih.gov/pubmed/20956527

43. Beug ST, Beauregard CE, Healy C, Sanda T, St-Jean M, Chabot J, et al. Publisher Correction: Smac mimetics synergize with immune checkpoint inhibitors to promote tumour immunity against glioblastoma (Nature Communications (2017) 8 (14278) DOI: 10.1038/ncomms14278). Nat Commun [Internet]. 2018;9:1–15. Available from: http://dx.doi.org/10.1038/ncomms14278

44. Langemann D, Trochimiuk M, Appl B, Hundsdoerfer P, Reinshagen K, Eschenburg G. Sensitization of neuroblastoma for vincristine-induced apoptosis by Smac mimetic LCL161 is attended by G2 cell cycle arrest but is independent of NFκB, RIP1 and TNF-α Oncotarget [Internet]. 2017 Oct 20 [cited 2018 Jul 9];8(50):87763–72. Available from: http://www.ncbi.nlm.nih.gov/pubmed/29152118

45. Frommann K, Appl B, Hundsdoerfer P, Reinshagen K, Eschenburg G. Vincristine resistance in relapsed neuroblastoma can be efficiently overcome by Smac mimetic LCL161 treatment. J Pediatr Surg [Internet]. 2018 Jan 31 [cited 2018 Feb 27]; Available from: http://www.ncbi.nlm.nih.gov/pubmed/29455885

46. Yang Q-H, Du C. Smac/DIABLO Selectively Reduces the Levels of c-IAP1 and c-IAP2 but Not That of XIAP and Livin in HeLa Cells. J Biol Chem [Internet]. 2004 Apr 23 [cited 2018 Jul 26];279(17):16963–70. Available from: http://www.ncbi.nlm.nih.gov/pubmed/14960576

47. Liu Z, Sun C, Olejniczak ET, Meadows RP, Betz SF, Oost T, et al. Structural basis for binding of Smac/DIABLO to the XIAP BIR3 domain. Nature [Internet]. 2000 Dec 21 [cited 2018 Jul 26];408(6815):1004–8. Available from: http://www.ncbi.nlm.nih.gov/pubmed/11140637

48. Probst BL, Liu L, Ramesh V, Li L, Sun H, Minna JD, et al. Smac mimetics increase cancer cell response to chemotherapeutics in a TNF-α-dependent manner. Cell Death Differ [Internet]. 2010 Oct [cited 2018 Aug 26];17(10):1645–54. Available from: http://www.ncbi.nlm.nih.gov/pubmed/20431601

49. Moriwaki K, Bertin J, Gough PJ, Orlowski GM, Chan FK. Differential roles of RIPK1 and RIPK3 in TNF-induced necroptosis and chemotherapeutic agent-induced cell death. Cell Death Dis [Internet]. 2015 Feb 12 [cited 2018 Aug 26];6(2):e1636. Available from: http://www.nature.com/doifinder/10.1038/cddis.2015.16

50. Schenk B, Fulda S. Reactive oxygen species regulate Smac mimetic/TNFα-induced

necroptotic signaling and cell death. Oncogene [Internet]. 2015 Nov 6 [cited 2018 Aug 26];34(47):5796–806. Available from: http://www.ncbi.nlm.nih.gov/pubmed/25867066

51. Varfolomeev E, Blankenship JW, Wayson SM, Fedorova A V., Kayagaki N, Garg P, et al. IAP Antagonists Induce Autoubiquitination of c-IAPs, NF-κB Activation, and TNFα-Dependent Apoptosis. Cell [Internet]. 2007 Nov 16 [cited 2018 Jun 22];131(4):669–81. Available from: http://www.ncbi.nlm.nih.gov/pubmed/18022362

52. Kearney CJ, Vervoort SJ, Hogg SJ, Ramsbottom KM, Freeman AJ, Lalaoui N, et al. Tumor immune evasion arises through loss of TNF sensitivity. Sci Immunol [Internet]. 2018 May 18 [cited 2018 Aug 26];3(23):eaar3451. Available from: http://www.ncbi.nlm.nih.gov/pubmed/29776993

53. Zhang B, Karrison T, Rowley DA, Schreiber H. IFN-gamma- and TNF-dependent bystander eradication of antigen-loss variants in established mouse cancers. J Clin Invest [Internet]. 2008 Apr [cited 2018 Aug 26];118(4):1398–404. Available from: http://www.ncbi.nlm.nih.gov/pubmed/18317595

54. Witt A, Seeger JM, Coutelle O, Zigrino P, Broxtermann P, Andree M, et al. IAP antagonization promotes inflammatory destruction of vascular endothelium. EMBO Rep [Internet]. 2015 Jun [cited 2018 Jun 23];16(6):719–27. Available from: http://www.ncbi.nlm.nih.gov/pubmed/25825408

55. Beug ST, Pichette SJ, St-Jean M, Holbrook J, Walker DE, LaCasse EC, et al. Combination of IAP Antagonists and TNF-α-Armed Oncolytic Viruses Induce Tumor Vascular Shutdown and Tumor Regression. Mol Ther - Oncolytics [Internet]. 2018 Sep 28 [cited 2018 Aug 18];10:28–39. Available from: https://www.sciencedirect.com/science/article/pii/S2372770518300147

56. Dougan M, Dougan S, Slisz J, Firestone B, Vanneman M, Draganov D, et al. IAP inhibitors enhance co-stimulation to promote tumor immunity. J Exp Med [Internet]. 2010 Sep 27 [cited 2018 Jul 31];207(10):2195–206. Available from: http://www.ncbi.nlm.nih.gov/pubmed/20837698

57. Beug ST, Cheung HH, LaCasse EC, Korneluk RG. Modulation of immune signalling by inhibitors of apoptosis. Trends Immunol [Internet]. 2012 Nov [cited 2018 Jul 19];33(11):535–45. Available from: http://linkinghub.elsevier.com/retrieve/pii/S147149061200110X

58. LaCasse EC, Mahoney DJ, Cheung HH, Plenchette S, Baird S, Korneluk RG. IAP-targeted therapies for cancer. Oncogene [Internet]. 2008 Oct 20 [cited 2018 Aug 26];27(48):6252–75. Available from: http://www.nature.com/articles/onc2008302

59. Owens TW, Gilmore AP, Streuli CH, Foster FM. Inhibitor of Apoptosis Proteins: Promising Targets for Cancer Therapy. J Carcinog Mutagen [Internet]. 2013 May 27 [cited 2018 Aug 26];Suppl 14. Available from: http://www.ncbi.nlm.nih.gov/pubmed/25328816

60. Dougan SK, Dougan M. Regulation of innate and adaptive antitumor immunity by IAP antagonists. Immunotherapy [Internet]. 2018 Jul 29 [cited 2018 Aug 26];10(9):787–96. Available from: https://www.futuremedicine.com/doi/10.2217/imt-2017-0185

61. Fischer K, Tognarelli S, Roesler S, Boedicker C, Schubert R, Steinle A, et al. The smac mimetic BV6 improves NK cell-mediated killing of rhabdomyosarcoma cells by simultaneously targeting tumor and effector cells. Front Immunol. 2017;8(MAR):1–11.

62. Brinkmann K, Hombach A, Seeger JM, Wagner-Stippich D, Klubertz D, Krönke M, et al. Second mitochondria-derived activator of caspase (SMAC) mimetic potentiates tumor susceptibility toward natural killer cell-mediated killing. Leuk Lymphoma [Internet]. 2014 Mar 26 [cited 2016 Nov 28];55(3):645–51. Available from: http://www.tandfonline.com/doi/full/10.3109/10428194.2013.807925

63. Dougan M, Dougan S, Slisz J, Firestone B, Vanneman M, Draganov D, et al. IAP inhibitors enhance co-stimulation to promote tumor immunity. J Exp Med [Internet]. 2010 Sep 27 [cited 2018 Jul 30];207(10):2195–206. Available from: http://www.ncbi.nlm.nih.gov/pubmed/20837698

64. Evans MK, Sauer SJ, Nath S, Robinson TJ, Morse MA, Devi GR. X-linked inhibitor of apoptosis protein mediates tumor cell resistance to antibody-dependent cellular cytotoxicity. Cell Death Dis [Internet]. 2016 Jan 28 [cited 2016 Nov 19];7(1):e2073. Available from: http://www.nature.com/doifinder/10.1038/cddis.2015.412

65. Costanzo MC, Kim D, Creegan M, Lal KG, Ake JA, Currier JR, et al. Transcriptomic signatures of NK cells suggest impaired responsiveness in HIV-1 infection and increased activity post-vaccination. Nat Commun [Internet]. 2018 Dec 23 [cited 2018 Jul 30];9(1):1212. Available from: http://www.nature.com/articles/s41467-018-03618-w

66. Ivagnès A, Messaoudene M, Stoll G, Routy B, Fluckiger A, Yamazaki T, et al. TNFR2/BIRC3-TRAF1 signaling pathway as a novel NK cell immune checkpoint in cancer. Oncoimmunology [Internet]. 2017 Oct 11 [cited 2018 Jul 30];00–00. Available from: https://www.tandfonline.com/doi/full/10.1080/2162402X.2017.1386826

67. Wicki S, Gurzeler U, Wei-Lynn Wong W, Jost PJ, Bachmann D, Kaufmann T. Loss of XIAP facilitates switch to TNFα-induced necroptosis in mouse neutrophils. Cell Death Dis [Internet]. 2016 Oct 13 [cited 2018 Jul 30];7(10):e2422–e2422. Available from: http://www.nature.com/articles/cddis2016311

68. Hasegawa T, Suzuki K, Sakamoto C, Ohta K, Nishiki S, Hino M, et al. Expression of the inhibitor of apoptosis (IAP) family members in human neutrophils: up-regulation of cIAP2 by granulocyte colony-stimulating factor and overexpression of cIAP2 in chronic neutrophilic leukemia. Blood [Internet]. 2003 Feb 1 [cited 2018 Jul 30];101(3):1164–71. Available from: http://www.ncbi.nlm.nih.gov/pubmed/12393423

69. Simons MP, Nauseef WM, Griffith TS, Apicella MA. Neisseria gonorrhoeae delays the onset of apoptosis in polymorphonuclear leukocytes. Cell Microbiol [Internet]. 2006 Nov [cited 2018 Jul 30];8(11):1780–90. Available from:

http://www.ncbi.nlm.nih.gov/pubmed/16803582

70. Jinesh G. G, Chunduru S, Kamat AM. Smac mimetic enables the anticancer action of BCG-stimulated neutrophils through TNF-α but not through TRAIL and FasL. J Leukoc Biol [Internet]. 2012 Jul [cited 2018 Jul 10];92(1):233–44. Available from: http://www.ncbi.nlm.nih.gov/pubmed/22517918

71. Nadella V, Mohanty A, Sharma L, Yellaboina S, Mollenkopf H-J, Mazumdar VB, et al. Inhibitors of Apoptosis Protein Antagonists (Smac Mimetic Compounds) Control Polarization of Macrophages during Microbial Challenge and Sterile Inflammatory Responses. Front Immunol [Internet]. 2017 [cited 2018 Jul 30];8:1792. Available from: http://www.ncbi.nlm.nih.gov/pubmed/29375545

72. McComb S, Cheung HH, Korneluk RG, Wang S, Krishnan L, Sad S. cIAP1 and cIAP2 limit macrophage necroptosis by inhibiting Rip1 and Rip3 activation. Cell Death Differ [Internet]. 2012 Nov [cited 2018 Jul 30];19(11):1791–801. Available from: http://www.ncbi.nlm.nih.gov/pubmed/22576661

73. Siegmund D, Kums J, Ehrenschwender M, Wajant H. Activation of TNFR2 sensitizes macrophages for TNFR1-mediated necroptosis. Cell Death Dis [Internet]. 2016 Sep 22 [cited 2018 Jul 30];7(9):e2375–e2375. Available from: http://www.nature.com/articles/cddis2016285

74. He S, Liang Y, Shao F, Wang X. Toll-like receptors activate programmed necrosis in macrophages through a receptor-interacting kinase-3-mediated pathway. Proc Natl Acad Sci U S A [Internet]. 2011 Dec 13 [cited 2018 Jul 30];108(50):20054–9. Available from: http://www.ncbi.nlm.nih.gov/pubmed/22123964

75. Bergsagel PL, Lacy MQ, Dingli D, Kumar SK, Ailawadhi S, Dispenzieri A, et al. Anti-Tumor Phagocytic Cell Activation in Multiple Myeloma By the IAP Antagonist LCL161: Results of a Phase II Clinical Trial. Blood [Internet]. 2015 [cited 2018 Jul 30];126(23). Available from: http://www.bloodjournal.org/content/126/23/3039?sso-checked=true

76. Dupoux A, Cartier J, Cathelin S, Filomenko R, Solary E, Dubrez-Daloz L. cIAP1-dependent TRAF2 degradation regulates the differentiation of monocytes into macrophages and their response to CD40 ligand. Blood [Internet]. 2009 Jan 1 [cited 2018 Jul 31];113(1):175–85. Available from: http://www.ncbi.nlm.nih.gov/pubmed/18827186

77. Müller-Sienerth N, Dietz L, Holtz P, Kapp M, Grigoleit GU, Schmuck C, et al. SMAC Mimetic BV6 Induces Cell Death in Monocytes and Maturation of Monocyte-Derived Dendritic Cells. Häcker G, editor. PLoS One [Internet]. 2011 Jun 30 [cited 2018 Jul 31];6(6):e21556. Available from: http://dx.plos.org/10.1371/journal.pone.0021556

78. Knights AJ, Fucikova J, Pasam A, Koernig S, Cebon J. Inhibitor of apoptosis protein (IAP) antagonists demonstrate divergent immunomodulatory properties in human immune subsets with implications for combination therapy. Cancer Immunol Immunother [Internet]. 2013 Feb 26 [cited 2018 Jul 31];62(2):321–35. Available from: http://link.springer.com/10.1007/s00262-012-1342-1

79. Emeagi PU, Thielemans K, Breckpot K. The role of SMAC mimetics in regulation of tumor cell death and immunity. Oncoimmunology [Internet]. 2012 Sep 28 [cited 2018 Jul 31];1(6):965–7. Available from: http://www.tandfonline.com/doi/abs/10.4161/onci.20369

80. Emeagi PU, Van Lint S, Goyvaerts C, Maenhout S, Cauwels A, McNeish IA, et al. Proinflammatory characteristics of SMAC/DIABLO-induced cell death in antitumor therapy. Cancer Res [Internet]. 2012 Mar 15 [cited 2018 Jul 10];72(6):1342–52. Available from: http://www.ncbi.nlm.nih.gov/pubmed/22379024

81. Gentle IE, Moelter I, Lechler N, Bambach S, Vucikuja S, Hacker G, et al. Inhibitors of apoptosis proteins (IAPs) are required for effective T-cell expansion/survival during antiviral immunity in mice. Blood [Internet]. 2014 Jan 30 [cited 2018 Jul 31];123(5):659–68. Available from: http://www.ncbi.nlm.nih.gov/pubmed/24335231

82. Hsieh W-C, Hsu T-S, Chang Y-J, Lai M-Z. IL-6 receptor blockade corrects defects of XIAP-deficient regulatory T cells. Nat Commun [Internet]. 2018 Dec 31 [cited 2018 Jul 31];9(1):463. Available from: http://www.nature.com/articles/s41467-018-02862-4

83. Dimberu PM, Leonhardt RM. Cancer immunotherapy takes a multi-faceted approach to kick the immune system into gear. Yale J Biol Med [Internet]. 2011 Dec [cited 2018 Aug 26];84(4):371–80. Available from: http://www.ncbi.nlm.nih.gov/pubmed/22180675

84. Galluzzi L, Vacchelli E, Bravo-San Pedro J-M, Buqué A, Senovilla L, Baracco EE, et al. Classification of current anticancer immunotherapies. Oncotarget [Internet]. 2014 Dec 30 [cited 2018 Aug 26];5(24):12472–508. Available from: http://www.ncbi.nlm.nih.gov/pubmed/25537519

85. Schuster M, Nechansky A, Kircheis R. Cancer immunotherapy. Biotechnol J [Internet]. 2006 Feb [cited 2018 Aug 26];1(2):138–47. Available from: http://www.ncbi.nlm.nih.gov/pubmed/16892244

86. Kellner C, Otte A, Cappuzzello E, Klausz K, Peipp M. Modulating Cytotoxic Effector Functions by Fc Engineering to Improve Cancer Therapy. Transfus Med Hemother [Internet]. 2017 Sep [cited 2018 Aug 26];44(5):327–36. Available from: http://www.ncbi.nlm.nih.gov/pubmed/29070978

87. Suzuki M, Kato C, Kato A. Therapeutic antibodies: their mechanisms of action and the pathological findings they induce in toxicity studies. J Toxicol Pathol [Internet]. 2015 Jul [cited 2018 Jul 24];28(3):133–9. Available from: http://www.ncbi.nlm.nih.gov/pubmed/26441475

88. Macor P, Tedesco F. Complement as effector system in cancer immunotherapy. Immunol Lett [Internet]. 2007 Jul 31 [cited 2018 Aug 26];111(1):6–13. Available from: http://www.ncbi.nlm.nih.gov/pubmed/17572509

89. Zhou X, Hu W, Qin X. The role of complement in the mechanism of action of rituximab for B-cell lymphoma: implications for therapy. Oncologist [Internet]. 2008 Sep 1 [cited 2018 Aug 26];13(9):954–66. Available from:

http://www.ncbi.nlm.nih.gov/pubmed/18779537

90. Baig NA, Taylor RP, Lindorfer MA, Church AK, Laplant BR, Pavey ES, et al. Complement dependent cytotoxicity in chronic lymphocytic leukemia: ofatumumab enhances alemtuzumab complement dependent cytotoxicity and reveals cells resistant to activated complement. Leuk Lymphoma [Internet]. 2012 Nov [cited 2018 Aug 26];53(11):2218–27. Available from: http://www.ncbi.nlm.nih.gov/pubmed/22475085

91. Boyerinas B, Jochems C, Fantini M, Heery CR, Gulley JL, Tsang KY, et al. Antibody-Dependent Cellular Cytotoxicity Activity of a Novel Anti-PD-L1 Antibody Avelumab (MSB0010718C) on Human Tumor Cells. Cancer Immunol Res [Internet]. 2015 Oct [cited 2018 Jul 24];3(10):1148–57. Available from: http://www.ncbi.nlm.nih.gov/pubmed/26014098

92. Wang W, Erbe AK, Hank JA, Morris ZS, Sondel PM. NK Cell-Mediated Antibody-Dependent Cellular Cytotoxicity in Cancer Immunotherapy. Front Immunol [Internet]. 2015 [cited 2018 Aug 26];6:368. Available from: http://www.ncbi.nlm.nih.gov/pubmed/26284063

93. Petricevic B, Laengle J, Singer J, Sachet M, Fazekas J, Steger G, et al. Trastuzumab mediates antibody-dependent cell-mediated cytotoxicity and phagocytosis to the same extent in both adjuvant and metastatic HER2/neu breast cancer patients. J Transl Med [Internet]. 2013 Dec 12 [cited 2018 Aug 26];11(1):307. Available from: http://translational-medicine.biomedcentral.com/articles/10.1186/1479-5876-11-307

94. Navid F, Santana VM, Barfield RC. Anti-GD2 antibody therapy for GD2-expressing tumors. Curr Cancer Drug Targets [Internet]. 2010 Mar [cited 2018 Mar 4];10(2):200–9. Available from: http://www.ncbi.nlm.nih.gov/pubmed/20201786

95. Shi Y, Fan X, Deng H, Brezski RJ, Rycyzyn M, Jordan RE, et al. Trastuzumab triggers phagocytic killing of high HER2 cancer cells in vitro and in vivo by interaction with Fcγ receptors on macrophages. J Immunol [Internet]. 2015 May 1 [cited 2018 Jan 2];194(9):4379–86. Available from: http://www.ncbi.nlm.nih.gov/pubmed/25795760

96. Kurdi AT, Glavey S V., Bezman NA, Jhatakia A, Guerriero JL, Manier S, et al. Antibody-Dependent Cellular Phagocytosis by Macrophages is a Novel Mechanism of Action of Elotuzumab. Mol Cancer Ther [Internet]. 2018 Jul [cited 2018 Aug 26];17(7):1454–63. Available from: http://www.ncbi.nlm.nih.gov/pubmed/29654064

97. Ribas A, Wolchok JD. Cancer immunotherapy using checkpoint blockade. Science [Internet]. 2018 Mar 23 [cited 2018 Aug 26];359(6382):1350–5. Available from: http://www.ncbi.nlm.nih.gov/pubmed/29567705

98. Thallinger C, Füreder T, Preusser M, Heller G, Müllauer L, Höller C, et al. Review of cancer treatment with immune checkpoint inhibitors. Wien Klin Wochenschr [Internet]. 2018 Feb 2 [cited 2018 Aug 26];130(3–4):85–91. Available from: http://www.ncbi.nlm.nih.gov/pubmed/29098404

99. Dyck L, Wilk MM, Raverdeau M, Misiak A, Boon L, Mills KHG. Anti-PD-1 inhibits Foxp3+ Treg cell conversion and unleashes intratumoural effector T cells thereby enhancing the efficacy of a cancer vaccine in a mouse model. Cancer Immunol Immunother [Internet]. 2016 Dec 28 [cited 2018 Aug 26];65(12):1491–8. Available from: http://www.ncbi.nlm.nih.gov/pubmed/27680570

100. Asano T, Kishi Y, Meguri Y, Yoshioka T, Iwamoto M, Maeda Y, et al. PD-1 Signaling Has a Critical Role in Maintaining Regulatory T Cell Homeostasis; Implication for Treg Depletion Therapy By PD-1 Blockade. Blood [Internet]. 2015 [cited 2018 Aug 26];126(23). Available from: http://www.bloodjournal.org/content/126/23/848?sso-checked=true

101. Shi F, Shi M, Zeng Z, Qi R-Z, Liu Z-W, Zhang J-Y, et al. PD-1 and PD-L1 upregulation promotes CD8+ T-cell apoptosis and postoperative recurrence in hepatocellular carcinoma patients. Int J Cancer [Internet]. 2011 Feb 15 [cited 2018 Aug 26];128(4):887–96. Available from: http://www.ncbi.nlm.nih.gov/pubmed/20473887

102. Chiu Y-M, Tsai C-L, Kao J-T, Hsieh C-T, Shieh D-C, Lee Y-J, et al. PD-1 and PD-L1 Up-regulation Promotes T-cell Apoptosis in Gastric Adenocarcinoma. Anticancer Res [Internet]. 2018 Mar 28 [cited 2018 Aug 26];38(4):2069–78. Available from: http://www.ncbi.nlm.nih.gov/pubmed/29599324

103. Jin H-T, Ahmed R, Okazaki T. Role of PD-1 in Regulating T-Cell Immunity. In: Current topics in microbiology and immunology [Internet]. 2010 [cited 2018 Aug 26]. p. 17–37. Available from: http://www.ncbi.nlm.nih.gov/pubmed/21061197

104. Sharpe AH, Pauken KE. The diverse functions of the PD1 inhibitory pathway. Nat Rev Immunol [Internet]. 2017 Nov 13 [cited 2018 Jul 24];18(3):153–67. Available from: http://www.nature.com/doifinder/10.1038/nri.2017.108

105. Thibult M-L, Mamessier E, Gertner-Dardenne J, Pastor S, Just-Landi S, Xerri L, et al. PD-1 is a novel regulator of human B-cell activation. Int Immunol [Internet]. 2013 Feb [cited 2018 Aug 26];25(2):129–37. Available from: http://www.ncbi.nlm.nih.gov/pubmed/23087177

106. Benson DM, Bakan CE, Mishra A, Hofmeister CC, Efebera Y, Becknell B, et al. The PD-1/PD-L1 axis modulates the natural killer cell versus multiple myeloma effect: a therapeutic target for CT-011, a novel monoclonal anti-PD-1 antibody. Blood [Internet]. 2010 Sep 30 [cited 2018 Jul 24];116(13):2286–94. Available from: http://www.ncbi.nlm.nih.gov/pubmed/20460501

107. Lim TS, Chew V, Sieow JL, Goh S, Yeong JP-S, Soon AL, et al. PD-1 expression on dendritic cells suppresses CD8 $^{+}$ T cell function and antitumor immunity. Oncoimmunology [Internet]. 2016 Mar 3 [cited 2018 Aug 26];5(3):e1085146. Available from: http://www.ncbi.nlm.nih.gov/pubmed/27141339

108. Rigo V, Emionite L, Daga A, Astigiano S, Corrias MV, Quintarelli C, et al. Combined immunotherapy with anti-PDL-1/PD-1 and anti-CD4 antibodies cures syngeneic

disseminated neuroblastoma. Sci Rep [Internet]. 2017 Dec 25 [cited 2018 Jul 11];7(1):14049. Available from: http://www.nature.com/articles/s41598-017-14417-6

109. Siebert N, Zumpe M, Jüttner M, Troschke-Meurer S, Lode HN. PD-1 blockade augments anti-neuroblastoma immune response induced by anti-GD2 antibody ch14.18/CHO. Oncoimmunology [Internet]. 2017 Oct 3 [cited 2018 Jan 2];6(10):e1343775. Available from: https://www.tandfonline.com/doi/full/10.1080/2162402X.2017.1343775

110. Wang X, Teng F, Kong L, Yu J. PD-L1 expression in human cancers and its association with clinical outcomes. Onco Targets Ther [Internet]. 2016 [cited 2018 Aug 26];9:5023–39. Available from: http://www.ncbi.nlm.nih.gov/pubmed/27574444

111. Pinto N, Park JR, Murphy E, Yearley J, McClanahan T, Annamalai L, et al. Patterns of PD-1, PD-L1, and PD-L2 expression in pediatric solid tumors. Pediatr Blood Cancer [Internet]. 2017 Nov [cited 2018 Feb 27];64(11):e26613. Available from: http://www.ncbi.nlm.nih.gov/pubmed/28488345

112. Dong Y, Sun Q, Zhang X. PD-1 and its ligands are important immune checkpoints in cancer. Oncotarget [Internet]. 2017 Jan 10 [cited 2018 Aug 26];8(2):2171–86. Available from: http://www.ncbi.nlm.nih.gov/pubmed/27974689

113. Lee S-J, Jang B-C, Lee S-W, Yang Y-I, Suh S-I, Park Y-M, et al. Interferon regulatory factor-1 is prerequisite to the constitutive expression and IFN-γ-induced upregulation of B7-H1 (CD274). FEBS Lett [Internet]. 2006 Feb 6 [cited 2018 Jul 24];580(3):755–62. Available from: http://www.ncbi.nlm.nih.gov/pubmed/16413538

114. Linsley PS, Golstein P. Lymphocyte activation: T-cell regulation by CTLA-4. Curr Biol [Internet]. 1996 Apr 1 [cited 2018 Aug 26];6(4):398–400. Available from: https://www.sciencedirect.com/science/article/pii/S0960982202005067

115. Jago CB, Yates J, Câmara NOS, Lechler RI, Lombardi G. Differential expression of CTLA-4 among T cell subsets. Clin Exp Immunol [Internet]. 2004 Jun [cited 2018 Aug 26];136(3):463–71. Available from: http://www.ncbi.nlm.nih.gov/pubmed/15147348

116. Lammas DA, Raza K, Sansom DM, Qureshi OS, Hewison M, Walker LSK, et al. FoxP3 Regulatory T Cells Expressing CTLA-4 and Cytokines and Promote Development of to Inhibit T Cell Production of Inflammatory and IL-2 Combine 3 1,25-Dihydroxyvitamin D. J Immunol Ref [Internet]. 2018 [cited 2018 Aug 26];183:5458–67. Available from: http://www.jimmunol.org/content/183/9/5458http://www.jimmunol.org/content/183/9/5458.full#ref-list-1

117. Matheu MP, Othy S, Greenberg ML, Dong TX, Schuijs M, Deswarte K, et al. Imaging regulatory T cell dynamics and CTLA4-mediated suppression of T cell priming. Nat Commun [Internet]. 2015 Dec 5 [cited 2018 Aug 26];6(1):6219. Available from: http://www.nature.com/articles/ncomms7219

118. Sotomayor EM, Borrello I, Tubb E, Allison JP, Levitsky HI. In vivo blockade of CTLA-4 enhances the priming of responsive T cells but fails to prevent the induction of tumor

antigen-specific tolerance. Proc Natl Acad Sci U S A [Internet]. 1999 Sep 28 [cited 2018 Aug 26];96(20):11476–81. Available from: http://www.ncbi.nlm.nih.gov/pubmed/10500201

119. Srinivasan P, Wu X, Basu M, Rossi C, Sandler AD. PD-L1 checkpoint inhibition and anti-CTLA-4 whole tumor cell vaccination counter adaptive immune resistance: A mouse neuroblastoma model that mimics human disease. PLoS Med [Internet]. 2018 Jan [cited 2018 Jul 11];15(1):e1002497. Available from: http://www.ncbi.nlm.nih.gov/pubmed/29377881

120. Son C-H, Bae J, Lee H-R, Yang K, Park Y-S. Enhancement of antitumor immunity by combination of anti-CTLA-4 antibody and radioimmunotherapy through the suppression of Tregs. Oncol Lett [Internet]. 2017 May [cited 2018 Aug 26];13(5):3781–6. Available from: http://www.ncbi.nlm.nih.gov/pubmed/28521478

121. Grosso JF, Jure-Kunkel MN. CTLA-4 blockade in tumor models: an overview of preclinical and translational research. Cancer Immun [Internet]. 2013 [cited 2018 Aug 26];13:5. Available from: http://www.ncbi.nlm.nih.gov/pubmed/23390376

122. PDQ Pediatric Treatment Editorial Board. Neuroblastoma Treatment (PDQ®): Patient Version [Internet]. PDQ Cancer Information Summaries. 2002 [cited 2016 Nov 19]. Available from: http://www.ncbi.nlm.nih.gov/pubmed/26389278

123. Davidoff AM. Neuroblastoma. Semin Pediatr Surg [Internet]. 2012 Feb [cited 2018 Aug 2];21(1):2–14. Available from: http://www.ncbi.nlm.nih.gov/pubmed/22248965

124. Brodeur GM, Pritchard J, Berthold F, Carlsen NL, Castel V, Castelberry RP, et al. Revisions of the international criteria for neuroblastoma diagnosis, staging, and response to treatment. J Clin Oncol [Internet]. 1993 Aug [cited 2016 Nov 19];11(8):1466–77. Available from: http://www.ncbi.nlm.nih.gov/pubmed/8336186

125. Teitz T, Wei T, Valentine MB, Vanin EF, Grenet J, Valentine VA, et al. Caspase 8 is deleted or silenced preferentially in childhood neuroblastomaswith amplification of MYCN. Nat Med [Internet]. 2000 May 1 [cited 2018 Feb 27];6(5):529–35. Available from: http://www.ncbi.nlm.nih.gov/pubmed/10802708

126. Castle VP, Heidelberger KP, Bromberg J, Ou X, Dole M, Nunezt G. Short Communication Expression of the Apoptosis-Suppressing Protein bcl-2, in Neuroblastoma Is Associated with Unfavorable Histology and N-myc Amplification [Internet]. Vol. 143, American Jouirntal of Pathology. 1993 [cited 2018 Aug 22]. Available from: https://www.ncbi.nlm.nih.gov/pmc/articles/PMC1887263/pdf/amjpathol00072-0043.pdf

127. Brodeur GM, Seeger RC, Barrett A, Berthold F, Castleberry RP, D'Angio G, et al. International criteria for diagnosis, staging, and response to treatment in patients with neuroblastoma. J Clin Oncol [Internet]. 1988 Dec [cited 2016 Nov 19];6(12):1874–81. Available from: http://www.ncbi.nlm.nih.gov/pubmed/3199170

128. Brodeur GM, Seeger RC, Schwab M, Varmus HE, Bishop JM. Amplification of N-myc in

untreated human neuroblastomas correlates with advanced disease stage. Science [Internet]. 1984 Jun 8 [cited 2016 Nov 19];224(4653):1121–4. Available from: http://www.ncbi.nlm.nih.gov/pubmed/6719137

129. Howman-Giles R, Shaw PJ, Uren RF, Chung DKV. Neuroblastoma and Other Neuroendocrine Tumors. Semin Nucl Med [Internet]. 2007 Jul [cited 2016 Nov 19];37(4):286–302. Available from: http://linkinghub.elsevier.com/retrieve/pii/S000129980700030X

130. Mueller S, Matthay KK. Neuroblastoma: biology and staging. Curr Oncol Rep [Internet]. 2009 Nov [cited 2018 Aug 24];11(6):431–8. Available from: http://www.ncbi.nlm.nih.gov/pubmed/19840520

131. Carén H, Kryh H, Nethander M, Sjöberg R-M, Träger C, Nilsson S, et al. High-risk neuroblastoma tumors with 11q-deletion display a poor prognostic, chromosome instability phenotype with later onset. Proc Natl Acad Sci U S A [Internet]. 2010 Mar 2 [cited 2018 Mar 12];107(9):4323–8. Available from: http://www.ncbi.nlm.nih.gov/pubmed/20145112

132. Houghton PJ, Kang MH, Reynolds CP, Morton CL, Kolb EA, Gorlick R, et al. Initial testing (stage 1) of LCL161, a SMAC mimetic, by the pediatric preclinical testing program. Pediatr Blood Cancer. 2012;58(4):636–9.

133. Czaplinski S, Abhari BA, Torkov A, Seggewiß D, Hugle M, Fulda S. Differential role of RIP1 in Smac mimetic-mediated chemosensitization of neuroblastoma cells. Oncotarget [Internet]. 2015 Dec 8 [cited 2018 Feb 27];6(39):41522–34. Available from: http://www.ncbi.nlm.nih.gov/pubmed/26575016

134. Langemann D, Trochimiuk M, Appl B, Hundsdoerfer P, Reinshagen K, Eschenburg G. Sensitization of neuroblastoma for vincristine-induced apoptosis by Smac mimetic LCL161 is attended by G2 cell cycle arrest but is independent of NFκB, RIP1 and TNF-α. Oncotarget [Internet]. 2017 Oct 20 [cited 2018 Feb 27];8(50):87763–72. Available from: http://www.ncbi.nlm.nih.gov/pubmed/29152118

135. Langdon CG, Wiedemann N, Held MA, Mamillapalli R, Iyidogan P, Theodosakis N, et al. SMAC mimetic Debio 1143 synergizes with taxanes, topoisomerase inhibitors and bromodomain inhibitors to impede growth of lung adenocarcinoma cells. Oncotarget [Internet]. 2015 Nov 10 [cited 2018 Aug 25];6(35):37410–25. Available from: http://www.ncbi.nlm.nih.gov/pubmed/26485762

136. Cabal-Hierro L, O'Dwyer PJ. TNF Signaling through RIP1 Kinase Enhances SN38-Induced Death in Colon Adenocarcinoma. Mol Cancer Res [Internet]. 2017 Apr [cited 2018 Aug 25];15(4):395–404. Available from: http://www.ncbi.nlm.nih.gov/pubmed/28087739

137. Abhari BA, Cristofanon S, Kappler R, von Schweinitz D, Humphreys R, Fulda S. RIP1 is required for IAP inhibitor-mediated sensitization for TRAIL-induced apoptosis via a RIP1/FADD/caspase-8 cell death complex. Oncogene [Internet]. 2013 Jul 13 [cited 2018

Feb 27];32(27):3263–73. Available from: http://www.ncbi.nlm.nih.gov/pubmed/22890322

138. Airoldi I, Lualdi S, Bruno S, Raffaghello L, Occhino M, Gambini C, et al. Expression of costimulatory molecules in human neuroblastoma. Evidence that CD40+ neuroblastoma cells undergo apoptosis following interaction with CD40L. Br J Cancer [Internet]. 2003 May 19 [cited 2018 Jan 2];88(10):1527–36. Available from: http://www.ncbi.nlm.nih.gov/pubmed/12771917

139. Saletta F, Vilain RE, Gupta AK, Nagabushan S, Yuksel A, Catchpoole D, et al. Programmed Death-Ligand 1 Expression in a Large Cohort of Pediatric Patients With Solid Tumor and Association With Clinicopathologic Features in Neuroblastoma. JCO Precis Oncol [Internet]. 2017 Jul 18 [cited 2018 Jan 2];(1):1–12. Available from: http://ascopubs.org/doi/10.1200/PO.16.00049

140. Williams EL, Dunn SN, James S, Johnson PW, Cragg MS, Glennie MJ, et al. Immunomodulatory monoclonal antibodies combined with peptide vaccination provide potent immunotherapy in an aggressive murine neuroblastoma model. Clin Cancer Res [Internet]. 2013 Jul 1 [cited 2018 Jan 2];19(13):3545–55. Available from: http://www.ncbi.nlm.nih.gov/pubmed/23649004

141. Chan R, Shirinbak S, Muthugounder S, Hung L, Gnanachandran J, Hajidaniel M, et al. Abstract 5021: Regulatory T-cells and effects of anti-CTLA4 and anti-PD1 therapy in a transgenic murine model of neuroblastoma. Cancer Res [Internet]. 2014 Oct 1 [cited 2018 Jan 2];74(19 Supplement):5021–5021. Available from: http://cancerres.aacrjournals.org/lookup/doi/10.1158/1538-7445.AM2014-5021

142. Dondero A, Pastorino F, Della Chiesa M, Corrias MV, Morandi F, Pistoia V, et al. PD-L1 expression in metastatic neuroblastoma as an additional mechanism for limiting immune surveillance. Oncoimmunology [Internet]. 2016 Jan 2 [cited 2018 Jul 11];5(1):e1064578. Available from: http://www.ncbi.nlm.nih.gov/pubmed/26942080

143. Aoki T, Hino M, Koh K, Kyushiki M, Kishimoto H, Arakawa Y, et al. Low Frequency of Programmed Death Ligand 1 Expression in Pediatric Cancers. Pediatr Blood Cancer [Internet]. 2016 Aug [cited 2018 Mar 3];63(8):1461–4. Available from: http://www.ncbi.nlm.nih.gov/pubmed/27135656

144. Saletta F, Vilain RE, Gupta AK, Nagabushan S, Yuksel A, Catchpoole D, et al. Programmed Death-Ligand 1 Expression in a Large Cohort of Pediatric Patients With Solid Tumor and Association With Clinicopathologic Features in Neuroblastoma. JCO Precis Oncol [Internet]. 2017 Jul 18 [cited 2018 Feb 27];(1):1–12. Available from: http://ascopubs.org/doi/10.1200/PO.16.00049

145. Chowdhury F, Dunn S, Mitchell S, Mellows T, Ashton-Key M, Gray JC. PD-L1 and CD8 $^{+}$ PD1 $^{+}$ lymphocytes exist as targets in the pediatric tumor microenvironment for immunomodulatory therapy. Oncoimmunology [Internet]. 2015 Oct 3 [cited 2018 Jul 11];4(10):e1029701. Available from: http://www.tandfonline.com/doi/full/10.1080/2162402X.2015.1029701

146. Srinivasan P, Wu X, Basu M, Rossi C, Sandler AD. PD-L1 checkpoint inhibition and anti-CTLA-4 whole tumor cell vaccination counter adaptive immune resistance: A mouse neuroblastoma model that mimics human disease. Mardis ER, editor. PLOS Med [Internet]. 2018 Jan 29 [cited 2018 Feb 27];15(1):e1002497. Available from: http://dx.plos.org/10.1371/journal.pmed.1002497

147. Rigo V, Emionite L, Daga A, Astigiano S, Corrias MV, Quintarelli C, et al. Combined immunotherapy with anti-PDL-1/PD-1 and anti-CD4 antibodies cures syngeneic disseminated neuroblastoma. Sci Rep [Internet]. 2017 Dec 25 [cited 2018 Mar 3];7(1):14049. Available from: http://www.nature.com/articles/s41598-017-14417-6

148. University Hospital of Southampton NFT. Phase I Study of Investigational Medicinal Products in Children With Relapsed/Refractory Neuroblastoma (Inbraced) [Internet]. [cited 2018 Aug 27]. Available from: https://clinicaltrials.gov/ct2/show/NCT02914405?term=pd-1&cond=neuroblastoma&rank=1

149. Amgen F. Cross discipline team leader review: dinutuximab. Cent Drug Eval Res. 2010;0–13.

150. Dhillon S. Dinutuximab: First Global Approval. Drugs [Internet]. 2015 May 5 [cited 2018 Aug 24];75(8):923–7. Available from: http://www.ncbi.nlm.nih.gov/pubmed/25940913

151. Berois N, Osinaga E. Glycobiology of neuroblastoma: impact on tumor behavior, prognosis, and therapeutic strategies. Front Oncol [Internet]. 2014 [cited 2018 Aug 25];4:114. Available from: http://www.ncbi.nlm.nih.gov/pubmed/24904828

152. Horwacik I, Golik P, Grudnik P, Kolinski M, Zdzalik M, Rokita H, et al. Structural Basis of GD2 Ganglioside and Mimetic Peptide Recognition by 14G2a Antibody. Mol Cell Proteomics [Internet]. 2015 Oct [cited 2018 Aug 27];14(10):2577–90. Available from: http://www.ncbi.nlm.nih.gov/pubmed/26179345

153. Sphyris N, Sarkar TR, Battula VL, Andreeff M, Mani SA. GD2 and GD3 synthase: novel drug targets for cancer therapy. Mol Cell Oncol [Internet]. 2015 [cited 2018 Jul 12];2(3):e975068. Available from: http://www.ncbi.nlm.nih.gov/pubmed/27308452

154. Sarkar TR, Battula VL, Werden SJ, Vijay G V, Ramirez-Peña EQ, Taube JH, et al. GD3 synthase regulates epithelial–mesenchymal transition and metastasis in breast cancer. Oncogene [Internet]. 2015 Jun 11 [cited 2018 Aug 25];34(23):2958–67. Available from: http://www.ncbi.nlm.nih.gov/pubmed/25109336

155. Wu ZL, Schwartz E, Seeger R, Ladisch S. Expression of GD2 ganglioside by untreated primary human neuroblastomas. Cancer Res [Internet]. 1986 Jan 1 [cited 2018 Jul 25];46(1):440–3. Available from: http://www.ncbi.nlm.nih.gov/pubmed/3940209

156. Fleurence J, Fougeray S, Bahri M, Cochonneau D, Clémenceau B, Paris F, et al. Targeting *O* -Acetyl-GD2 Ganglioside for Cancer Immunotherapy. J Immunol Res [Internet]. 2017 Jan 5 [cited 2018 Aug 24];2017:1–16. Available from:

https://www.hindawi.com/journals/jir/2017/5604891/

157. Zhang S, Cordon-Cardo C, Zhang HS, Reuter VE, Adluri S, Hamilton WB, et al. Selection of tumor antigens as targets for immune attack using immunohistochemistry: I. Focus on gangliosides. Int J cancer [Internet]. 1997 Sep 26 [cited 2018 Aug 25];73(1):42–9. Available from: http://www.ncbi.nlm.nih.gov/pubmed/9334808

158. Svennerholm L, Boström K, Fredman P, Jungbjer B, Lekman A, Månsson JE, et al. Gangliosides and allied glycosphingolipids in human peripheral nerve and spinal cord. Biochim Biophys Acta [Internet]. 1994 Sep 15 [cited 2018 Aug 25];1214(2):115–23. Available from: http://www.ncbi.nlm.nih.gov/pubmed/7918590

159. Roth M, Linkowski M, Tarim J, Piperdi S, Sowers R, Geller D, et al. Ganglioside GD2 as a therapeutic target for antibody-mediated therapy in patients with osteosarcoma. Cancer [Internet]. 2014 Feb 15 [cited 2018 Aug 25];120(4):548–54. Available from: http://www.ncbi.nlm.nih.gov/pubmed/24166473

160. Fleurence J, Cochonneau D, Fougeray S, Oliver L, Geraldo F, Terme M, et al. Targeting and killing glioblastoma with monoclonal antibody to <i>O</i>-acetyl GD2 ganglioside. Oncotarget [Internet]. 2016 Jul 5 [cited 2018 Aug 25];7(27):41172–85. Available from: http://www.ncbi.nlm.nih.gov/pubmed/27172791

161. Woo SR, Oh YT, An JY, Kang BG, Nam D-H, Joo KM. Glioblastoma specific antigens, GD2 and CD90, are not involved in cancer stemness. Anat Cell Biol [Internet]. 2015 Mar [cited 2018 Aug 25];48(1):44–53. Available from: http://www.ncbi.nlm.nih.gov/pubmed/25806121

162. Battula VL, Shi Y, Evans KW, Wang R-Y, Spaeth EL, Jacamo RO, et al. Ganglioside GD2 identifies breast cancer stem cells and promotes tumorigenesis. J Clin Invest [Internet]. 2012 Jun [cited 2018 Jul 24];122(6):2066–78. Available from: http://www.ncbi.nlm.nih.gov/pubmed/22585577

163. Orsi G, Barbolini M, Ficarra G, Tazzioli G, Manni P, Petrachi T, et al. GD2 expression in breast cancer. Oncotarget [Internet]. 2017 May 9 [cited 2018 Aug 25];8(19):31592–600. Available from: http://www.ncbi.nlm.nih.gov/pubmed/28415563

164. Tsao C-Y, Sabbatino F, Cheung N-K V, Hsu JC-F, Villani V, Wang X, et al. Anti-proliferative and pro-apoptotic activity of GD2 ganglioside-specific monoclonal antibody 3F8 in human melanoma cells. Oncoimmunology [Internet]. 2015 [cited 2018 Jul 23];4(8):e1023975. Available from: http://www.ncbi.nlm.nih.gov/pubmed/26405581

165. Hersey P, Jamal O, Henderson C, Zardawi I, D'Alessandro G. Expression of the gangliosides GM3, GD3 and GD2 in tissue sections of normal skin, naevi, primary and metastatic melanoma. Int J cancer [Internet]. 1988 Mar 15 [cited 2018 Aug 25];41(3):336–43. Available from: http://www.ncbi.nlm.nih.gov/pubmed/3346097

166. Cahan LD, Irie RF, Singh R, Cassidenti A, Paulson JC. Identification of a human neuroectodermal tumor antigen (OFA-I-2) as ganglioside GD2. Proc Natl Acad Sci U S A

[Internet]. 1982 Dec 1 [cited 2018 Aug 25];79(24):7629–33. Available from: http://www.ncbi.nlm.nih.gov/pubmed/6296843

167. Longee DC, Wikstrand CJ, M&#65533;nsson J-E, He X, Fuller GN, Bigner SH, et al. Disialoganglioside GD2 in human neuroectodermal tumor cell lines and gliomas. Acta Neuropathol [Internet]. 1991 Jun [cited 2018 Aug 25];82(1):45–54. Available from: http://link.springer.com/10.1007/BF00310922

168. Yeh S-C, Wang P-Y, Lou Y-W, Khoo K-H, Hsiao M, Hsu T-L, et al. Glycolipid GD3 and GD3 synthase are key drivers for glioblastoma stem cells and tumorigenicity. Proc Natl Acad Sci U S A [Internet]. 2016 May 17 [cited 2018 Jul 24];113(20):5592–7. Available from: http://www.ncbi.nlm.nih.gov/pubmed/27143722

169. Liang Y-J, Wang C-Y, Wang I-A, Chen Y-W, Li L-T, Lin C-Y, et al. Interaction of glycosphingolipids GD3 and GD2 with growth factor receptors maintains breast cancer stem cell phenotype. Oncotarget [Internet]. 2017 Jul 18 [cited 2018 Jul 24];8(29):47454–73. Available from: http://www.ncbi.nlm.nih.gov/pubmed/28537895

170. Liu Y, Wondimu A, Yan S, Bobb D, Ladisch S. Tumor gangliosides accelerate murine tumor angiogenesis. Angiogenesis [Internet]. 2014 Jul 29 [cited 2018 Jul 25];17(3):563–71. Available from: http://link.springer.com/10.1007/s10456-013-9403-4

171. Hettmer S, Malott C, Woods W, Ladisch S, Kaucic K. Biological Stratification of Human Neuroblastoma by Complex “B” Pathway Ganglioside Expression. Cancer Res. 2003;63(21).

172. Yang RK, Sondel PM. Anti-GD2 Strategy in the Treatment of Neuroblastoma. Drugs Future [Internet]. 2010 [cited 2018 Aug 25];35(8):665. Available from: http://www.ncbi.nlm.nih.gov/pubmed/21037966

173. Cheung NK, Kushner BH, Yeh SD, Larson SM. 3F8 monoclonal antibody treatment of patients with stage 4 neuroblastoma: a phase II study. Int J Oncol [Internet]. 1998 Jun [cited 2018 Aug 25];12(6):1299–306. Available from: http://www.ncbi.nlm.nih.gov/pubmed/9592190

174. Doronin II, Kholodenko I V, Molotkovskaya IM, Kholodenko R V. Preparation of Fab-fragments of GD2-specific antibodies and analysis of their antitumor activity in vitro. Bull Exp Biol Med [Internet]. 2013 Mar [cited 2018 Jul 9];154(5):658–63. Available from: http://www.ncbi.nlm.nih.gov/pubmed/23658893

175. Gur H, Ozen F, Can Saylan C, Atasever-Arslan B. Dinutuximab in the Treatment of High-Risk Neuroblastoma in Children. Clin Med Insights Ther [Internet]. 2017 Jan 30 [cited 2018 Aug 25];9:1179559X1771910. Available from: http://journals.sagepub.com/doi/10.1177/1179559X17719106

176. Yu AL, Gilman AL, Ozkaynak MF, London WB, Kreissman SG, Chen HX, et al. Anti-GD2 antibody with GM-CSF, interleukin-2, and isotretinoin for neuroblastoma. N Engl J Med [Internet]. 2010 Sep 30 [cited 2018 Mar 3];363(14):1324–34. Available from:

http://www.ncbi.nlm.nih.gov/pubmed/20879881

177. Lehmann C, Zeis M, Uharek L. Activation of natural killer cells with interleukin 2 (IL-2) and IL-12 increases perforin binding and subsequent lysis of tumour cells. Br J Haematol [Internet]. 2001 Sep [cited 2018 Aug 25];114(3):660–5. Available from: http://www.ncbi.nlm.nih.gov/pubmed/11552995

178. Bober LA, Grace MJ, Pugliese-Sivo C, Rojas-Triana A, Waters T, Sullivan LM, et al. The effect of GM-CSF and G-CSF on human neutrophil function. Immunopharmacology [Internet]. 1995 Mar [cited 2018 Aug 25];29(2):111–9. Available from: http://www.ncbi.nlm.nih.gov/pubmed/7539779

179. Doronin II, Vishnyakova PA, Kholodenko I V, Ponomarev ED, Ryazantsev DY, Molotkovskaya IM, et al. Ganglioside GD2 in reception and transduction of cell death signal in tumor cells. BMC Cancer [Internet]. 2014 Dec 28 [cited 2018 Mar 3];14(1):295. Available from: http://bmccancer.biomedcentral.com/articles/10.1186/1471-2407-14-295

180. Kowalczyk A, Gil M, Horwacik I, Odrowąż Ż, Kozbor D, Rokita H. The GD2-specific 14G2a monoclonal antibody induces apoptosis and enhances cytotoxicity of chemotherapeutic drugs in IMR-32 human neuroblastoma cells. Cancer Lett [Internet]. 2009 Aug [cited 2016 Nov 19];281(2):171–82. Available from: http://linkinghub.elsevier.com/retrieve/pii/S0304383509001347

181. Yoshida S, Kawaguchi H, Sato S, Ueda R, Furukawa K. An anti-GD2 monoclonal antibody enhances apoptotic effects of anti-cancer drugs against small cell lung cancer cells via JNK (c-Jun terminal kinase) activation. Jpn J Cancer Res [Internet]. 2002 Jul [cited 2018 Aug 25];93(7):816–24. Available from: http://www.ncbi.nlm.nih.gov/pubmed/12149148

182. Mahata B, Banerjee A, Kundu M, Bandyopadhyay U, Biswas K. TALEN mediated targeted editing of GM2/GD2-synthase gene modulates anchorage independent growth by reducing anoikis resistance in mouse tumor cells. Sci Rep [Internet]. 2015 Mar 12 [cited 2018 Jan 23];5:9048. Available from: http://www.ncbi.nlm.nih.gov/pubmed/25762467

183. Cheresh DA, Klier FG. Disialoganglioside GD2 distributes preferentially into substrate-associated microprocesses on human melanoma cells during their attachment to fibronectin. J Cell Biol [Internet]. 1986 May [cited 2018 Jan 19];102(5):1887–97. Available from: http://www.ncbi.nlm.nih.gov/pubmed/3084502

184. Ribatti D. Anti-angiogenesis in neuroblastoma. Crit Rev Oncol Hematol [Internet]. 2013 Jun [cited 2016 Nov 29];86(3):212–21. Available from: http://linkinghub.elsevier.com/retrieve/pii/S1040842812002302

185. Khanna C, Jaboin JJ, Drakos E, Tsokos M, Thiele CJ. Biologically relevant orthotopic neuroblastoma xenograft models: primary adrenal tumor growth and spontaneous distant metastasis. In Vivo [Internet]. [cited 2016 Nov 27];16(2):77–85. Available from: http://www.ncbi.nlm.nih.gov/pubmed/12073775

186. RIBATTI D. Angiogenesis in Neuroblastoma. Ann N Y Acad Sci [Internet]. 2004 Dec 1 [cited 2016 Nov 29];1028(1):133–42. Available from: http://doi.wiley.com/10.1196/annals.1322.014

187. Hatzi E, Breit S, Zoephel A, Ashman K, Tontsch U, Ahorn H, et al. MYCN oncogene and angiogenesis: down-regulation of endothelial growth inhibitors in human neuroblastoma cells. Purification, structural, and functional characterization. Adv Exp Med Biol [Internet]. 2000 [cited 2018 Jul 25];476:239–48. Available from: http://www.ncbi.nlm.nih.gov/pubmed/10949669

188. Ribatti D, Raffaghello L, Pastorino F, Nico B, Brignole C, Vacca A, et al. In vivo angiogenic activity of neuroblastoma correlates withMYCN oncogene overexpression. Int J Cancer [Internet]. 2002 Dec 1 [cited 2018 Jul 25];102(4):351–4. Available from: http://www.ncbi.nlm.nih.gov/pubmed/12402304

189. Jakovljević G, Čulić S, Stepan J, Bonevski A, Seiwerth S. Vascular endothelial growth factor in children with neuroblastoma: a retrospective analysis. J Exp Clin Cancer Res [Internet]. 2009 Nov 6 [cited 2018 Jul 25];28(1):143. Available from: http://jeccr.biomedcentral.com/articles/10.1186/1756-9966-28-143

190. Weng W-C, Lin K-H, Wu P-Y, Ho Y-H, Liu Y-L, Wang B-J, et al. VEGF expression correlates with neuronal differentiation and predicts a favorable prognosis in patients with neuroblastoma. Sci Rep [Internet]. 2017 Dec 11 [cited 2018 Jul 25];7(1):11212. Available from: http://www.ncbi.nlm.nih.gov/pubmed/28894229

191. Kang J, Rychahou PG, Ishola TA, Mourot JM, Evers BM, Chung DH. N-myc is a novel regulator of PI3K-mediated VEGF expression in neuroblastoma. Oncogene [Internet]. 2008 Jun 18 [cited 2018 Jul 25];27(28):3999–4007. Available from: http://www.nature.com/articles/onc200815

192. Segerström L, Fuchs D, Bäckman U, Holmquist K, Christofferson R, Azarbayjani F. The Anti-VEGF Antibody Bevacizumab Potently Reduces the Growth Rate of High-Risk Neuroblastoma Xenografts. Pediatr Res [Internet]. 2006 Nov [cited 2018 Jul 25];60(5):576–81. Available from: http://www.ncbi.nlm.nih.gov/pubmed/16988184

193. Schmid TA, Gore ME. Sunitinib in the treatment of metastatic renal cell carcinoma. Ther Adv Urol [Internet]. 2016 Dec [cited 2018 Aug 25];8(6):348–71. Available from: http://www.ncbi.nlm.nih.gov/pubmed/27904651

194. Le Tourneau C, Raymond E, Faivre S. Sunitinib: a novel tyrosine kinase inhibitor. A brief review of its therapeutic potential in the treatment of renal carcinoma and gastrointestinal stromal tumors (GIST). Ther Clin Risk Manag [Internet]. 2007 Jun [cited 2018 Aug 25];3(2):341–8. Available from: http://www.ncbi.nlm.nih.gov/pubmed/18360643

195. Calero R, Morchon E, Johnsen JI, Serrano R. Sunitinib Suppress Neuroblastoma Growth through Degradation of MYCN and Inhibition of Angiogenesis. Castresana JS, editor. PLoS One [Internet]. 2014 Apr 23 [cited 2018 Jul 25];9(4):e95628. Available from: http://www.ncbi.nlm.nih.gov/pubmed/24759734

196. Zhang L, Smith KM, Chong AL, Stempak D, Yeger H, Marrano P, et al. In vivo antitumor and antimetastatic activity of sunitinib in preclinical neuroblastoma mouse model. Neoplasia [Internet]. 2009 May [cited 2018 Jul 25];11(5):426–35. Available from: http://www.ncbi.nlm.nih.gov/pubmed/19412427

197. Kumar S, Sun JD, Zhang L, Mokhtari RB, Wu B, Meng F, et al. Hypoxia-Targeting Drug Evofosfamide (TH-302) Enhances Sunitinib Activity in Neuroblastoma Xenograft Models. Transl Oncol [Internet]. 2018 Aug 1 [cited 2018 Jul 25];11(4):911–9. Available from: https://www.sciencedirect.com/science/article/pii/S193652331730298X

198. National Institue of Health. Clinical trials investigating angiogenesis in neuroblastoma [Internet]. [cited 2018 Aug 27]. Available from: https://clinicaltrials.gov/ct2/results?cond=Neuroblastoma&term=angiogenesis&cntry=&state=&city=&dist=

199. Creagh EM, Murphy BM, Duriez PJ, Duckett CS, Martin SJ. Smac/Diablo Antagonizes Ubiquitin Ligase Activity of Inhibitor of Apoptosis Proteins. J Biol Chem [Internet]. 2004 Jun 25 [cited 2016 Nov 19];279(26):26906–14. Available from: http://www.jbc.org/cgi/doi/10.1074/jbc.M313859200

200. National Institute of Health. Investigation of using Smac Mimetic therapies in cancer [Internet]. [cited 2018 Aug 27]. Available from: https://clinicaltrials.gov/ct2/results?cond=&term=smac+mimetics&cntry=&state=&city=&dist=

201. Hao Q, Tang H. Interferon-γ and Smac mimetics synergize to induce apoptosis of lung cancer cells in a TNFα-independent manner. Cancer Cell Int [Internet]. 2018 Dec 14 [cited 2018 Aug 23];18(1):84. Available from: https://cancerci.biomedcentral.com/articles/10.1186/s12935-018-0579-y

202. Marschall V, Fulda S. Smac mimetic-induced upregulation of interferon-β sensitizes glioblastoma to temozolomide-induced cell death. Cell Death Dis [Internet]. 2015 Sep 17 [cited 2018 Aug 23];6(9):e1888. Available from: http://www.ncbi.nlm.nih.gov/pubmed/26379193

203. Rathore R, McCallum JE, Varghese E, Florea A-M, Büsselberg D. Overcoming chemotherapy drug resistance by targeting inhibitors of apoptosis proteins (IAPs). Apoptosis [Internet]. 2017 [cited 2018 Aug 27];22(7):898–919. Available from: http://www.ncbi.nlm.nih.gov/pubmed/28424988

204. Najem S, Langemann D, Appl B, Trochimiuk M, Hundsdoerfer P, Reinshagen K, et al. Smac mimetic LCL161 supports neuroblastoma chemotherapy in a drug class-dependent manner and synergistically interacts with ALK inhibitor TAE684 in cells with ALK mutation F1174L. Oncotarget [Internet]. 2016 Nov 8 [cited 2018 Feb 27];7(45):72634–53. Available from: http://www.ncbi.nlm.nih.gov/pubmed/27655666

205. Cheung HH, Mahoney DJ, LaCasse EC, Korneluk RG. Down-regulation of c-FLIP enhances death of cancer cells by Smac mimetic compound. Cancer Res.

2009;69(19):7729–38.

206. Teitz T, Wei T, Valentine MB, Vanin EF, Grenet J, Valentine VA, et al. Caspase 8 is deleted or silenced preferentially in childhood neuroblastomaswith amplification of MYCN. Nat Med [Internet]. 2000 May 1 [cited 2018 Aug 22];6(5):529–35. Available from: http://www.nature.com/articles/nm0500_529

207. Bate-Eya LT, den Hartog IJM, van der Ploeg I, Schild L, Koster J, Santo EE, et al. High efficacy of the BCL-2 inhibitor ABT199 (venetoclax) in BCL-2 high-expressing neuroblastoma cell lines and xenografts and rational for combination with MCL-1 inhibition. Oncotarget [Internet]. 2016 May 10 [cited 2018 Aug 10];7(19):27946–58. Available from: http://www.ncbi.nlm.nih.gov/pubmed/27056887

208. Nakamura-López Y, Sarmiento-Silva RE, Moran-Andrade J, Gómez-García B. Staurosporine-induced apoptosis in P388D1 macrophages involves both extrinsic and intrinsic pathways. Cell Biol Int [Internet]. 2009 Sep 1 [cited 2018 Aug 24];33(9):1026–31. Available from: https://www.sciencedirect.com/science/article/pii/S1065699509001449

209. Kaufmann SH, Desnoyers S, Ottaviano Y, Davidson NE, Poirier GG. Specific proteolytic cleavage of poly(ADP-ribose) polymerase: an early marker of chemotherapy-induced apoptosis. Cancer Res [Internet]. 1993 Sep 1 [cited 2018 Aug 10];53(17):3976–85. Available from: http://www.ncbi.nlm.nih.gov/pubmed/8358726

210. Witt A, Seeger JM, Coutelle O, Zigrino P, Broxtermann P, Andree M, et al. IAP antagonization promotes inflammatory destruction of vascular endothelium. EMBO Rep [Internet]. 2015 Jun [cited 2018 Jan 2];16(6):719–27. Available from: http://www.ncbi.nlm.nih.gov/pubmed/25825408

211. Roy Choudhury S, Karmakar S, Banik NL, Ray SK, Roy Choudhury S, Karmakar S, et al. Targeting angiogenesis for controlling neuroblastoma. J Oncol [Internet]. 2012 [cited 2016 Nov 29];2012:782020. Available from: http://www.ncbi.nlm.nih.gov/pubmed/21876694

212. Demetri GD, van Oosterom AT, Garrett CR, Blackstein ME, Shah MH, Verweij J, et al. Efficacy and safety of sunitinib in patients with advanced gastrointestinal stromal tumour after failure of imatinib: a randomised controlled trial. Lancet (London, England) [Internet]. 2006 Oct 14 [cited 2018 Aug 27];368(9544):1329–38. Available from: http://www.ncbi.nlm.nih.gov/pubmed/17046465

213. Draghiciu O, Nijman HW, Hoogeboom BN, Meijerhof T, Daemen T. Sunitinib depletes myeloid-derived suppressor cells and synergizes with a cancer vaccine to enhance antigen-specific immune responses and tumor eradication. Oncoimmunology [Internet]. 2015 Mar [cited 2018 Jul 10];4(3):e989764. Available from: http://www.ncbi.nlm.nih.gov/pubmed/25949902

214. Prapa M, Caldrer S, Spano C, Bestagno M, Golinelli G, Grisendi G, et al. A novel anti-GD2/4-1BB chimeric antigen receptor triggers neuroblastoma cell killing. Oncotarget

[Internet]. 2015 Sep 21 [cited 2016 Nov 19];6(28):24884–94. Available from: http://oncotarget.com/abstract/4670

215. Neal ZC, Yang JC, Rakhmilevich AL, Buhtoiarov IN, Lum HE, Imboden M, et al. Enhanced activity of hu14.18-IL2 immunocytokine against murine NXS2 neuroblastoma when combined with interleukin 2 therapy. Clin Cancer Res [Internet]. 2004 Jul 15 [cited 2018 Jan 19];10(14):4839–47. Available from: http://www.ncbi.nlm.nih.gov/pubmed/15269160

216. National Cancer Institute. Lenalidomide and Dinutuximab With or Without Isotretinoin in Treating Younger Patients With Refractory or Recurrent Neuroblastoma - Full Text View - ClinicalTrials.gov [Internet]. [cited 2018 Aug 27]. Available from: https://clinicaltrials.gov/ct2/show/NCT01711554?id=NCT01711554&rank=1&load=cart

217. Doronin II, Vishnyakova PA, Kholodenko I V, Ponomarev ED, Ryazantsev DY, Molotkovskaya IM, et al. Ganglioside GD2 in reception and transduction of cell death signal in tumor cells. BMC Cancer [Internet]. 2014 Dec 28 [cited 2016 Nov 19];14(1):295. Available from: http://bmccancer.biomedcentral.com/articles/10.1186/1471-2407-14-295

218. Zhao XJ, Cheung NK. GD2 oligosaccharide: target for cytotoxic T lymphocytes. J Exp Med [Internet]. 1995 Jul 1 [cited 2018 Mar 30];182(1):67–74. Available from: http://www.ncbi.nlm.nih.gov/pubmed/7540657

219. MASUCCI G, WERSÄLL P, NIELSEN J, NIELSEN HK, WIGZELL H, MELLSTEDT H. Lymphokine Activated Killer (LAK) Cells in Antibody Dependent Cellular Cytotoxicity (ADCC) Using MAb 17-1A: A Combination of Potential Usefulness in Tumor Therapy. Hybridoma [Internet]. 1989 Oct [cited 2018 Jan 23];8(5):507–16. Available from: http://www.ncbi.nlm.nih.gov/pubmed/2807310

220. Thurin J, Koprowski H, Herlyn M, Steplewski Z. United States Patent: 4849509: Monoclonal antibodies against melanoma-associated antigens and hybrid cell lines producing these antibodies [Internet]. 4849509, 1987 [cited 2018 Aug 27]. Available from: http://patft.uspto.gov/netacgi/nph-Parser?Sect1=PTO2&Sect2=HITOFF&p=1&u=%2Fnetahtml%2FPTO%2Fsearch-bool.html&r=1&f=G&l=50&co1=AND&d=PTXT&s1=4,849,509.PN.&OS=PN/4,849,509 &RS=PN/4,849,509

221. Srinivasan P, Wu X, Basu M, Rossi C, Sandler AD. PD-L1 checkpoint inhibition and anti-CTLA-4 whole tumor cell vaccination counter adaptive immune resistance: A mouse neuroblastoma model that mimics human disease. Mardis ER, editor. PLOS Med [Internet]. 2018 Jan 29 [cited 2018 Mar 3];15(1):e1002497. Available from: http://dx.plos.org/10.1371/journal.pmed.1002497

222. Sanda T, Korneluk RG. Smac mimetic compounds used in combination with CTLA-4 antibody treatment. University of Ottawa;

223. Manguso RT, Pope HW, Zimmer MD, Brown FD, Yates KB, Miller BC, et al. In vivo

CRISPR screening identifies Ptpn2 as a cancer immunotherapy target. Nature [Internet]. 2017 Jul 19 [cited 2018 Aug 27];547(7664):413–8. Available from: http://www.ncbi.nlm.nih.gov/pubmed/28723893

224. Maris JM, Hogarty MD, Bagatell R, Cohn SL. Neuroblastoma. Lancet [Internet]. 2007 Jun [cited 2016 Nov 19];369(9579):2106–20. Available from: http://linkinghub.elsevier.com/retrieve/pii/S0140673607609830

225. Kushner BH, Cheung IY, Modak S, Kramer K, Ragupathi G, Cheung N-K V. Phase I Trial of a Bivalent Gangliosides Vaccine in Combination with β-Glucan for High-Risk Neuroblastoma in Second or Later Remission. Clin Cancer Res [Internet]. 2014 Mar 1 [cited 2018 Aug 24];20(5):1375–82. Available from: http://www.ncbi.nlm.nih.gov/pubmed/24520094

226. Grupp SA, Prak EL, Boyer J, McDonald KR, Shusterman S, Thompson E, et al. Adoptive Transfer of Autologous T Cells Improves T-cell Repertoire Diversity and Long-term B-cell Function in Pediatric Patients with Neuroblastoma. Clin Cancer Res [Internet]. 2012 Dec 15 [cited 2018 Aug 24];18(24):6732–41. Available from: http://clincancerres.aacrjournals.org/cgi/doi/10.1158/1078-0432.CCR-12-1432

227. Heczey A, Louis CU, Savoldo B, Dakhova O, Durett A, Grilley B, et al. CAR T Cells Administered in Combination with Lymphodepletion and PD-1 Inhibition to Patients with Neuroblastoma. Mol Ther [Internet]. 2017 Sep 6 [cited 2018 Aug 24];25(9):2214–24. Available from: http://www.ncbi.nlm.nih.gov/pubmed/28602436

228. Chen K-F, Lin J-P, Shiau C-W, Tai W-T, Liu C-Y, Yu H-C, et al. Inhibition of Bcl-2 improves effect of LCL161, a SMAC mimetic, in hepatocellular carcinoma cells. Biochem Pharmacol [Internet]. 2012 [cited 2018 Mar 5];84:268–77. Available from: https://journals-scholarsportal-info.proxy.bib.uottawa.ca/pdf/00062952/v84i0003/268_iobieosmihcc.xml

229. Johnsen JI, Pettersen I, Ponthan F, Sveinbjørnsson B, Flaegstad T, Kogner P. Synergistic induction of apoptosis in neuroblastoma cells using a combination of cytostatic drugs with interferon-gamma and TRAIL. Int J Oncol [Internet]. 2004 Dec [cited 2018 Aug 24];25(6):1849–57. Available from: http://www.ncbi.nlm.nih.gov/pubmed/15547726

230. Chaitanya GV, Steven AJ, Babu PP. PARP-1 cleavage fragments: signatures of cell-death proteases in neurodegeneration. Cell Commun Signal [Internet]. 2010 Dec 22 [cited 2016 Nov 19];8:31. Available from: http://www.ncbi.nlm.nih.gov/pubmed/21176168

231. Lecis D, De Cesare M, Perego P, Conti A, Corna E, Drago C, et al. Smac mimetics induce inflammation and necrotic tumour cell death by modulating macrophage activity. Cell Death Dis [Internet]. 2013 Nov 14 [cited 2018 Aug 27];4(11):e920. Available from: http://www.ncbi.nlm.nih.gov/pubmed/24232096

232. Motzer RJ, Michaelson MD, Redman BG, Hudes GR, Wilding G, Figlin RA, et al. Activity of SU11248, a Multitargeted Inhibitor of Vascular Endothelial Growth Factor Receptor and Platelet-Derived Growth Factor Receptor, in Patients With Metastatic Renal

Cell Carcinoma. J Clin Oncol [Internet]. 2006 Jan 1 [cited 2018 Aug 27];24(1):16–24. Available from: http://www.ncbi.nlm.nih.gov/pubmed/16330672

233. Liu D, Li G, Avella DM, Kimchi ET, Kaifi JT, Rubinstein MP, et al. Sunitinib represses regulatory T cells to overcome immunotolerance in a murine model of hepatocellular cancer. Oncoimmunology [Internet]. 2018 Jan 2 [cited 2018 Jul 10];7(1):e1372079. Available from: http://www.ncbi.nlm.nih.gov/pubmed/29296523

234. Finke JH, Rini B, Ireland J, Rayman P, Richmond A, Golshayan A, et al. Sunitinib Reverses Type-1 Immune Suppression and Decreases T-Regulatory Cells in Renal Cell Carcinoma Patients. Clin Cancer Res [Internet]. 2008 Oct 15 [cited 2018 Jul 10];14(20):6674–82. Available from: http://www.ncbi.nlm.nih.gov/pubmed/18927310

235. Hsieh W-C, Hsu T-S, Chang Y-J, Lai M-Z. IL-6 receptor blockade corrects defects of XIAP-deficient regulatory T cells. Nat Commun [Internet]. 2018 Dec 31 [cited 2018 Jul 10];9(1):463. Available from: http://www.nature.com/articles/s41467-018-02862-4

236. Patel K, Rossell R, Pemberton L, Cheung N, Walsh F, Moore S, et al. Monoclonal antibody 3F8 recognises the neural cell adhesion molecule (NCAM) in addition to the ganglioside GD2. Br J Cancer [Internet]. 1989 Dec 1 [cited 2018 Aug 27];60(6):861–6. Available from: http://www.nature.com/articles/bjc1989380

237. Agrawal V, Frankel AE. 14G2a Anti-GD2 Crossreactivity With the CD166 Antigen. J Immunother [Internet]. 2010 Nov [cited 2018 Jul 19];33(9):1014–5. Available from: https://insights.ovid.com/crossref?an=00002371-201011000-00012

238. Kozbor D. Cancer vaccine with mimotopes of tumor-associated carbohydrate antigens. Immunol Res [Internet]. 2010 Mar 10 [cited 2018 Jul 9];46(1–3):23–31. Available from: http://www.ncbi.nlm.nih.gov/pubmed/19763891

239. Gerardy-Schahn R, Delannoy P (Philippe R, Itzstein M von. SialoGlyco chemistry and biology. II, Tools and techniques to identify and capture sialoglycans [Internet]. [cited 2018 Aug 27]. 254 p. Available from: https://books.google.ca/books?id=6dhECgAAQBAJ&dq=need+fixative+agent+for+ganglioside&source=gbs_navlinks_s

240. Poon VI, Roth M, Piperdi S, Geller D, Gill J, Rudzinski ER, et al. Ganglioside GD2 expression is maintained upon recurrence in patients with osteosarcoma. Clin Sarcoma Res [Internet]. 2015 [cited 2018 Jul 17];5(1):4. Available from: http://www.ncbi.nlm.nih.gov/pubmed/25642322

241. Schulz G, Cheresh DA, Varki NM, Yu A, Staffileno LK, Reisfeld RA. Detection of ganglioside GD2 in tumor tissues and sera of neuroblastoma patients. Cancer Res [Internet]. 1984 Dec [cited 2016 Dec 3];44(12 Pt 1):5914–20. Available from: http://www.ncbi.nlm.nih.gov/pubmed/6498849

242. Aixinjueluo W, Furukawa K, Zhang Q, Hamamura K, Tokuda N, Yoshida S, et al. Mechanisms for the apoptosis of small cell lung cancer cells induced by anti-GD2

monoclonal antibodies: roles of anoikis. J Biol Chem [Internet]. 2005 Aug 19 [cited 2018 Aug 27];280(33):29828–36. Available from: http://www.ncbi.nlm.nih.gov/pubmed/15923178

243. Kang N-Y, Kim C-H, Kim K-S, Ko J-H, Lee J-H, Jeong Y-K, et al. Expression of the human CMP-NeuAc:GM3 α2,8-sialyltransferase (GD3 synthase) gene through the NF-κB activation in human melanoma SK-MEL-2 cells. Biochim Biophys Acta - Gene Struct Expr [Internet]. 2007 Nov [cited 2018 Aug 27];1769(11–12):622–30. Available from: http://www.ncbi.nlm.nih.gov/pubmed/17913261

244. Nguyen K, Battula VL. Targeting NFκB signaling in GD2+ BCSCs. Aging (Albany NY) [Internet]. 2017 Aug 3 [cited 2018 Jul 12];9(8):1847–8. Available from: http://www.ncbi.nlm.nih.gov/pubmed/28858852

245. Battula VL, Nguyen K, Sun J, Pitner MK, Yuan B, Bartholomeusz C, et al. IKK inhibition by BMS-345541 suppresses breast tumorigenesis and metastases by targeting GD2+ cancer stem cells. Oncotarget [Internet]. 2017 Jun 6 [cited 2018 Jul 12];8(23):36936–49. Available from: http://www.ncbi.nlm.nih.gov/pubmed/28415808

246. Burke JR, Pattoli MA, Gregor KR, Brassil PJ, MacMaster JF, McIntyre KW, et al. BMS-345541 is a highly selective inhibitor of I kappa B kinase that binds at an allosteric site of the enzyme and blocks NF-kappa B-dependent transcription in mice. J Biol Chem [Internet]. 2003 Jan 17 [cited 2018 Jul 12];278(3):1450–6. Available from: http://www.ncbi.nlm.nih.gov/pubmed/12403772

247. Dewald JH, Cavdarli S, Steenackers A, Delannoy CP, Mortuaire M, Spriet C, et al. TNF differentially regulates ganglioside biosynthesis and expression in breast cancer cell lines. PLoS One [Internet]. 2018 [cited 2018 Jul 19];13(4):e0196369. Available from: http://www.ncbi.nlm.nih.gov/pubmed/29698439

248. Bocca P, Di Carlo E, Caruana I, Emionite L, Cilli M, De Angelis B, et al. Bevacizumab-mediated tumor vasculature remodelling improves tumor infiltration and antitumor efficacy of GD2-CAR T cells in a human neuroblastoma preclinical model. Oncoimmunology [Internet]. 2018 Jan 2 [cited 2018 Jul 10];7(1):e1378843. Available from: http://www.ncbi.nlm.nih.gov/pubmed/29296542

249. Androulla MN, Lefkothea PC. CAR T-cell Therapy: A New Era in Cancer Immunotherapy. Curr Pharm Biotechnol [Internet]. 2018 May 31 [cited 2018 Aug 27];19(1):5–18. Available from: http://www.ncbi.nlm.nih.gov/pubmed/29667553

250. Jinesh G G, Chunduru S, Kamat AM. Smac mimetic enables the anticancer action of BCG-stimulated neutrophils through TNF-α but not through TRAIL and FasL. J Leukoc Biol [Internet]. 2012 Jul [cited 2018 Jul 30];92(1):233–44. Available from: http://www.ncbi.nlm.nih.gov/pubmed/22517918

251. Mansky P, Brown WM, Park JH, Choi JW, Yang SY. The second kappa B element, kappa B2, of the HLA-A class I regulatory complex is an essential part of the promoter. J Immunol [Internet]. 1994 Dec 1 [cited 2018 Aug 8];153(11):5082–90. Available from:

http://www.ncbi.nlm.nih.gov/pubmed/7963567

252. Ghosh S, Paul A, Sen E. Tumor necrosis factor α-induced hypoxia-inducible factor 1α-β-catenin axis regulates major histocompatibility complex class I gene activation through chromatin remodeling. Mol Cell Biol [Internet]. 2013 Jul [cited 2018 Aug 8];33(14):2718–31. Available from: http://www.ncbi.nlm.nih.gov/pubmed/23671189

253. Ou J-N, Wiedeman AE, Stevens AM. TNF-α and TGF-β counter-regulate PD-L1 expression on monocytes in systemic lupus erythematosus. Sci Rep [Internet]. 2012 [cited 2018 Aug 8];2:295. Available from: http://www.ncbi.nlm.nih.gov/pubmed/22389764

254. Hartley G, Regan D, Guth A, Dow S. Regulation of PD-L1 expression on murine tumor-associated monocytes and macrophages by locally produced TNF-α. Cancer Immunol Immunother [Internet]. 2017 Apr 9 [cited 2018 Aug 8];66(4):523–35. Available from: http://link.springer.com/10.1007/s00262-017-1955-5

255. Chowdhury F, Dunn S, Mitchell S, Mellows T, Ashton-Key M, Gray JC. PD-L1 and CD8 $^{+}$ PD1 $^{+}$ lymphocytes exist as targets in the pediatric tumor microenvironment for immunomodulatory therapy. Oncoimmunology [Internet]. 2015 Oct 3 [cited 2018 Mar 3];4(10):e1029701. Available from: http://www.tandfonline.com/doi/full/10.1080/2162402X.2015.1029701

256. National Institute of Health. Clinical trials investigating PD-1 or CTLA-4 therapy to treat neuroblastoma [Internet]. [cited 2018 Aug 27]. Available from: https://clinicaltrials.gov/ct2/results?cond=neuroblastoma&term=pd-1&cntry=&state=&city=&dist=

257. Shen S, Dolnikov A, O'Brien T. Use of HDACi and PD-1/PD-L1 Blockade to Enhance Cytolytic Activity of Ex Vivo Expanded NK Cells Against Neuroblastoma. Cytotherapy [Internet]. 2016 Jun 1 [cited 2018 Jul 11];18(6):S101. Available from: http://linkinghub.elsevier.com/retrieve/pii/S1465324916302365

258. Hank JA, Surfus J, Gan J, Albertini M, Lindstrom M, Schiller JH, et al. Distinct clinical and laboratory activity of two recombinant interleukin-2 preparations. Clin Cancer Res [Internet]. 1999 Feb 15 [cited 2018 Jan 19];5(2):281–9. Available from: http://www.ncbi.nlm.nih.gov/pubmed/10037176

259. Erbe AK, Wang W, Carmichael L, Kim K, Mendonça EA, Song Y, et al. Neuroblastoma Patients' KIR and KIR-Ligand Genotypes Influence Clinical Outcome for Dinutuximab-based Immunotherapy: A Report from the Children's Oncology Group. Clin Cancer Res [Internet]. 2018 Jan 1 [cited 2018 Aug 3];24(1):189–96. Available from: http://www.ncbi.nlm.nih.gov/pubmed/28972044